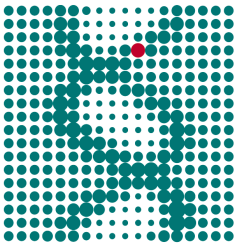

Max Planck Institute for Molecular Genetics

Freie Universität Berlin

Identification of novel genetic loci for non-syndromic autosomal recessive mental retardation and molecular genetic characterization of a causative *GRIK2* mutation

DISSERTATION

zur Erlangung des akademischen Grades

doctor rerum naturalium

(Dr. rer. nat.)

Vorgelegt von

Mohammad Mahdi Motazacker

Aus Esfahan, Iran

Eingereicht im Fachbereich

Biologie, Chemie, Pharmazie

der

Freien Universität Berlin

September 2008

Diese Dissertation wurde in der Zeit vom Februar 2004 bis July 2007 am Max-Planck-Institut für molekulare Genetik in Berlin, in der Abteilung von Herrn Prof. Dr. Hans-
Hilger Ropers, Arbeitsgruppe Dr. Andreas W. Kuss angefertigt.

This thesis has been conducted from February 2004 till July 2007 at the Max Planck Institute for Molecular Genetics in Berlin in the department of Prof. Dr. Hans-Hilger Ropers, Research group Familial cognitive disorders (Dr. Andreas W. Kuss)

1. Gutachter: **Prof. Dr. Hans-Hilger Ropers**
Max Planck Institut für molekulare Genetik

Ihnestr. 73, D-14195 Berlin

First Referee: **Prof. Dr. Hans-Hilger Ropers**
Max Planck Institute for molecular Genetics

Ihnestr. 73, D-14195 Berlin

2. Gutachter: **Prof. Dr. Gerd Multhaup**
Freie Universität

Thielallee 63, D-14195 Berlin

Second Referee: **Prof. Dr. Gerd Multhaup**
Free University

Thielallee 63, D-14195 Berlin

Tag der Disputation: September 23rd, 2008
Day of the Disputation: September 23rd, 2008

I hereby declare that the work presented in this thesis has been conducted independentlyand without any inappropriate support and that all sources of information, be it experimental or intellectual, are aptly referenced.
I hereby declare that this thesis has not been submitted, either in the same or a differentform, to this or any other university for a degree.

Mohammad Mahdi Motazacker
Berlin, September 2008

1. Introduction

1.1. Mental retardation

Mental retardation (MR) or intellectual and developmental disability (IDD) is characterized by significant limitations both in intellectual functioning and in adaptive behaviour as expressed in conceptual, social and practical adaptive skills before age 18. Conceptual skills include receptive and expressive language, reading and writing, money concepts and self-directions. Social skills are responsibility, self-esteem, gullibility, i.e. likelihood of being tricked or manipulated, following the rules, obey laws and avoiding victimization. Practical adaptive skills are personal activities of daily living such as eating, dressing, mobility and toileting and instrumental activities of daily living such as preparing meals, taking medication, using the telephone, managing money, using transportation and doing housekeeping activities, occupational skills and maintaining a safe environment (APA 1994; AAMR 2005).

MR is a highly heterogeneous condition with a prevalence of 1-3% in the general population. It is the most common reason for referral to genetic services and one of the important unsolved problems in health care (Roeleveld et al. 1997; Leonard and Wen 2002; Ropers 2006). If MR is an isolated feature in the patients, it is referred to as non-syndromic MR while if it is observed together with other clinical features, it is referred to as syndromic MR. An important tool for defining and standardizing the extent of MR is the intelligence quotient (IQ).

The IQ is usually determined by standardized tests i.e. Wechsler's test (Wechsler 1981), which are designed to measure intellectual ability. Using these tests, it is possible to characterize mental disability in a semi-standardized manner. Mild forms of mental retardation are defined by an IQ of 50 to 70. Mild MR is thought to represent the lower end of the normal IQ distribution and might be the result of the interaction of many genes and environmental factors. In contrast, severe forms with an IQ <50 which have an incidence about ~0.4%, might be caused by catastrophic events such as perinatal hypoxia or, more often, specific genetic factors such as chromosomal aberrations and defects in specific genes (Ropers 2006).

The genetic factors involved in the aetiology of MR can be classified as follows:

- Large chromosome abnormalities, which can be detected by normal karyotyping using light microscopy. They include aneuploidies, large chromosomal deletion/insertions, inversions and translocations. Down syndrome, for example, was the first identified chromosomal abnormality associated with MR (Penrose 1938; Lejeune et al. 1959).

- Microdeletions, which are detectable with fluorescence in situ hybridization (FISH), Comparative Genomic Hybridization (CGH) and array based CGH (array-CGH). Common microdeletion syndromes are Wolf-Hirschhorn syndrome, Cri du Chat syndrome, Williams syndrome, Prader-Willi syndrome, Angelman syndrome, Rubinstein-Taybi syndrome, Miller-Dieker lissencephaly, Smith-Magenis syndrome, Alagille and Di George syndromes. These syndromes are associated with varying degrees of mental retardation in addition to their own characteristic distinguishing features.

- Functionally relevant sequence variation in single genes. Identification of these genes relies on the characterization of familial cases.

1.2. X-linked mental retardation (XLMR)

The majority of genes that have been identified in mental retardation are located on the X chromosome. This is because XLMR has been disproportionately well studied due to the following reasons:

First, there is a marked (e.g., 25 to 40%) excess of male over female MR patients (Yeargin-Allsopp et al. 1997; Leonard and Wen 2002).

Second, it is comparatively easy to identify XLMR families because of their characteristic inheritance patterns. Finally, the X-chromosome comprises only 4% of all human genes which has greatly facilitated the identification of genetic defects underlying X-linked mental retardation.

The fragile X mental retardation syndrome was the first of the various forms of XLMR that could be elucidated (Verkerk et al, 1991), and it still remains the most common single gene defect underlying XLMR (Martin and Bell 1943; Oberle et al. 1991; Crawford et al. 2001).

In non-syndromic XLMR (NSXLMR), about 30 genes have been identified so far (Lugtenberg et al. 2006), either by mutation screening in families or by studying patients with balanced or small X-chromosomal aberrations. Some of these genes with known function are listed in Table 1-1 (Chiurazzi et al. 2008).

Table 1-1: Genes involved in non-syndromic X-linked mental retardation.

Gene	Reference	OMIM	Function
Genes involved in only non-syndromic XLMR.			
AGTR2	(Vervoort et al. 2002)	+300034	Dephosphorylation of mitogen-activated protein kinase
ARHGEF6	(Kutsche et al. 2000)	*300267	RhoGTPase Pathway
DLG3	(Tarpey et al. 2004)	+300189	Synaptic vesicle component
FACL4 (ACSL4)	(Meloni et al. 2002)	*300157	Long chain fatty acid CoA ligase
FMR2	(Gecz 2000)	+309548	Putative transcription transactivation
FTSJ1	(Freude et al. 2004)	*300499	Methylase
GDI	(D'Adamo et al. 1998)	+300104	RhoGTPase Pathway
IL1RAPL1	(Carrie et al. 1999)	*300206	Interleukin 1 receptor accessory protein-related
NLGN3	(Jamain et al. 2003)	300336	Synaptic vesicle component
NLGN4	(Jamain et al. 2003)	300427	Synaptic vesicle component
PAK3	(Allen et al. 1998)	*300142	RhoGTPase Pathway
RPL10	(Klauck et al. 2006)	312173	Transcription regulatory protein
TM4SF2	(Zemni et al. 2000)	*300096	Control of neurite outgrowth
ZNF41	(Shoichet et al. 2003)	+314995	Transcription factor
ZNF674	(Lugtenberg et al. 2006)	+300573	Transcription factor
ZNF81	(Kleefstra et al. 2004)	*314998	Transcription factor

Genes involved in both syndromic and non-syndromic XLMR			
AP1S2	(Tarpey et al. 2006)	300630	Assembly of endocytic vesicles
ARX	(Stromme et al. 2002)	300382	Aristaless-related homeobox gene
ATRX	(Guerrini et al. 2000)	300032	Chromatin remodelling
FGD1	(Lebel et al. 2002)	305400	Cdc42-specific GDP-GTP exchange factor.
HUWE1	(Turner et al. 1994)	-	E3 ubiquitin-protein ligase
MECP2	(Meloni et al. 2000; Orrico et al. 2000; Klauck et al. 2002)	300005	Transcription repression
OPHN1	(Billuart et al. 1998)	300127	Repression of the Rho signalling pathway to maintain dendritic spine length
PQBP1	(Kalscheuer et al. 2003)	300463	Transcriptional activator
RPS6KA3 (RSK2)	(Merienne et al. 1999)	300075	Chromatin remodelling
SLC16A2	(Friesema et al. 2004)	300523	Thyroid hormone transporter
SLC6A8	(Salomons et al. 2001)	300036	Sodium- and chloride-dependent creatine transporter 1
SMCX	(Jensen et al. 2005)	314690	Transcriptional repressor
SYN1	(Garcia et al. 2004)	313440	Regulation of neurotransmitter release
UPF3B	(Tarpey et al. 2007)	300676	mRNA nuclear export and mRNA surveillance

However, it is not always easy to discern between syndromic and non-syndromic forms of MR as several genes have been shown to be involved in both (Kerr et al. 1991; Frints et al. 2002) indicating that there is no reliable molecular basis for strictly distinguishing between genes for syndromic and non-syndromic MR. However, as the possibilities for classifying families through molecular studies improve, and as patients are examined in more detail, it can be expected that the proportion of syndromic cases that are diagnosed will increase, while at the same time the number of non-syndromic cases will shrink correspondingly (Ropers and Hamel 2005).

1.3. Autosomal forms of mental retardation

As severely retarded individuals are unlikely to reproduce, the vast majority of patients with autosomal dominant mutations must be sporadic, and familial cases must be extremely rare. This has greatly hampered the identification of genes for autosomal dominant MR, and there are no reliable data on its prevalence.

Up to now, studies aiming to identify causative gene defects have mostly focused on recurrent MR syndromes with recognizable dysmorphic features. Smith-Magenis syndrome and Rubinstein-Taybi syndrome are examples of such conditions, and the single genes that are sufficient to cause these phenotypes have been identified by systematic deletion mapping and point mutation analysis (Petrij et al. 1995; Slager et al. 2003; Baptista et al. 2005). Other clinically recognizable autosomal MR syndromes such as Williams-Beuren syndrome, Cohen syndrome or Angelman syndrome have a much lower frequency in all MR patients (Roeleveld et al. 1997; Leonard and Wen 2002; Rauch et al. 2006).

Although functional considerations as well as epidemiological data suggest that ARMR is more common than X-linked and autosomal dominant forms of MR which appear to include 8-10% of moderate to severe MR cases (Ropers 2007), the molecular basis of non-syndromic ARMR (NS-ARMR) is still poorly understood.

To date, only three genes have been found to be directly linked to NS-ARMR. These genes are PRSS12 (neurotrypsin [MIM 606709]), a trypsin-like serine protease (Molinari et al. 2002), CRBN (cereblon [MIM 609262]), an ATP-dependent Lon protease (Higgins et al. 2004) and CC2D1A [MIM 610055] (Basel-Vanagaite et al. 2006).

Neurotrypsin is a synaptic serine protease. It cleaves the extracellular proteoglycan agrin redominantly at or in the vicinity of synapses, resulting in increased concentrations of agrin fragments and decreased full-length agrin at synapses (Stephan et al. 2008).

Cereblon, belongs to an Adenosine 5'-triphosphate-dependent Lon protease gene family represented by multi-domain enzymes associated with diverse functions from proteolysis to membrane trafficking (Jo et al. 2005).

CC2D1A is a protein which is highly homologous to the rat Freud-1 which is a repressor element of the 5-HT1A receptor gene (Ou et al. 2003). Freud-1 negatively regulates basal 5-HT1A receptor expression in neurons via binding to the repressor element of the 5-HT1A receptor gene and is inactivated by calcium/calmodulin-dependent protein kinase-mediated phosphorylation (Ou et al. 2000; Ou et al. 2003). Therefore, disruption of the CC2D1A protein is expected to lead to an upregulation of 5-HT1A receptor expression. Studies indicate that 5-HT1A receptors are important in dendritic maturation in the hippocampus and in the control of adult neurogenesis (Yan et al. 1997; Brezun and Daszuta 1999). It has been shown that activation of the 5-HT1A receptors can impair learning and memory (Buhot et al. 2000; Yasuno et al. 2003).

In western civilizations, most patients with ARMR are sporadic cases, due to small family sizes and low rates of parental consanguinity, and pedigrees with several affected sibs are rare, which has precluded linkage analysis and gene mapping.

In contrast, up to 40% of all children are born to consanguineous parents in Iran, and large families are very common. Therefore, the structure of the Iranian population is ideal for homozygosity mapping of autosomal recessive traits. In 2003, this has prompted two groups from Iran and Germany to embark on a collaborative project aiming at the systematic identification of genes that have a role in ARMR. This thesis reports on the first 48 ARMR families recruited and analysed in the course of this large-scale collaborative study.

1.4. Kainate receptors (KARs), a subset of ionotropic glutamate receptors

Fast excitatory neurotransmission in the mammalian nervous system is mainly mediated by glutamate. Glutamate acts as the transmitter at most excitatory synapses and is involved in the induction of long-lasting changes in the efficacy of neurotransmission, which is thought to be cellular correlates of memory formation. Glutamate has also a pivotal role during the ontogeny of the nervous system, in the formation, outgrowth and elimination of synapses as well as in the activity dependent fine tuning of exquisitely precise patterns of connectivity in several brain areas (Lerma et al. 2001).

Alterations of glutamatergic neurotransmission have been related to the neuronal damage observed after episodes of ischemia and hypoglycemia, as well as to various neurological conditions including epilepsy, Alzheimer's disease and Chorea Huntington. Therefore, it is not surprising that ionotropic glutamate receptors, cationic channels responsible for converting the synaptic release of the amino acid into an immediate neuronal response, are among the most studied and best-understood molecules of the nervous system (Jonas and Monyer 1999).

Glutamate receptors are integral membrane proteins, which are responsible for mediating information transfer at most excitatory synapses in the brain. Ionotropic glutamate receptors belong to three receptor families, which have been named after their preferred ligands: N-methyl-D-aspartate (NMDA receptors or NMDARs), Alpha-amino-3-hydroxy-5-methyl-4-isoxazole propionic acid (AMPA receptors or AMPARs), and Kainate (KA receptors or KARs; Lerma 2006).

Kainic acid was first isolated from seaweed more than 50 years ago and was known, together with domoic acid, to cause amnesic shellfish poisoning. By the mid-1970s, the excitatory and neurotoxic actions of kainate were well established and the hypothesis that this compound acts on a specific subset of receptors was formulated (Watkins and Evans 1981). This was supported by the demonstration of high-affinity binding sites for [3H] kainate in the rat brain (London and Coyle 1979) and of distinct

depolarizing and desensitizing responses to kainate in C-fibres of the dorsal root ganglia (DRG; Agrawal and Evans 1986; Huettner 1990).

Similarly to the AMPARs and NMDARs, KARs are tetrameric combinations of five subunits: GLUR5, GLUR6 and GLUR7 that can associate and form functional homomeric receptors both in vitro (Cui and Mayer 1999; Paternain et al. 2000) and in vivo (Mulle et al. 2000; Christensen et al. 2004). Additional subunits are KA1 and KA2 that can, however, only form part of a functional receptor when coassembled with at least one of the GLUR5-GLUR7 subunits (Chittajallu et al. 1999; Lerma et al. 2001).

GLUR5, GLUR6 and GLUR7 subunits form functional homomeric receptor-channels activated by kainate and glutamate when expressed in heterologous systems and show an affinity for kainate in the range of 50–100 nM ("low-affinity" subunits; Egebjerg et al. 1991; Sommer et al. 1992; Schiffer et al. 1997). KA1 and KA2 subunits show high-affinity [3H]Kainate binding, with dissociation constants in the range of 5–15 nM (Werner et al. 1991; Herb et al. 1992). There is 75%–80% homology between GLUR5, GLUR6 and GLUR7, and 68% between KA1 and KA2, whereas these two subclasses of Kainate receptors (high-affinity versus low-affinity subunits) share just 45% homology. KAR subunits display less than 40% homology with the AMPAR subunits GLUR1-4 and do not co-assemble with these subunits.

KARs are tetrameric assemblies of subunits that have a structure similar to those of the other ionotropic glutamate receptors (iGLURs; Dingledine et al. 1999). They are transmembrane proteins with an extracellular N-terminal domain followed by a first transmembrane domain and a "p-loop" that dips into the lipid bilayer and forms part of the pore. Two other successive transmembrane domains are connected by an extracellular loop and are followed by an intracellular sequence containing C-terminus (Figure 1-1A).

Cells from different regions of the brain express distinct subsets of KAR subunits (Wisden and Seeburg 1993) that display distinct pharmacological and electrophysiological properties (Wilding and Huettner 2001).

The mRNAs coding for KARs are subject to post-translational modifications of editing and/or alternative splicing (Bettler and Mulle 1995; Lerma 2003; Jaskolski et al. 2005). All splice variants of KARs, with the exception of a GLUR5 isoform, which contains an alternative 15-amino-acid exon in the N-terminal domain, differ in their cytoplasmic C-terminal domain. Two main splice variants of GLUR6 have been described, GLUR6a and GLUR6b (Gregor et al. 1993).

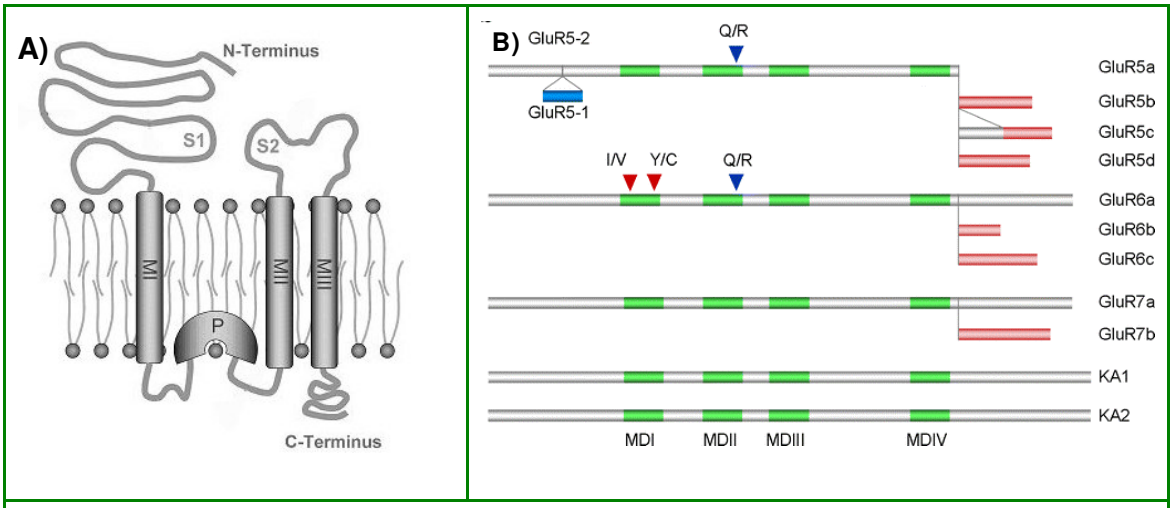

Figure 1-1: Kainate receptors and their subunits: A) Schematic view of Kainate proteins. The subunit topology is conserved with AMPA and NMDA receptor subunits (Motazacker et al. 2007). B) Subunits of KARs. Splice variants and editing sites (Pinheiro and Mulle 2006).

These are expressed in the same brain regions and co-assemble in native receptors (Coussen et al. 2005). A third variant, GLUR6c, contains an insertion of the C-terminal exon 15 and has only been described in human (Barbon et al. 2001; Jamain et al. 2002; Figure 1-1B).

For all the C-terminal splice variants, a stretch of 16 amino acids just behind the last transmembrane domain is conserved between GLUR5, GLUR6 and GLUR7. The physiological properties of the KAR subtypes do not appear to be affected by alternative splicing of the C-terminal domains; however, these modifications have a strong impact on intracellular trafficking and regulatory processes of Kainate receptors and their interacting partners (Schiffer et al. 1997; Jaskolski et al. 2004; Coussen et al. 2005). GLUR5 and GLUR6 can also be edited at a Q/R

(glutamine/arginine) site in the second membrane domain (Figure 1-1B) and this determines the extent to which KARs allow the permeation of Ca^{2+} ions. In analogy with the GLUR2 AMPA receptor, the presence of an arginine residue results in receptors that have low permeability to Ca^{2+}, whereas the presence of a glutamine residue leads to receptors with higher Ca^{2+} permeability (Burnashev et al. 1995). These different ion permeation properties are correlated with the blockage of calcium influx by intracellular polyamines at positive potentials, leading to inwardly rectifying current-voltage relationships for unedited receptors and linear current-voltage relationships for edited receptors (Bowie and Mayer 1995; Bahring et al. 1997). With GLUR6, in addition to the Q/R site, Ca^{2+} permeability is also dependent on the edited state of two other codons in the first transmembrane domain: the I/V (isoleucine/valine) and the Y490C (tyrosine/cysteine) sites (Figure 1-1B; Kohler et al. 1993). Fully edited GLUR6 subunits are essentially impermeable to Ca^{2+}. Fully unedited receptors also show a higher unitary conductance compared with receptors that include one or more edited subunits (Howe 1996; Swanson et al. 1996).

KARs are distributed in higher brain structures, such as the amygdala and related cortical areas (Hollmann and Heinemann 1994; Li and Stys 2001). In the hippocampus, KARs contribute to presynaptic regulation and postsynaptic responses to repetitive stimulation (Frerking and Nicoll 2000; Kullmann 2001; Huettner et al. 2002; Lerma 2003). Low to moderate activation of KARs enhances while strong KAR activation reduces synaptic transmission (Schmitz et al. 2001).

A prominent feature of AMPA and KARs is profound desensitization in response to glutamate. This is thought to protect the neuron from overexcitation. Stabilization of the binding domain dimer by generation of intermolecular disulfid bonds not only blocks desensitization of GLUR6 but also drastically reduces surface expression of nondesensitizing mutants independent from channel activity. This proposes an interacellular role for desensitization in controling maturation and traffiking of GLUR6 in addition to its role at the synapse (Priel et al. 2006). Furthermore the GLUR6 Y490C L752C dimer has shown relaxation from the active conformation, which is not sufficient to trigger desensitization (Weston et al. 2006).

1.5. KAR synaptic localization and function

KARs are present both at pre- and post-synaptic sites (Figure 1-2).

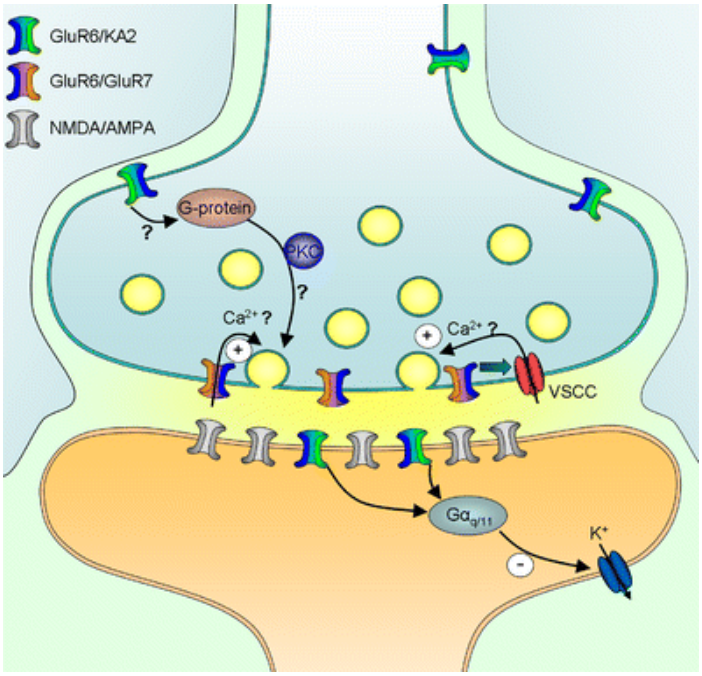

Figure 1-2: Schematic and hypothetical representation of the mechanisms of action of presynaptic and postsynaptic KARs (*PKC* protein kinase C, *VSCC* voltage-gated Ca^{2+} channels). This representation takes the mossy fibre synapse as an example. Presynaptic KARs acting as autoreceptors are probably localized close to the synaptic release site where they function as fast facilitatory receptors, either by a direct influx of Ca^{2+} through the Kainate-receptor channel or through depolarization of the presynaptic membrane. Heterosynaptic KARs are thought to be localized at some distance from the neurotransmitter release site, are activated by the diffusion of glutamate from its source and act with a slower time course to facilitate or depress synaptic transmission. Activation of postsynaptic KARs generates an EPSC (excitatory post synaptic current) with integrative properties that leads to the cumulative depolarization of the postsynaptic membrane and induces a down-regulation of the slow after hyperpolarizing current (I_{sAHP}), leading to an increase in neuronal excitability (Pinheiro and Mulle 2006).

The first evidence for the existence of postsynaptic KARs has come from observations at synapses between mossy fibers and CA3 pyramidal cells in the hippocampus (Castillo et al. 1997). In the presence of antagonists for both AMPA

(GYKI 53655) and NMDA receptors, a slow excitatory post synaptic current (EPSC) can be recorded in response to the stimulation of mossy fibers. Because this slow EPSC can be inhibited by CNQX (6-cyano-7-nitroquinoxaline-2,3-dione), it is reported to be mediated by KARs. CNQX is a compound from the quinoxalinedione family and acts as a competitive antagonist on native and recombinant KARs and exhibits little selectivity for KARs over AMPARs (Mayer et al. 2006).

KARs composed of at least GLUR6 and KA2 (Mulle et al. 1998; Contractor et al. 2003) are involved in mossy fiber EPSCs (excitatory post synaptic currents). The analysis of GLUR6–/– mice has further demonstrated that the GYKI-resistant EPSCs are mediated by KARs (Mulle et al. 1998; Figure 1-3). KAR-mediated EPSCs have also been observed in GABAergic interneurons of the CA1 region (Cossart et al. 1998; Frerking et al. 1998), in cerebellar Golgi cells (Bureau et al. 2000), in Purkinje cells (Huang et al. 2004), in both pyramidal cells and interneurons of the neocortex (Kidd and Isaac 1999; Ali 2003; Eder et al. 2003; Wu et al. 2005), in the superficial dorsal horn of the spinal cord (Li et al. 1999), in “Off” bipolar cells of the retina (DeVries and Schwartz 1999) and in the basolateral amygdala (Li and Rogawski 1998).

Glutamatergic synapses in hippocampal CA1 pyramidal cells (Bureau et al. 1999), medium spiny neurons of the dorsal striatum and nucleus accumbens (Chergui et al. 2000; Casassus and Mulle 2002) and possibly many other neuronal populations do not display KAR-mediated EPSCs, although functional postsynaptic KARs can be activated pharmacologically in these cell types. Thus postsynaptic KARs show restricted cellular and subcellular expression.

At mossy fiber synapses, presynaptic KARs are probably composed of GLUR6 and GLUR7 and might be located in the presynaptic active zone close to a glutamate release site (Figure 1-3). Their activation triggers either depolarization of the nerve terminal or direct Ca^{2+} influx that may lead to Ca^{2+} release from intracellular stores.

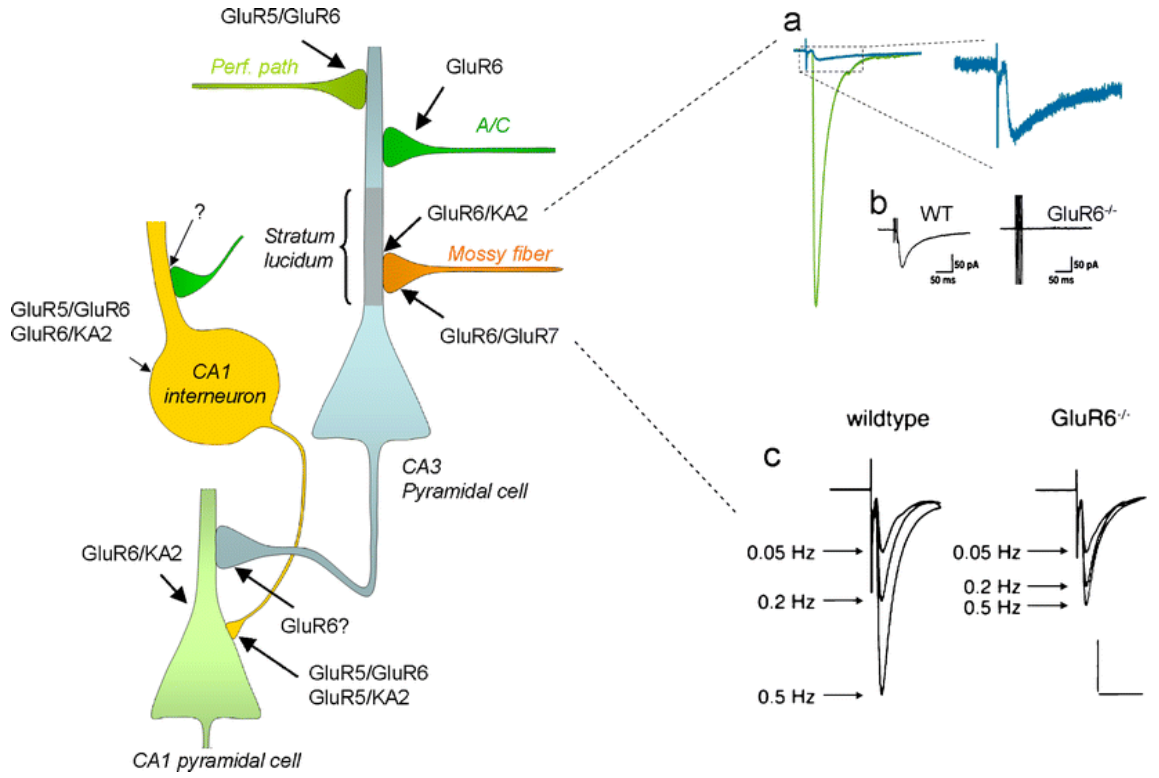

Figure 1-3: ***Left*** Schematic representation of the expression and subcellular localization of KARs in the network of hippocampal CA3 neurons. ***Right*** a) Mossy-fibre-mediated EPSCs affected by AMPA receptors (green) and by KARs (blue; enlarged upper right). b) A train of mossy fibre stimuli evokes a compound EPSC mediated by KARs, which is absent in GLUR6$^{-/-}$ mice (Mulle et al. 1998). c) The role of presynaptic KARs in frequency facilitation of mossy-fibre-mediated EPSCs. Increasing the stimulation frequency from 0.05 Hz to 0.5 Hz markedly increases the amplitude of mossy fibre EPSCs in wild-type but not in GLUR6$^{-/-}$ mice. These experiments demonstrate that presynaptic KARs are implicated in synaptic facilitation (Contractor et al. 2001); Whole figure taken from (Pinheiro and Mulle 2006).

Presynaptic KARs are involved in long term potentiation (LTP) (Henze et al. 2000), a form of plasticity that is induced and expressed presynaptically in mossy fibers. Presynaptic KARs are not essential for mossy fiber LTP but strongly influence it by changing the induction threshold, possibly by their direct facilitatory effect on synaptic transmission (Schmitz et al. 2003).

1.6. KAR interaction partners

Kainate-receptor-interacting proteins are involved in the trafficking, synaptic localization and modulation of the properties of KARs. Like other glutamate receptors, KARs contain a PDZ [post synaptic density protein (PSD-95), Drosophila disc large tumor suppressor (DlgA), and zonula occuldens-1 protein (zo-1)]-binding motif at their C-terminus that can bind to prototypic PDZ-domain-containing proteins such as PSD-95, SAP97 and SAP102. In heterologous systems, the binding of GLUR6a to PSD-95 causes the clustering of KARs (Garcia et al. 1998; Mehta et al. 2001; Coussen et al. 2002). Interestingly, the moderate specificity in the association of KARs with this family of proteins may dictate the subcellular localization of the receptors; both SAP90 and SAP102 can associate with KA2 and GLUR6 but the presynaptically localized SAP97 has been found only to associate with GLUR6 (Garcia et al. 1998). The PDZ-domain-containing proteins PICK1, GRIP and syntenin also associate with several subunits of KARs (Hirbec et al. 2003), but none of them is specific for this class of receptors. These proteins differentially regulate the function and synaptic stability of Kainate and AMPA receptors. However, PSD-95, PICK1 and GRIP do not seem to play any role in the exit from the endoplasmic reticulum (ER) of either GLUR5 or GLUR6 (Ren et al. 2003; Jaskolski et al. 2004). The association between GLUR6a and PSD-95 might also play an important role in triggering excitotoxicity, by initiating the formation of a complex with MLK2/3 proteins eventually leading to the activation of c-Jun N-terminal kinase (JNK) (Savinainen et al. 2001).

KARs can also bind to beta-catenin and proteins of the cadherin/catenin complex through an indirect interaction with the extreme C-terminus of GLUR6. Activation of the cadherin/catenin complex, in conditions mimicking the establishment of cell-cell contacts in heterologous cells, triggers the recruitment of GLUR6a. Overexpression of PSD-95 appears to disrupt the interaction between GLUR6a and the cadherin/catenin complex. This sequence of events suggests that interactions with cadherin/catenin complexes play an initial role in recruiting and stabilizing KARs at the synaptic membrane during synapse formation (Coussen et al. 2002).

Although the two splice variants GLUR6a and GLUR6b do not significantly differ in their functional properties, they can co-assemble into the same heteromeric complex

in native and recombinant receptors, bringing different sets of interacting cytosolic proteins into close proximity (Coussen et al. 2005). The set of proteins identified by a proteomic approach as interacting with GLUR6a/GLUR6b includes dynamin-1, NSF, dynamitin and 14-3-3 protein, which are possibly involved in the assembly and trafficking of membrane receptors, and also spectrin and profillin II, which may participate in cytoskeletal organization. GLUR6b also interacts with a group of proteins including calcineurin, calmodulin (Coussen et al. 2005), VILIP-1 and VILIP-3 (Burgoyne and Weiss 2001), which are involved in the regulation of receptors and ion channels by Ca^{2+}. Given the apparent complexity of the processes of kainate-receptor trafficking and polarized targeting in neurons, additional still unknown protein interaction partners are probably involved in these processes.

1.7. KAR trafficking

The relative level of surface expression of KARs depends on subunits and alternative splicing of their C-terminal domain and on subunit composition of heteromeric receptors. Some subunit splice variants are endowed with a forward trafficking motif, whereas others are strongly retained in the ER by intracellular retention signals (Figure 1-4).

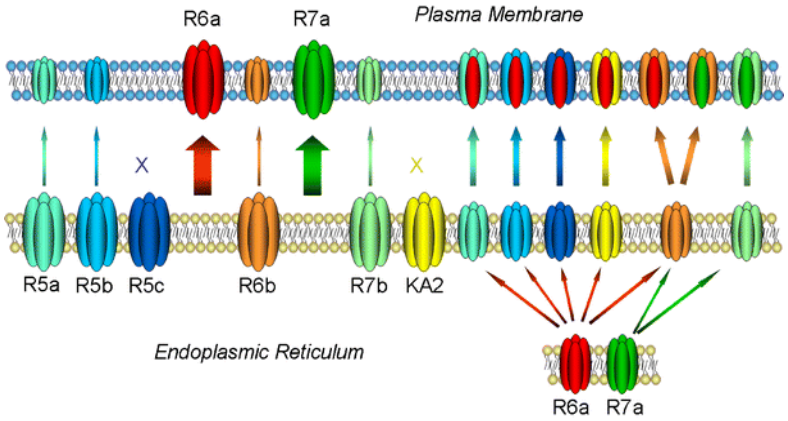

Figure 1-4: Trafficking of KARs: Exit from the endoplasmic reticulum and targeting of KARs to the plasma membrane depends on the composition in terms of subunits and splice variants (Pinheiro and Mulle 2006).

GLUR5, GLUR6 and GLUR7 can form functional homomeric receptor channels and have multiple isoforms derived from alternative splicing and RNA editing. These isoforms display different patterns of expression at the plasma membrane, strongly depending on the alternative splicing at their C-terminus (Ren et al. 2003; Jaskolski et al. 2004). GLUR6a and GLUR7a are expressed at high levels in the plasma membrane and can promote the surface expression of other subunits that contain ER retention motifs (Jaskolski et al. 2004; Yan et al. 2004; Jaskolski et al. 2005), because of the existence of a forward trafficking motif in their C-terminal portion. This stretch of positively charged amino acids (CQRRLKHK) is crucial for ER exit but, when mutated, the receptors can nevertheless reach the plasma membrane if associated with other receptors containing the intact sequence. The molecular mechanisms by which the CQRRLKHK motif acts as a forward trafficking signal are not known. The other subunit splice variants studied (GLUR5a, GLUR5b, GLUR6b, GLUR7b) are present at low levels at the plasma membrane when expressed as homomers. Cis-acting regulatory elements encoded within the C-terminal domain of Kainate-receptor subunits affect the trafficking and surface expression of these receptors. Contrary to findings from NMDA receptor subunits, these processes are not regulated by C-terminal PDZ-binding domains of KARs (Ren et al. 2003; Jaskolski et al. 2004; Yan et al. 2004). In addition, it has been demonstrated that the N-terminal domain of KARs also plays an important role in their trafficking and surface expression and the formation of an intact glutamate-binding site has been suggested to act as a quality control measure for the forward trafficking of intracellular KARs (Fleck et al. 2003; Mah et al. 2005; Valluru et al. 2005).

The surface expression of glutamate receptors is dynamically regulated. GLUR6-containing receptors are subject to rapid endocytosis followed by sorting to either recycling or degradation pathways, depending on the endocytic stimulus. In cultured hippocampal neurons, while exogenous Kainate causes a PKC-dependent internalization of KARs targeted to lysosomes for degradation, NMDA triggers a Ca^{2+}-, PKA- and PKC-dependent endocytosis of KARs to early endosomes for recycling to the plasma membrane (Martin and Henley 2004).

1.8. Pathophysiological roles of KARs

So far, no disease causing mutation has been reported in the *GRIK2* gene, but associations between *GRIK2* polymorphisms and several disorders such as autism, Huntington disease, schizophrenia and epilepsy, have been studied, as briefly summarized below.

GRIK2 and autism

A transmission disequilibrium test (TDT)-based study has shown association between *GRIK2* and autism in 174 Chinese Han parent-offspring trios (Shuang et al. 2004). The analysis, performed in 51 affected sib pair (ASP) families and in an independent data set of 107 parent-offspring trios, indicated a significant *GRIK2* maternal transmission disequilibrium (TDT all P = 0.0004). Another TDT analysis with only one affected proband per family has also shown significant association between *GRIK2* and autism (TDT association P = 0.008; (Jamain et al. 2002). The most prominent change found in this cohort of autistic patients was an amino acid change (M867I) in a highly conserved domain of the intracytoplasmic C-terminal region of the protein (Strutz-Seebohm et al. 2006). However, although a gain of function (an increase in current amplitudes) was reported for the M867I allele, no explanation has been given for the fact that this change is not only present in 8% of the autistic subjects but also in 4% of the control population.

GRIK2 and Huntington disease (HD)

A variety of experimental data suggests that glutamate excitotoxicity may play a role in the pathology of HD (Feigin and Zgaljardic 2002). Changes in three genes encoding glutamate receptor subunits have been reported to be associated with HD: *GRIK2* (Rubinsztein et al. 1997; MacDonald et al. 1999; Chattopadhyay et al. 2003), *GRIN2B* (Arning et al. 2005), and *GRIN2A* (Arning et al. 2005). Association between the age of onset of HD with a $(TAA)_n$ triplet repeat polymorphism in the 3' untranslated region of *GRIK2*, has been reported for English, New England, Eastern

Indian, French and Italian populations (Rubinsztein et al. 1997; MacDonald et al. 1999; Naze et al. 2002; Chattopadhyay et al. 2003; Cannella et al. 2004). Still, despite the robustness of this association in several populations, the result of an additional study with 359 HD patients in a cohort of 629 Venezuelan individuals was inconclusive (Andresen et al. 2007).

GRIK2 and Schizophrenia

In multiple genome-wide scanning studies, schizophrenia susceptibility was mapped to 6q21–q22.3 (Cao et al. 1997; Kaufmann et al. 1998; Martinez et al. 1999). In addition, a significant decrease of *GRIK2* mRNA expression level has been reported in schizophrenic brains (Porter et al. 1997). This evidence suggests *GRIK2* as a candidate gene for schizophrenia susceptibility. Even though association for a microsatellite in the untranslated region of *GRIK2* with the disease could not be established (Chen et al. 1996) there is still the possibility that the susceptibility locus lies in other parts of the gene since its size (~700 kb) by far exceeds the average range of linkage disequilibrium (LD) reported for the human genome (60 kb;Reich et al. 2001).

Study of 15 SNPs evenly distributed in the entire *GRIK2* region has not shown any association with schizophrenia in a cohort of 100 Japanese patients (and 100 controls; (Shibata et al. 2002). In contrast, evaluation of *GRIK2* transmission in 356 schizophrenic patients has indicated a maternal transmission disequilibrium ($p= 0.05$; Bah et al. 2004).

GRIK2 and Obsessive Compulsive Disorder (OCD)

No association has been observed between *GRIK2* polymorphisms and OCD in a case-control study comprising156 patients and 141 controls nor in a transmission disequilibrium test including 124 parent-offspring trios. However in this study, the *GRIK2* allele (M867I), which is also associated with autism has been transmitted less

often than expected ($p < 0.03$), which could indicate a functional role for this variant (Delorme et al. 2004).

GRIK2 and Idiopathic Generalized Epilepsies (IGEs)

Classical studies have shown that systemic or intracerebral injections of kainate in rodents cause seizures and epileptiform discharges in the hippocampus that propagate to other limbic structures. The finding that submicromolar concentrations of kainate generate epileptogenic effects in slice preparations in the CA3 region, an area enriched with high-affinity kainate-binding sites, is highly suggestive that KARs (and not AMPARs that are also activated by kainate) are primarily responsible for the epileptogenic action of kainate (Ben-Ari and Cossart 2000). In the absence of selective ligands for KARs, the direct demonstration of their involvement has come from the use of $GLUR6^{-/-}$ mice, which proved to be resistant to epileptic seizures induced by Kainate injection. In these mice, high-affinity kainate binding sites in the hippocampus and activation of currents by submicromolar concentrations of kainate were abolished (Mulle et al. 1998). The lack of GLUR6 prevents both kainate-induced gamma oscillations and epileptiform bursts in slice preparations (Fisahn et al. 2004). Conversely, over-expression of fully edited GLUR6a in the hippocampus by viral delivery rapidly leads to seizures and spontaneous bursting in vitro (Telfeian et al. 2000). Finally, mice engineered to express unedited GLUR6 have been found to be more vulnerable to Kainate-induced seizures, either because of enhanced GLUR6-mediated currents or because of increased Ca^{2+} permeability (Vissel et al. 2001). The high levels of Kainate-receptor expression in CA3 pyramidal cells (Wisden and Seeburg 1993; Bureau et al. 1999) and their recurrent connectivity render this region especially sensitive to the epileptogenic effects of kainate.

However, linkage and association analyses in 63 families with juvenile myoclonic epilepsy, juvenile absence epilepsy, or childhood absence epilepsy using *GRIK2* 3' untranslated region polymorphism suggest that allelic variants of *GRIK2* are not involved in the expression of the common familial IGEs (Sander et al. 1995).

1.9. Aim of the study

MR patients need life-long medical care, which puts a heavy psychological as well as financial burden not only on the affected families but also on society as a whole. In fact it can amount to as much as 25% of the total health care budget of a society (Polder et al. 2002). Although autosomal recessive forms of MR may be responsible for a large proportion of MR cases (Ropers 2007) only 3 genes have been implicated in NS-ARMR to date.Therefore, the first objective of this study was to identify new loci for NS-ARMR, by performing large-scale homozygosity mapping in numerous consanguineous Iranian families with a minimum of two affected children, and to rule out the possibility that there are common genes for non-syndromic ARMR in this populationSecond, homozygous intervals carrying novel genes for NS-ARMR were screened for potentially relevant sequence variants, and finally, functional studies were performed to verify the pathogenetic relevance of these changes and to shed light on the underlying functional mechanisms.

2. Patients, Materials and Methods

2.1. Patients

Families with a minimum of two mentally retarded children were identified through collaboration with local genetic counselors in several provinces of Iran. A subset of 48 families whose pedigree patterns and clinical data seemed to be compatible with moderate to severe NS-ARMR were selected and visited by experienced clinical geneticists, or invited to the Genetics Research Centre in Tehran. Patients and unaffected relatives were examined in a standardized way using a questionnaire (see appendix 1), and photographs were taken to document physical findings. The clinical geneticists assessed the mental status of the probands by monitoring their verbal and motor abilities, by interviewing the parents about developmental milestones and, in a minority of cases, by using more sophisticated tests such as a modified version of the Wechsler Intelligence Test for children or adults. After obtaining written consent from the parents, blood was taken and DNA was isolated using a standard salting out method (see section 2.3.2.1) from all mentally retarded individuals, the parents and as many of the unaffected sibs as possible, particularly in smaller families with closely related (first cousin) parents. For one patient of each nuclear family, Fragile X testing was carried out by PCR and Southern blot analysis, especially if X-linkage could not be excluded (Najmabadi et al. 2006). Filter-dried blood of one patient per family was screened by tandem mass spectrometry to exclude disorders of the amino acid, fatty acid (e.g. phenylketonuria) or organic acid metabolism (Chace et al. 2003; Wilcken et al. 2003). Standard 450 G-band karyotyping was also performed in order to exclude cytogenetically visible chromosomal aberrations.

2.2. Materials

2.2.1. General reagents

Table 2-1: Chemicals	
Chemical	**Supplier**
[α-32P]dCTP	Amersham Biosciences
Acrylamide (Molecular biology grade)	Sigma
Agarose	Invitrogen
Ammonium persulfate	Sigma
Ampicillin	Sigma
Aqua ad inectabilia	Baxter
Betaine	Sigma
Bromophenol Blue	Sigma
BSA	Sigma
Chloroform	Merck
Chloroform	Sigma
Complete, Mini Protease Inhibitor Cocktail Tablets	Roche
DAPI	Serva
Diethylpyrocarbonate (DEPC)	Aldrich
DMSO	Sigma
dNTPs	Roth
Dreamfect Cell transfection reagent	OZ bioscience
EDTA	Merck
Ethanol	Merck
Ethidium bromide	Serva
First strand buffer 5x	Merk
Formaldehyde-37.0% (v/v)	Fluka Biochemika
Formamide	Fluka Biochemika

Glycerol	Roth
Glycin	Merck
HEPES	Calbiochem
Herring sperm DNA	Roche
Hybridime human placental DNA	HT Biotechnology
Hydrogen Chloride	Merck
Kanamycin	Invitrogen
L-Glutamine (200 mM/ml)	Cambrex
Magnesium chloride	Merck
Methanol	Merck
Milk powder	Protifar
Northern blot hybridization buffer	Ambion
OptiMEM	Invitrogen
Penicillin-Streptomycin (10000 U/ml Pen., 10 mg/ml Strep.)	Cambrex
PFA (Paraformaldehyde)	Merck
Phenol	Sigma
Polyethylenglycol (PEG)	Merck
Poly-L-Lysine aqueous solution (0.1 w/v)	Sigma
Ponceau S dye	Invitrogen
Potassium Chloride	Sigma
SDS	Roth
Sodium Acetate	Sigma-Aldrich
Sodium Chloride	Roth
Sodium Hydroxide	Merck
Sodium Hydroxide	Sigma
Sodium perchlorate	Merck
Sodium triphosphate	Merck
TEMED	Gibco BRL

Triton X100	Invitrogen
TRIzol reagent	Gibco BRL
Trypsin EDTA (500 mg/ml Trypsin, 200 mg/ml EDTA)	Cambrex
Tween 20	Invitrogen
Whatman paper	Sigma
β-mercaptoethanol	Whatman

2.2.2. Buffers and Media

Table 2-2: Buffers and Media

Buffer/Medium	Composition
APS 10%	10% w/v APS in water, aliqouted and stored at –20°C
Blocking buffer	5% milk powder in PBST
DEPC H2O	0.1% DEPC was overnight stirred in water and autoclaved afterwards.
DMEM	From Cambrex + 10% FCS + 100 U/ml Penicillin + 100 µg/ml Streptomycin + 2 mM L-Glutamine
DNA re-suspension buffer	0,4M Tris-HCl PH=8, 0.06M NaEDTA, 0,15M NaCl
DNA-Loading buffer	15% Ficoll, 0,25% Bromphenolblue in bidest H_2O
Ethidium bromide	10 mg/ml EtBr in bidest H_2O
Fetal Calf Serum (FCS)	Sigma
First strand buffer 5x	250 mM Tris-HCl (pH 8.3 at room temperature), 375 mM KCl, 15 mM $MgCl_2$
Inverse PCR ligation buffer	50 mM Tris-Hcl pH=7.4, 10 mM $MgCl_2$, 10 mM DTT, 1 mM ATP, 10% gelatin
Laemmli protein loading buffer (5X)	Aqueous solution containing 62.5 mM Tris HCl (pH 6.8), 5% beta-mercaptoethanol (v/v), 50% Glycerol (v/v), 2% SDS (w/v), 0.1% (w/v) Bromo phenol Blue.
Lymphoblastoid cell lines	RPMI-1640 containing 10.0% (v/v) FBS; 100 U/ml Penicillin; 68.6 µM Streptomycin; 2.00 mM L-Glu.
MOPS 10 x	0,4 M MOPS; 0,1 M NaAc; 10 mM EDTA pH 7,0
Northern blot running	2.2 M formaldehyde, 1x MOPS in DEPC H2O

buffer	
Northern blot sample buffer	50% formamid, 2.2M formaldehyde, 1x MOPS, 40 µg/ml Ethidium Bromide
Northern blot wash buffer	2x SSC / 0.1% SDS
PBS 1 x buffer	137 mM NaCl; 2,7 mM KCl; 10,1 mM Na2HPO4; 1,8 mM KH_2PO_4
PBST buffer	1 x PBS; 1:1000 Tween 20
Ponceau Red solution	2% (w/v) Ponceau S dye, 5% (v/v) Acetic acid
RPMI 1640	From Cambrex + 10%FCS + 100 U/ml Penicillin + 100 µg/ml Streptomycin + 2 mM L-Glutamine
SDS-PAGE running buffer (1X)	196 mM glycine, 0.1% SDS, 50 mM Tris-HCl (pH 8.3)
Western blot Separating gel buffer	1,5 M Tris-HCl, 0,4 % SDS pH 8,8
Southern blot denaturing buffer	1.5M NaCl + 0.5M NaOH
Southern blot wash buffer	40 mM Na_3PO_4 + 0.5% SDS
SSC 10x	3M NaCl, 0,3M Na-citrate in bidest H2O, adjust pH 7 with 1M HCl
Stacking gel buffer	0,5 M Tris-HCl, 0,4 % SDS pH 6,8
Stripping buffer	1% SDS, 20 mM TRIS/HCl (pH 6.8), 1% (v/v) β-Mercaptoethanol
TAE buffer 50 x	50 mM EDTA, 5,71% v/v acetic acid, 2M Tris-HCl
TBE buffer	0.1 M Tris, 0.1 M boric acid, 2 mM EDTA
TBS	20 mM Tris, 150 mM NaCl
TBST buffer	20 mM Tris, 150 mM NaCl. 0.1% (w/v) Tween-20
TE	10 mM Tris-HCl pH 7,5; 1 mM EDTA
WB Transfer buffer 1x	5x blotting buffer: Methanol: bidest H_2O 1:1:3
Western Blot Blotting buffer 5x	29,11g Tris; 14,65g Glycin; 18,75 ml SDS in 1L bidest water

2.2.3. Instruments

Table 2-3: Instruments	
Instrument	**Manufacturer**
B 5050 E incubator	Heraeus
Capillary Sequencer ABI 377	Applied Biosystems
Centrifuge 5810R	Eppendorf
Centrifuge Rotanta 46R/Rotina 4R	Hettich zentrifugen
Centrifuge Rotina 48R	Hettich zentrifugen
Clean bench Herasafe	Heraeus
CO_2 water jacketed incubator	Forma Scientific
Concentrator 5301	Eppendorf
Control environment incubator shaker	New Brunswick Scientific
E.A.S.Y. 440K Gel Documentation System	Herolab
Electrophoresis power supply 2	Heathkit
Geiger Counter, Series 900 mini-monitor	Artisan Electronics Corp.
Hamilton syringe	Hamilton
Horizontal gel apparatus Horizon® 11.14 and 20.25	Life technologies
HyperCassette BioMAX (Northern blot)	Amersham
Inverted light microscope, Eclipse TS100	Nikon
L8-70M ultracentrifuge	Beckmann
Laminar flow hood, CA/REV 6 Cleanbench	Clean Air
Mini-Gel apparatus	Bio-Rad
Multichannel pipette	Rainin
Phase lock gel light	Eppendorf
pH-meter	Knick
Pipett boy	Integra biosciences
Pipettes	Gilson
Power Pac 300 electrophoresis power supply	Bio-Rad

PTC-225 Tetrad and Dyad thermal cycler	Bio-Rad
REAX 2000 vortexer	Heidolph
Rnase ZapWipes	Ambion
Rotating mini hybridization oven	Appligene
Rotors TLA120.1, TLS-55, SW40	Beckmann
Scanner, Expression 1680 Pro	Epson
Sonifier cell disruptor B-30	Branson Sonic Power
Sorvall RC-5B refrigerated super speed centrifuge	Du Pont instrument
Southern blot cassette (HyperCassette)	Amersham
SPD 111V Speed Vac	Savant
Spectrophotometer NanoDrop ND-1000	PEQLAB
Steri-cycle CO_2 incubator 371	Thermo Electron Corp.
Table centrifuge 5415C	Eppendorf
ThermoForma 758 Ultrafreezer	Thermo Electron Corp.
Thermomixer 5436	Eppendorf
TL100 ultracentrifuge	Beckmann
UV stratalinker 1800	Stratagene
UV trasilluminator	UVPinc
Western blot cassette (HyperCassette)	Amersham
Western blot Trans Blot SD	Bio-Rad
X-ray film developing machine, Curix 60	Agfa

2.2.4. Consumables (Disposable materials)

Table 2-4: Consumables (disposable materials)

Name	**Supplier**
Adhesive PCR film	Abgene
Biomax MS X-ray film (sensitive)	Kodak

Cell culture flask (75 & 100 cm^2)	TTP
Cell scraper	TTP
Chromatography paper	Whatman
Disposable reaction tube 14 ml	Greiner BioOne
Disposable reaction tube 30 ml	Sarstedt
Falcon tube	Greiner BioOne
Glass coverslip	Menzel-Gläser
Hybond-N+ (Southern blot membrane)	Amersham
Hybond-XL (Northern blot membrane)	Amersham
Immobilon-P transfer membrane (Western blot membrane)	Millipore
MS Photographic film	Kodak
MS X-ray film	Kodak
Parafilm	Pechiney Plastic Packaging
Pasteur pipette	Roth
PCR plate (96 well)	Abgene
Pipette tip (0.1 – 10, 1-20, 20 – 200 & 1000 µl)	Biozyme
Reaction tube (1.5 & 2 ml)	Eppendorf
Scalpel	Aesculap
Serological pipette (2, 5, 10 & 25 ml)	Corning
Superfrost Plus glass slide	Menzel-Gläser

2.2.5. Kits and markers

Table 2-5: Kits and Markers

Name	**Supplier**
0.24-9.5 Kb RNA ladder	Invitrogen
1 kb DNA ladder	Roth
BigDye Terminatormix	Applied Biosystems

Bio-X-ACT (Bioline) PCR Kit	Bioline
DC protein assay kit	BIO-RAD
Dithiothreitol (DTT)	Invitrogen
Dynabeads Oligo (dT)25 kit	DYNAL Biotech
ECL kit	Amersham Biosciences
Expand Long Template PCR system kit	Roche
FastPlasmid Mini kit	Eppendorf
GeneChip® Human Mapping 10K Array and Assay Kit	Affymetrix
Human Fetal Brain Total RNA	BD Bioscience
Hyper Ladder I	Bioline
Hyper ladder IV	Bioline
Lambda DNA/*Hind*III marker	Fermentas
Micro Spin G-50 column	Amersham
MiniElute PCR purification kit	Qiagen
Oligo(dT)12-18 primer	Invitrogen
Oligo(dT)20 primer	Invitrogen
PENTR directional TOPO cloning kits	Invitrogen
pENTR/D-TOPO Directional TOPO cloning kit	Invitrogen
Pinpoint cell surface protein isolation kit	Pierce
pUC Mix marker, 8	Fermentas
QIAquick Gel Extraction Kit	QIAGEN
QuickChange site-directed mutagenesis kit	Stratagene
Random Primers	Promega
SDS-PAGE protein marker - High range	Sigma
Taq PCR core kit	Qiagen
TOPO TA Cloning kit for sequencing	Invitrogen

2.2.6. Plasmids

Table 2-6: Plasmids	
Plasmid	**Supplier**
Modified pcDNA-DEST47	Received from Dr. Kalscheuer
pENTR/D-TOPO	Invitrogen
pCR4-TOPO	Invitrogen

2.2.7. Antibodies

Table 2-7: Antibodies		
Primary antibody	**Supplier**	**Dilution, time, Temperature**
Anti GLUR6/7, Clone NL9 Ab.	Upstate	1:2000, 1h, Room T.
GAPDH monoclonal Ab. (HRP. Conjugated)	Abcam	1:1000, 1h, Room T.
Mouse monoclonal alpha-tubulin Ab. (DM1A)	Sigma	1 :400, 1h, Room T.
panCadherin Ab.	Abcam plc	1:2000, 1h, Room T.
Secondary antibody		
Alexa Fluor® 488 chicken anti-mouse	Invitrogen	1:1000, 1h, Room T.
Alexa Fluor® 488 chicken anti-rabbit	Invitrogen	1:1000, 1h, Room T.
Donkey Anti-Mouse HRP	Diavona	1:1000, 1h, Room T.
Donkey Anti-Rabbit HRP	Amersham	1:2000, 1h, Room T.

2.2.8. Enzymes

Table 2-8: Enzymes	
Enzymes	**Supplier**
*Bgl*II restriction enzyme (10 U/µl)	NEB
DNA polymerase 1, Klenow fragment	USB

*EcoR*V restriction enzyme	NEB
Gateway LR Clonase Enzyme Mix	Invitrogen
Proteinase K	Fermentas
Rnase-Free DNase	Promega
RNAsin	Promega
SuperScript III Reverse Transcriptase	Invitrogen
T4 DNA ligase	Promega

2.2.9. Software

Table 2-9: Software

Name	Application and Source
Allegro	Parametric linkage analysis http://www.decode.com/software/allegro
Alohomora	Conversion Tool http://gmc.mdc-berlin.de/alohomora/
CodonCode	sequence assembly, contig editing and mutation detection. http://www.codoncode.com/
GCG package	DNA sequences analysis http://www.accelrys.com/products/gcg/
GeneHunter	Parametric and non-parametric linkage analysis http://www.broad.mit.edu/ftp/distribution/software/genehunter/
GRR	Pedigree based relationship evaluation http://www.sph.umich.edu/csg/abecasis/GRR/
Haplopainter	Visualization of haplotypes created by GeneHunter or Merlin http://haplopainter.sourceforge.net/html/ManualIndex.htm
Merlin	Non-parametric linkage analysis http://www.sph.umich.edu/csg/abecasis/Merlin/download
PedCheck	Finding mendelian errors and unlikely genotypes http://watson.hgen.pitt.edu/register

STADEN package	DNA sequences analysis http://portal.litbio.org/Registered/Option/staden.html
Zeiss LSM image examiner	Provided with Zeiss laser scanning microscope

2.2.10. Bioinformatic databases and web-based tools

Table 2-10: Bioinformatic databases and tools

Databse	Type	Internet Address
European Bioinformatics Institute, Hinxton, UK and The Wellcome Trust Sanger Institute, Hinxton, UK	Ensembl	http://www.ensembl.org
ExPaSy	Proteomics Server	http://www.expasy.org/
GenBank	Genome database	http://www.ncbi.nlm.nih.gov/Genbank/
Genome Bioinformatics Group, University of California, Santa Cruz, CA, USA	Genome Browser, Blat Search, PCR	http://genome.ucsc.edu/
National Center for Biotechnology Information, Bethesda, MD, USA	PubMed, UniGene, Nucleotide, Blast Search	http://www.ncbi.nlm.nih.gov/
Online Mendelian Inheritance in Man (OMIM)	Database of human genes and genetic disorders	http://www.ncbi.nlm.nih.gov/Omim
POSMED	Positional cloning gene ranking	http://omicspace.riken.jp/PosMed/
Primer3	Primer design	http://frodo.wi.mit.edu/cgi-bin/primer3/primer3_www.cgi
Webcutter	DNA restriction map	http://rna.lundberg.gu.se/cutter2/

2.3. Methods

2.3.1. Linkage analysis methods

The aim of genetic mapping is to determine how often two chromosome locations (two polymorphisms, two genes, two loci or a disease locus and a marker) are separated by meiotic recombination.

In order to determine linkage, informative meioses are required. A meiosis is informative for linkage when we can identify whether or not the gamete is recombinant (Strachan and Read 2004). The proportion of gametes that are recombinant for two chromosomal locations is the recombination fraction between these two locations (θ):

$$\theta = \text{Recombination fraction} = \frac{\text{Recombinant meioses}}{\text{Recombinant M.} + \text{Nonrecombinant M.}}$$

Recombination fraction values vary between 0 and 0.5. Ten meiosis are sufficient to give evidence of linkage if there are no recombinants for the given markers.

The probability of linkage is the ratio between the overall likelihood given linkage and the likelihood given no linkage:

$$\text{Odds of linkage} = \frac{\text{Likelihood if recombination fraction } \theta=\theta_1}{\text{Likelihood if recombination fraction } \theta=0.5}$$

The generally accepted measure for the likelihood of linkage between genetic loci is the LOD score, the logarithm to the base 10 of the odds of linkage.

All LOD scores at θ = 0.5 are zero because they are then measuring the ratio of two identical probabilities, and log (1) = 0. Positive LOD scores give evidence in favor of linkage while negative LOD scores argue against linkage. LOD score 3 is the threshold for accepting linkage, with a 5% chance of error. Linkage is rejected if the LOD score is less than –2 and values between –2 and +3 are inconclusive (Strachan and Read 2004).

Recombination rarely separates loci that lie very close together on a chromosome, because only a crossover located precisely in the small space between the two loci can create recombinants. Therefore sets of alleles on the same small chromosomal segment tend to be transmitted as a block through a pedigree. Such a block is known as a haplotype.

Human genetic mapping depends on “markers”. A marker is any polymorphic Mendelian character that can be used to follow a chromosomal segment through a pedigree. It helps if the marker can be scored easily and cheaply using readily available material (e.g. blood cells) but more crucial is that it should be sufficiently polymorphic that a randomly selected person has a good chance of being heterozygous. An overview over human genetic markers is shown in Table 2-11.

Table 2-11: Development of human genetic markers. (Strachan and Read 2004)

Type of marker	No. Of Loci	Features
Blood groups (1910-1960)	~ 20	May need frech blood, rare antisera Genotype not always inferred from phenotype because of dominance
Electrophoretic mobility variants of serum proteins (1960-75)	~30	May need fresh serum, specialized assays, limited polymorphism
HLA tissue types (1970-)	1 (Haplotype)	One linked set, highly informative, can only be tested for linkage to 6p21.3
DNA RFLPs (1975-)	> 10^5 (potentially)	Two allele markers, maximum heterozygosity 0.5, initially required Southern blotting but no PCR, Easy physical localization
Minisatellites (VNTRs) (1985-)	> 10^4 (potentially)	Many alleles, highly informative, type by Southern blotting, easy physical localization, tend to cluster near end of chromosomes
Microsatellites (STRs) (1989-)	> 10^5 (potentially)	Many alleles, highly informative, type by automated multiplex PCR, easy physical localization, Distributed throughout genome
Single Nucleotide Polymorphisms (SNPs)	> 4 x 10^6	Less informative than Microsatellites, Can be typed on a very large scale by automated equipments without gel electrophoresis

When the linkage between 2 markers is evaluated, it is referred to as two-point linkage analysis. But in linkage analysis using genome wide genetic markers, data for more than two loci are analyzed simultaneously, a procedure called multi-point linkage analysis. The relative order of these loci and the distance between them may be extracted from a genetic map. Thus, upon multipoint linkage analysis, the likelihood of the pedigree data is sequentially calculated for any position of the disease gene within a known map of markers. The hypothesis of linkage between the disease gene and map of markers is compared to the hypothesis that the disease gene and the markers constituting the map are unlinked. Multipoint linkage analysis helps overcome problems caused by the limited informativeness of markers.

If these calculations are carried out under the assumption of a specific mode of inheritance for the trait locus, linkage analysis is referred to as parametric. In contrast, non-parametric linkage analysis does not require a genetic model and is based on shared chromosomal segments in affected individuals. In this study, both approaches were used to analyze the NS-ARMR families and to determine the location of disease loci.

Individuals with rare recessive diseases in consanguineous families are likely to be autozygous for all markers in the vicinity of the disease locus. Autozygosity means homozygosity for marker alleles that are identical by descent, i.e. inherited from a recent common ancestor (Figure 2-1).

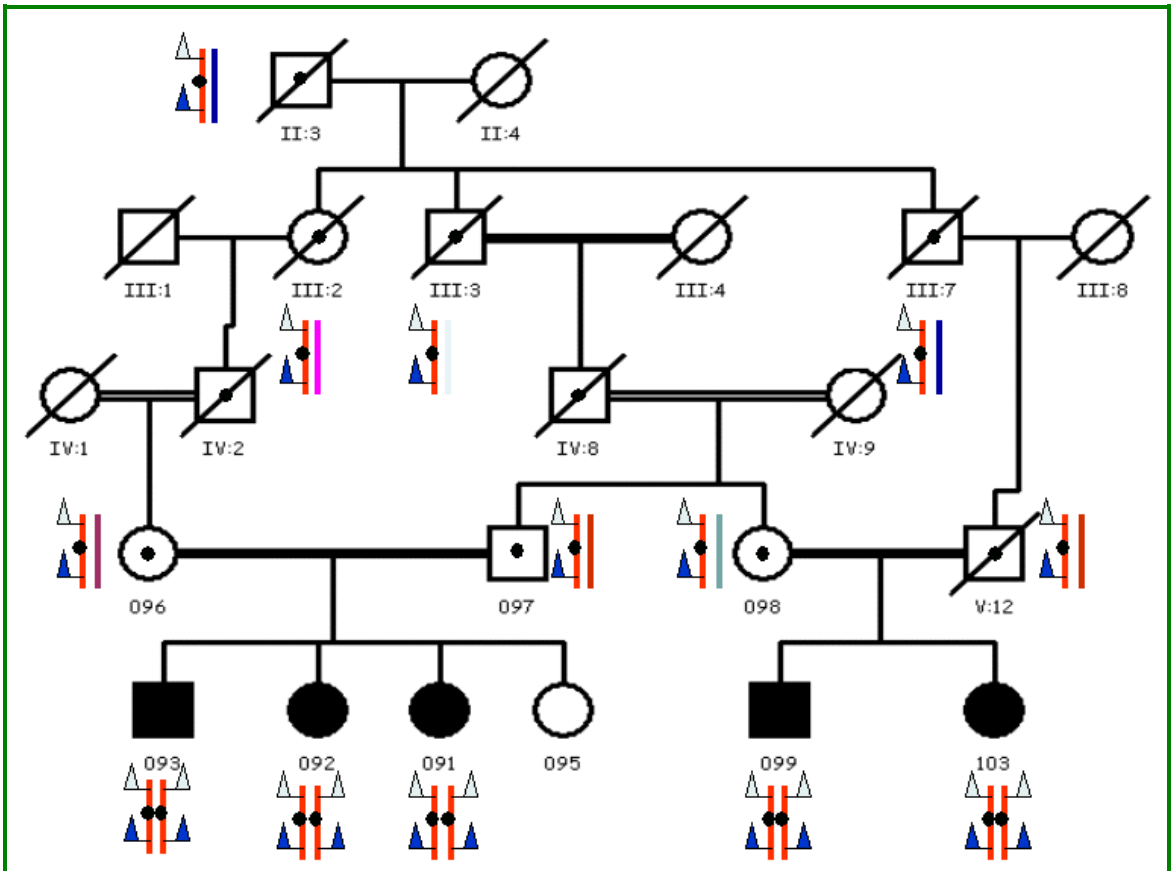

Figure 2-1: Autozygosity in consanguineous families with autosomal recessive conditions. Segregation of a mutation (back circle) and its linked neighbouring markers (small flags) is shown in a consanguineous family with ARMR. Consanguinity loops give a great value to the pedigree information. If the frequency of the mutant allele is 0.001, the probability of the existence of 4 carrier parents in the presence of consanguinity is 2 x 10^{-6} versus 10^{-12} in the absence of consanguinity in this pedigree. By searching for regions of autozygosity, it is possible to obtain information on the chromosomal location of the mutation.

Autozygosity mapping is a very powerful tool if applied to multiple affected individuals with the same condition in two or more related sibships. For example, the genetic causes of autosomal recessive hearing loss and benign recurrent intra-hepatic cholestasis have been identified by autozygosity mapping (Houwen et al. 1994; Chaib et al. 1996).

2.3.1.1. Pitfalls of linkage analysis

Standard linkage analysis is a powerful method for scanning a genome to find disease loci, but it can also run into difficulties. Two major difficulties are:

- Vulnerability to errors: These errors can occur during sample preparation (e.g. mis-labeling, sample swap), genotyping (due to mis-hybridization or wrong SNP detection), phenotype evaluation (which might happen when a trait does not have a complete penetration or when the phenotype in the affected individuals is not distinct from unaffecteds), mode of inheritance assumption and pooling information (e.g. for a trait with locus heterogeneity). Use of quality control software can help in detection sample mixups or genotyping errors. Detailed clinical evaluation of the family members helps to reduce phenotype related errors.

- Computational limits as to the size of pedigrees that can be analysed: Despite the great increase in the calculation power of the computers during the last decade, it is still very time consuming if not impossible to analyse linkage for large pedigrees. Analysis of split pedigree information is a way to tackle limitations in computing power.

2.3.1.2. Whole genome SNP typing

For each individual, whole genome SNP typing was performed with the Affymetrix Human Mapping 10 K Array Version 2 (Kennedy et al. 2003) according to previously described protocols (Matsuzaki et al. 2004). This oligonucleotide microarray allows to genotype a total of 10,204 SNPs in a single experiment. The GeneChip® Mapping Assay uses a simple approach for reducing complexity of the genome, allowing efficient genotyping with a microarray containing over 10,000 SNPs. The experimental steps are outlined in Figure 2-2.

Total genomic DNA (250ng) was digested with the restriction enzyme *Xba*I and ligated to adapters that recognize the cohesive four base pair (bp) overhangs. All fragments resulting from the restriction enzyme digestion, regardless of size, were used as substrates for adapter ligation. A generic primer that recognizes the adapter

sequence was used to amplify adapter ligated DNA fragments. PCR conditions have been optimized to preferentially amplify fragments in the 250 to 1,000 bp size range. The amplified DNA was then fragmented, labeled, and hybridized to the GeneChip Mapping 10K Array.

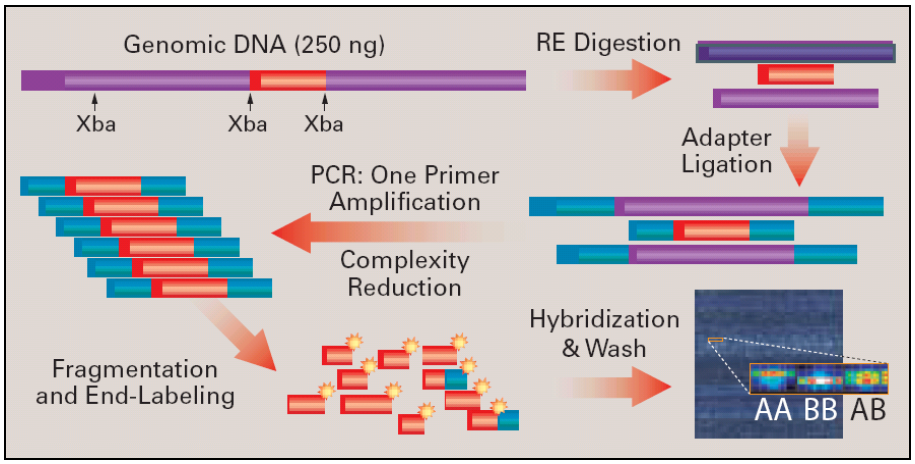

Figure 2-2: GeneChip ® mapping assay overview (from Affymetrix website).

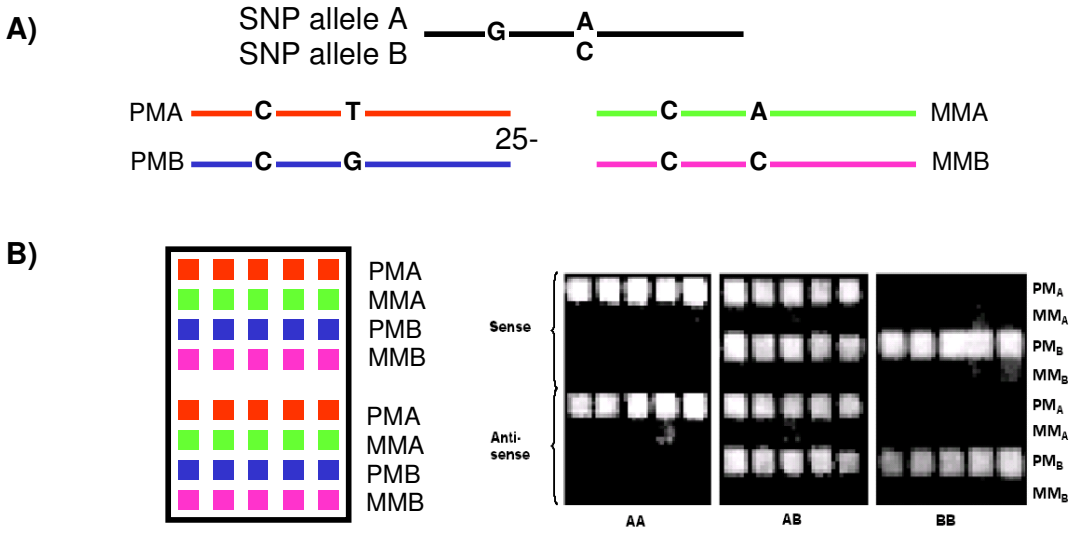

Figure 2-3: A) Design of mismatch and perfect match oligos for each SNP. PM: Perfect match (Specific for each allele) MM: Mismatch (one mismatch in the center of PM oligo). **B) Example of Allele-Specific Hybridization with 40 probes** (Hybridization figure and content taken from Affymetrix GeneChip® Human Mapping 10K Array manual, Affymetrix website).

For each SNP, 40 different 25 bp oligos are tiled on the chip to increase specificity. Perfectly matching oligos are specific for each allele and mismatch oligos have one mismatch in the center of perfect match sequence. In an optimal hybridization condition, only perfect match oligos can hybridize to their respective alleles and lack of hybridization with mismatch oligos indicates the specificity of hybridization. An example of allele specific hybridization is shown in Figure 2-3B. Each SNP lies within one of the 250 to 1,000 base *Xba*I fragments amplified by the Mapping Assay. The median physical distance between SNPs is approximately 105 kb, and the average distance between SNPs is 210 kb. The average heterozygosity of these SNPs is 0.37. Detailed specifications of Affymetrix Human Mapping 10 K Array are given in Table 2-12.

Table 2-12: Affymetrix Human Mapping 10 K Array Critical Specifications

DNA Required	250 ng per sample
Number of SNPs on Array	11,555
Call Rate	>90%
Reproducibility	99.96%
Concordance	Concordance >99.6%
Genotype Calling	Automated with quality score
SNP Annotation	NetAffx™ Analysis Center
PCR Primers	1 per sample
PCR Reactions	4 per sample
Capital Equipment	Standard Affymetrix® Instrument Platform

2.3.1.3. Data conversion

The ALOHOMORA software (Ruschendorf and Nurnberg 2005) was used to convert Affymetrix GeneChip® Human Mapping 10K Array SNP genotype data together with pedigree and SNP allele frequency data into input files suitable for downstream software such as GRR, PedCheck, Allegro, GeneHunter and Merlin.

2.3.1.4. Examination of pedigree data for consistency with genotypes

Prior to linkage analysis, elimination of all Mendelian inconsistencies in the pedigree data is essential. Errors at this stage can come from sample mix-up, non-paternity or wrongly called genotypes.

Therefore, the program PedCheck (O'Connell and Weeks 1998) was implemented in order to detect Mendelian errors with four error-checking algorithms. The applications of these algorithms range from simple parent-offspring-compatibility checks to a single-locus likelihood-based statistic that identifies and ranks the individuals most likely to be in error. If more than 1% of the investigated SNPs indicating Mendelian errors, the sample genotype was excluded from linkage analysis.

In addition, the software GRR (graphical representation of relationship errors; Abecasis et al. 2001) was used to verify relationships between individuals in a given pedigree. The correct genetic relationship between any two individuals defines a specific pattern of allele-sharing between them. The details of this pattern can be complex, and depend on the exact type of relationship, marker characteristics, population history and inbreeding. Unlike other approaches, GRR does not require specification of allele frequencies or any other population parameter. It is robust, tolerates a small number of random errors in the data and can be applied to large inbred samples. In addition to relationship misspecification, GRR can detect some other problems such as sample duplications and switches. The method is defined as follows: First, classify each pair of individuals according to their assumed relationship (such as sib-pairs, parent–offspring pairs, unrelated individuals, etc.). Second,

calculate the mean and variance of identical-by-state allele sharing over a number of polymorphic loci for each pair of individuals. If the sample is homogeneous, each group is expected to display a characteristic pattern of allele sharing. For example, sib-pairs are expected to share more alleles on average than unrelated individuals, while parent–offspring pairs (which have exactly 50 percent of their genetic material in common) are expected to show less variability in allele sharing than sib-pairs (which may share zero, one or two copies of each chromosome pair).

GRR then offers a convenient way to identify individuals with patterns of allele sharing that are inconsistent with their specified relationship by coloring code and plotting the mean-variance statistics. Relationships whose mean variance does not fit to the assumed category can be considered as falsely classified.

2.3.1.5. Data formatting for linkage analysis

Pedigree information was prepared in a tab-delimited text file as shown in Figure 2-4A and B.

A)

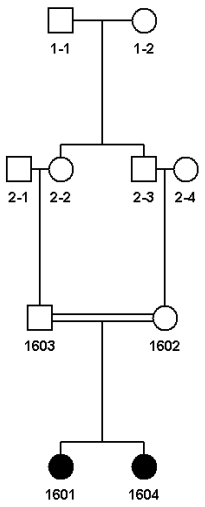

B)

PID	IID	FID	MID	SEX	AS
M090	1-1	0	0	1	1
M090	1-2	0	0	2	1
M090	2-1	0	0	1	1
M090	2-2	1-1	1-2	2	1
M090	2-3	1-1	1-2	1	1
M090	2-4	0	0	2	1
M090	1603	2-1	2-2	1	1
M090	1602	2-3	2-4	2	1
M090	1601	1603	1602	2	2
M090	1604	1603	1602	2	2

C)

SNP ID	1601	1602	1603	1604
SNP_A-1513509	AB	BB	AB	AB
SNP_A-1518411	AB	AB	AB	NoCall
SNP_A-1511066	AA	AA	AA	AA
SNP_A-1517367	BB	AB	BB	BB
⋮	⋮	⋮	⋮	⋮

D)

CHR	Affymetrix ID	deCODE_Gen_Map	Position
01	SNP_A-1509443	3.422940287	2882121
01	SNP_A-1518557	5.678250775	3985402
01	SNP_A-1517286	8.05555011	4804829
⋮	⋮	⋮	⋮

E)

SNP_ID	freq. A	freq. B	Heterozygosity
SNP_A-1513509	0.371	0.629	0.467
SNP_A-1513556	0.580	0.420	0.487
SNP_A-1518411	0.199	0.801	0.319
SNP_A-1511066	0.891	0.109	0.194
SNP_A-1517367	0.764	0.236	0.361
SNP_A-1512567	0.460	0.540	0.497
SNP_A-1519604	0.811	0.189	0.307
SNP_A-1507932	0.261	0.739	0.386
SNP_A-1519685	0.365	0.635	0.464
⋮	⋮	⋮	⋮

Figure 2-4: Data formatting for linkage analysis. A) An example pedigree and B) its representative pedfile used for linkage analysis ; PID : Pedigree ID, IID : Individual ID, FID : Father ID, MID : Mother ID, AS : Affection Status , C) Excerpt from genotyping data file , D) Excerpt from genetic map file ; CHR : Chromosome, Gen_Map : Genetic map , E) Excerpt from allele frequency file, freq. A : frequency of allele A, freq. B : frequency of allele B.

Genotype information was delivered in a text file that contains SNP IDs in one column followed by the genotype for each sample in a tab-delimited separate column (Figure 2-4C). The genetic Map file was provided by deCODE (Figure 2-4D), the

allele frequency file for the Caucasian population was provided by Affymetrix (Figure 2-4E).

2.3.1.6. Parametric and non-parametric linkage analysis

For parametric linkage analysis, the Allegro V1.2 (Gudbjartsson et al. 2000) and GeneHunter V2.1 (Kruglyak et al. 1996) software were applied, and non-parametric linkage analysis was performed using GeneHunter and Merlin (Abecasis et al. 2002).

Allegro, GeneHunter and Merlin use the Lander-Green algorithm and have a pedigree size restriction per analysis (2n-f<16: where “f” and “n” are the number of founders and non-founders respectively). With this algorithm, the time required for the calculation will increase exponentially with the number of individuals, and linearly with the number of markers, missing data have only a modest effect on calculation time.

2.3.1.7. Graphical haplotype reconstruction

For easy visualization of the complex haplotype information that resulted from the analysis of genome-wide high-density SNP marker panels, the software Haplopainter V.027b (Thiele and Nurnberg 2005) was used. It is a pedigree-drawing application, which has been developed to facilitate gene mapping in Mendelian diseases in terms of fast and reliable definition of the smallest critical interval harbouring the underlying gene defect.

2.3.2. Nucleic acid methods

2.3.2.1. DNA isolation from immortalized lymphoblastoid cells

As a permanent source of material for DNA, RNA or protein studies, lymphoblastoid cell lines were established from at least one affected individual per family (in Family M097, cell lines were established for 5 affected and 2 healthy siblings). Pellets containing 10^8 cells from these cell lines were frozen at -80°C and used for DNA, RNA or protein isolation. Information about the medium that was used to culture lymphoblastoid cell lines is given in Table 2-2.

For DNA isolation, 10^8 EBV-transformed lymphocytes were resuspended in buffer solution. The tube was then vortexed until the cell pellet was completely dissolved. The solution was incubated for 1h at 37°C after adding 30 µl RNase A (10 mg/ml). Subsequently, 5 ml Sodium perchlorate were added and the tube was inverted 10-15 times. 20 ml ice-cold Chloroform were then added under the extractor hood and the tube was again inverted 10-15 times before centrifuging at 4000U/min for 10 min.

The upper phase was transferred to a new tube with a glass Pasteur pipette. An equal volume of ice-cold ethanol (100%) was added to the tube and the DNA was precipitated by inverting the tube several times. The DNA was then transferred to a 1.5 ml Eppendorf tube using a plastic loop and centrifuged in 7500 U/min for 1 min after adding 1 ml cold ethanol (70%). The supernatant ethanol was removed and this step repeated with 500 µl ethanol. The DNA was then dried at room temperature (or alternatively at 50°C) and subsequently dissolved in an appropriate amount of Tris-EDTA (TE) buffer. The DNA concentration was then measured using a Nanodrop Spectrophotometer (Table 2-3).

2.3.2.2. RNA extraction from lymphoblastoid cell lines

Total RNA was isolated from lymphoblastoid cells using the following protocol:

A cell pellet (5 x 10^7 cells) was resuspended in 10 ml Trizol reagent in a 30 ml RNase free tube and was vortexed vigorously for 5 min at room temperature.

After adding 2 ml Chloroforom, the tube content was again mixed vigorously for 15 sec and was kept at room temperature for 2-3 min, before it was centrifuged with 5000 rpm at 4℃ for 20 min.

The supernatant was then removed and mixed with 5 ml Isopropanol in a new tube and kept at room temperature for additional 5-10 min before it was centrifuged at 10000 rpm at 4℃ for 10 min.

The upper phase was discarded and RNA was precipitated from the lower phase by adding 10 ml 70% Ethanol and centrifuging with 10000 rpm at 4℃ for 5 min.

The supernatant was removed and the pellet dried at room temperature, then dissolved in 500 µl DEPC-H_2O, (10 min on ice) and heated at 65℃ for 5 min.

The RNA concentration and purity was measured using a Nanodrop spectrophotometer (Table 2-3).

This total RNA was used for direct cDNA synthesis or for mRNA isolation using a Dynabeads Oligo$(dT)_{25}$ kit based according to the manufacturer's instructions.

2.3.2.3. cDNA synthesis

cDNA was synthesized following the procedure shown in Table 2-13.

Table 2-13: Conditions and material for cDNA synthesis from total RNA/mRNA

Prepare reaction mix as follows:	
Random primers	50-250ng (4 µl)
RNA	4 µg (10 µl)
10 mM dNTPs	2 µl
H2O	Up to 28 µl
Heat-shock reaction mix at 65℃ for 5 min	
Put reaction mix on ice for at least 1 min	
Add 5x first strand buffer to the mix	8 µl

Add 0.1M DTT to the mix	2 µl
Add *RNaseOut® to the mi	1 µl
Add SuperScriptIII® reverse transcriptase to the mix	2 µl
Put reaction tube at 25℃ for 5 min	
Put reaction tube at 50℃ for 1h	
Put reaction tube at 70℃ for 15 min	

* Necessary if initial RNA concentration is less than 50 ng/µl

In order to verify the success of the cDNA synthesis, control PCR reactions were carried out using primers for HUWE1, a gene located on chromosome X, with exon spanning primers CAAGTGAGGAAAAGGGCAAA (exon64) and GTTCATGAGCTGCCCCAGT (exon65), which give rise to a 568 bp amplicon.

2.3.2.4. Polymerase Chain Reaction (PCR)

PCR reactions were carried out in order to amplify DNA fragments for further sequencing, cloning or other downstream applications.

All PCR reactions were performed according to the conditions shown in Table 2-14 using either the Taq PCR core kit or Expand Long Template PCR system kit.

Table 2-14: Touchdown polymerase chain reaction program

	Temp	Time	Cycle number
Initial denaturation	94℃	2 min	1x
Denaturation	94℃	30 sec	
Annealing	65℃ >> 55℃*	30 sec	20x
Extension	72℃	30 sec**	
Denaturation	94℃	30 sec	
Annealing	55℃	30 sec	30x
Extension	72℃	30 sec**	
Final extension	72℃	10 min	1x

*Annealing temperature was reduced 0.5℃ after each cycle

** 1 min extension time was considered for each 1000 bp

The primers used for mutation screening, sequencing and cDNA amplification are listed in supplementary data A.

2.3.2.5. Agarose gel electrophoresis

DNA or RNA fragments were separated and visualized by agarose gel electrophoresis. The gel composition was 1% agarose (Invitrogen) in TBE buffer (Table 2-2) supplemented with 0.5 µg/ml Ethidium-bromide. At least 0.2 volumes of gel loading buffer containing 0.25% Bromophenol blue, 0.25% Xylene cyanol FF, and 30% Glycerol were added to the nucleic acid solutions before loading into the wells. HyperLadder IV, pUC mix 8 or Lambda DNA/*EcoR*I+*Hind*III were used as size markers. Gels were run at 100 V for 30-45 min. Nucleic acids were visualized and pictures taken using the E.A.S.Y Win32 gel documentation system (Herolab).

2.3.2.6. Sequencing

Sequencing was performed according to the Sanger sequencing method with fluorescently labeled didesoxynucleotides. Quality and quantity of PCR products/clones were evaluated by agarose gel electrophoresis and spectrophotometry (if necessary, amplicon bands were excised from the agarose gel and purified using the Qiagen MiniElute PCR purification kit). The labeling reaction was carried out using the BigDye Terminatormix (Applied Biosystems; Table 2-15 and Table 2-16) and the primers used for PCR product amplification.

Table 2-15: PCR reaction mix for sequencing reaction

Name	Amount
Primer (10pmol)	1 µl
BigDye Terminator mix	2 µl
DNA (PCR Product)	10 ng/100bp
DNA (Plasmid)	150-200 ng
H2O	10 µl
Total volume	20 µl

Table 2-16: PCR conditions for sequencing reaction			
	Temperature	**Time**	**Cycle number**
Initial denaturation	96°C	3 min	1x
Denaturation	96°C	10 sec	
Annealing	Primer ann. °C	5 sec	25x
Extension	60°C	4 min	

For DNA precipitation, 25 µl absolute EtOH (room temperature) were mixed with the sequencing reaction. The mixture was then incubated for 1h at room temperature and subsequently centrifuged for 1h at 4000 rpm (Eppendorf 5810R). The supernatant was carefully removed and the pellet was washed twice with 150 µl 70% EtOH. Samples were then centrifuged at 4000 rpm for at least 15min. After the second washing step, the pellets were dried by centrifugation of the tubes in an inverted position at 500rpm (samples were stored at -20°C if they were not immediately analysed). Electrophoresis and base calling were done by the "Sequencing Service Group" of the Max-Planck-Institute for Molecular Genetics using an ABI 377 DNA sequencer.

2.3.2.7. Northern blot analysis

Membrane preparation:

Prior to loading, a voltage of 60V for 10 min at room temperature was applied to a 1% agarose gel, which was prepared with Northern blot running buffer (Table 2-2).

The RNA was mixed with northern blot sample buffer (Table 2-2), denatured (65°C, 5 min) and kept on ice before loading onto the gel. Electrophoresis was carried out (~16h, 50V/~30mA).

The gel was afterwards soaked in DEPC H2O for 20 min in order to remove formaldehyde before it was photographed using a UV sensitive ruler (0 cm of the ruler placed beside loading wells) in order to permit subsequent band localization.

The gel was then soaked in 10x SSC for 20 min.

The blotting setup for transferring RNA onto the Hybond-XL membrane was prepared as shown in Figure 2-5:

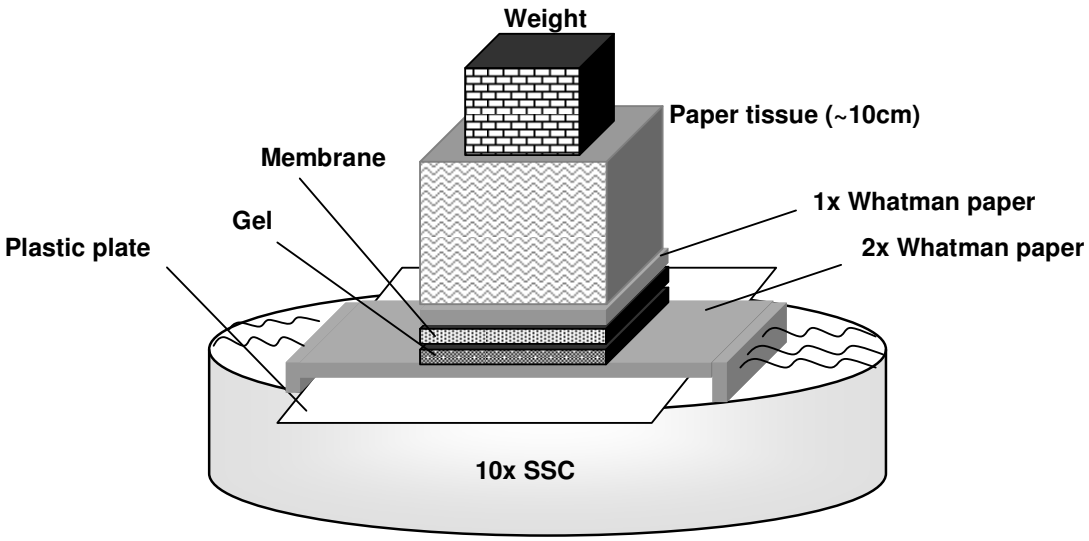

Figure 2-5: Northern blot setup. The whatman paper on which the gel lies has to be soaked in and dip into the 10x SSC.

The transfer was performed overnight at room temperature.

Using a needle, the well positions were marked on the membrane. The membrane was then soaked in 10x SSC (Table 2-2) for 2 min and dried on paper tissue with the RNA side facing away from the tissue. Subsequently, the RNA was crosslinked to the membrane using 2 times autocrosslink setting (1200 microjoules in 25 sec) of a UV Stratalinker 1800 machine (Table 2-3).

The blot was then sealed and stored at –20°C for hybridization.

Probe preparation:

An RT-PCR was performed using a primer combination from *GRIK2* exons 4 and 10 (Table 2-17).

Table 2-17: Primers used for amplification of Northern blot probe.

Forward (Exon 4)	GCTCATCAAAGCTCCATCAAG
Reverse (Exon 10)	ATCCTGGGCTCCATATTTCC

Membrane pre-hybridization:

Prior to probe hybridization, the membrane was incubated at 42°C with 20 ml hybridization buffer (Table 2-1) in a rotating glass tube.

Probe labeling:

For radioactive labeling the following protocol was applied:

20ng RT-PCR amplicon were mixed with 4 ml 5x OLB buffer (Table 2-2) in a final volume of 16 µl, denatured for 2 min at 95°C (in order to obtain single stranded DNA) and put on ice. Subsequently, 5 µl p32-dCTP and 1 µl Klenow fragment of DNA polymerase I enzyme were added and the mixture was then incubated at 37°C for 60 min.

Probe purification:

To remove of unincorporated nucleotides, a G50 microspin column was used. First, the tube solution was homogenized by vortexing. Then, after breaking the bottom of the tube it was centrifuged for 1 min with 735 rcf and 80 µl of the flow-through were added to the labeled probe. The rest of the flow-through was discarded and the entire

volume of the probe was loaded on the column and centrifuged for 2 min at 735 rcf. The flow-through was used for hybridization.

Hybridization:

Prior to hybridization, the purified probe was denatured at 95°C for 5 min, added directly to the hybridization solution (without touching the membrane) and incubated with the membrane overnight at 42°C in a rotating glass tube.

Washing and imaging:

Wash buffer (Table 2-2) was pre-warmed at 42°C. The hybridization solution was discarded and the hybridization tube was filled with 100 ml of wash buffer and rotated at 42°C for 10 min. Subsequently, the wash solution was discarded and the process was repeated 2 more times. For imaging, the membrane was sealed in plastic foil, exposed to sensitive Biomax X-ray film at -80°C in a HyperCassette and developed using a Curix 60 X-ray film-developing machine.

2.3.2.8. Inverse PCR

The principle of the Inverse PCR method (Ochman et al. 1988) is shown in Figure 2-6.

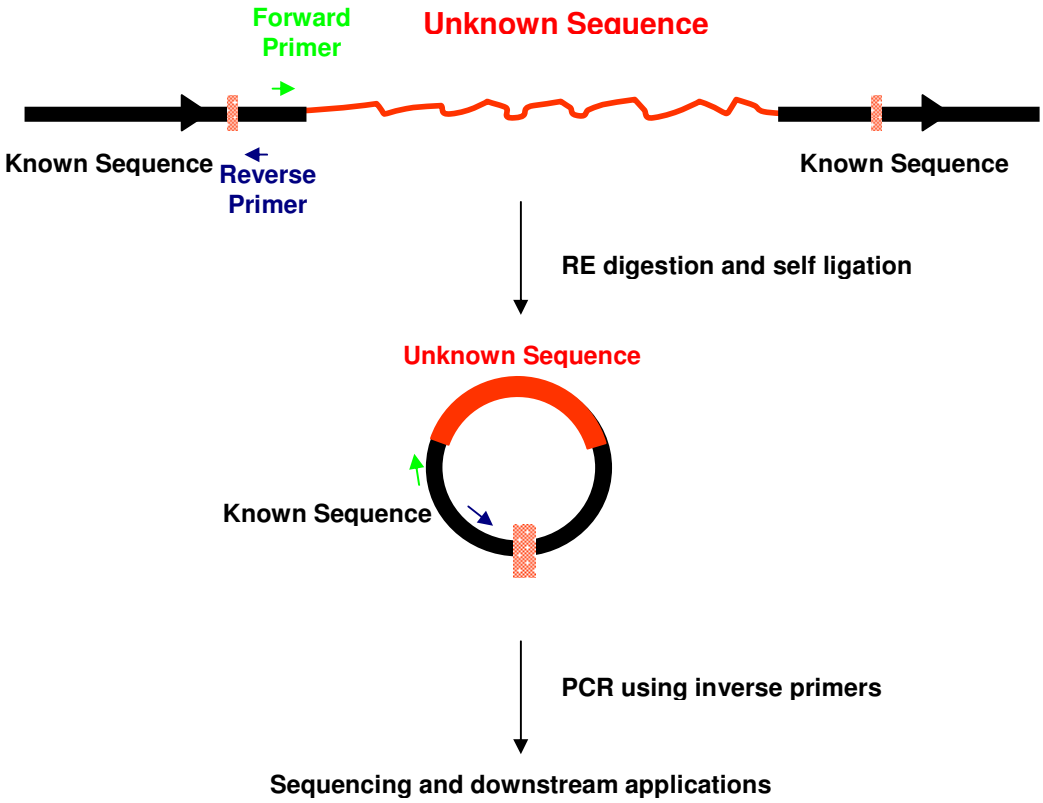

Figure 2-6: Inverse-PCR strategy.

In this study the following procedure was used:

5 µg genomic DNA were restricted using 10 units *Bgl*II restriction enzyme (in 1x NEB3 reaction buffer) for 1 h at room temperature. To obtain a complete DNA restriction, an additional overnight restriction was set up by adding 10 units fresh restriction enzyme. In order to remove the enzyme and buffer after restriction, gel electrophoresis was performed, the relevant band was excised from the gel and DNA was extracted using the Qiagen gel extraction kit. The DNA was then purified by Phenol-Chloroform as follows:

The equal volume of Phenol:Chloroform (Table 2-1) was mixed well with the extract and centrifuged, the aqueous phase was then transferred to a new tube and mixed with an equal volume of Chloroform and centrifuged again. Subsequently the DNA was precipitated from the aqueous phase by adding the same volume of Ethanol and centrifuging. The DNA was then re-dissolved in 25 µl H_2O. All centrifuging steps were perofrmed at 10000 rpm for 3 min in an Eppendorf Centrifuge (5415D).

After preparation and purification, 1 µg of the digested DNA from each sample was circularized by incubation with 1.5 units T4 DNA ligase in 10 µl 10x ligation buffer (Table 2-2, Table 2-1) for 16 h at 12°C. The enzyme was subsequently inactivated by incubating the reaction at 65°C for 10 min. After self ligation, the reaction mix was loaded onto a 1% agarose gel and electrophoresis was performed (1h at 100V). After separation, fragments with the expected size were excised from the gel and purified using the Qiagen MiniElute PCR purification kit. These fragments were then used for inverse PCR. The used conditions, primers and temperature profile are shown in Table 2-18, Table 2-19 and Table 2-20.

Table 2-18: Inverse-PCR mix

Solution	Amount
Forward Primer (10µM)	1.5 µl
Reverse Primer (10µM)	1.5 µl
BIO-X_ACT mix	25 µl
H_2O	12 µl
Ligated DNA	10 µl (100ng)

Table 2-19: Primers used for Inverse PCR*

Direction	Position	Sequence
Forward	chr6:102,244,436-102,244,461	CATGCTCCTAGAGGTGTGCAAATACC
Reverse	chr6:102,243,882-102,244,115	CTACAATGGCAAGCGAAGTG

*Primers were located in the reverse order on the 5' region of the deletion, which was known to be present in all individuals.

Table 2-20: Inverse PCR program			
	Temperature	**Time**	**Cycle number**
Initial denaturation	94°C	3 min	1x
Denaturation	94°C	30 sec	
Annealing	55°C	30 sec	25x
Extension	72°C	10 min	
Final extension	72°C	10 min	1x

The I-PCR products were then isolated by agarose gel electrophoresis, excised, purified (see above) and analyzed by cloning and sequencing.

2.3.2.9. Southern Blot analysis

DNA restriction and electrophoresis

10 µg DNA were submitted to enzymatic restriction (overnight, 37°C) with 1 µl *Bgl*II (10 U/µl) or 1 µl *EcoR*V (20 U/µl) in a volume of 25 µl, containing 2.5 µl NEB3 buffer and 2.5 µl BSA (10x).

The digested DNA was separated by agarose gel electrophoresis (1% agarose, without Ethidium Bromide, 50V, 8h) using Bromophenol-Blue loading buffer (Table 2-2). Afterwards, the gel was stained in an Ethidium Bromide bath (5mg/l) for 15 min. Gel documentation was done using a UV sensitive ruler beside the DNA 1kb ladder marker for subsequent band localization (Table 2-5).

DNA denaturation and transfer

The gel was then rinsed in the denaturing buffer for 30 min. The blotting set up was prepared as previously described (Figure 2-5) using a Hybond-N+ membrane.

After blotting, the membrane was rinsed in 10x SSC and the gel was checked in UV light to verify complete DNA transfer to the membrane.

The membrane was then dried on paper towels before the DNA was fixed on the membrane using 2x autocrosslink programs (1200µJoules, x100) in UV Stratalinker 1800 (Table 2-3). Afterwards the membrane was kept sealed in plastic foil at room temperature.

Probe preparation and labeling

Probes were amplified by touchdown PCR with 1 min extension time (See Table 2-14) and afterwards purified using a Qiagen gel extraction kit. The used primer sequences are shown in Table 2-21.

Table 2-21: Primers for Southern blot probes

Primer	Sequence	Product size
Upstream Deletion (Forward)	GCCATTGTGTAAGATCATAGTGCTCAGAC	
Upstream Deletion (Reverse)	GTATATTAGAACCACTGGGAAGG	802 bp
Downstream Inversion (Forward)	TGGAAATTCATAGTAAAGGTATGTGG	
Downstream Inversion (Reverse)	CTGAGTAGAAAGAGAGAGAAACAATG	930 bp

For labelling, 20ng of the probes were mixed with 4 µl 5x OLB buffer (Table 2-2) in 17 µl aqueous solution, denatured at 95°C for 2 min and then chilled on ice.

Subsequently, 2 µl [α-32P] dCTP and 1 µl Klenow enzyme were added and the mixture was incubated at 37°C for 45 min.

In order to remove unincorporated nucleotides a Micro Spin G-50 column (Table 2-5) was used according to the manufacturer's instructions.

Hybridization

To block unspecific sites on the membrane, reduce background signal and get a clear and specific result, the membrane was pre-hybridized with 20 ml pre-warmed (65°C) PEG buffer containing 0.1 mg/µl denatured (at 95°C for 5 min and then chilled on ice before adding to PEG) sonicated Herring sperm DNA in a rotating hybridization tube for 1 h.

The purified radioactively labelled probe was denatured at 95°C for 5 min, added directly to the PEG hybridization buffer and incubated overnight with the membrane in rotating a hybridization tube at 65°C. Subsequently, the hybridization solution was discarded and the membrane washed (3 times for 10 min at 65°C) using pre-warmed (65 °C) wash buffer.

Detection

The membrane was then sealed in plastic foil, exposed overnight to MS X-ray film in a HyperCassette at –80°C. The film was then developed using a Curix 60 X-ray film developing machine (Table 2-3).

2.3.2.10. Cloning of wild type *GRIK2* and *GRIK2* without exons 7 and 8

For cloning full length *GRIK2* (NM_021956), the wildtype transcript was amplified from fetal brain cDNA by touchdown PCR using the following primers:

Forward: CACCATGAAGATTATTTTCCCG

Reverse: TGCCATGGTTTCTTTACCTG

The forward primer contains a CACC sequence at the 5' end in order to facilitate the directional cloning of the amplicon into the pENTR/TOPO vector.

As the expression vector used in the experiments contained the coding sequence for a C-terminal c-Myc tag to be joined to the insert, the reverse primer did not contain a TAA stop codon.

The cDNA was cloned into the pENTR/D-TOPO entry vector (Figure 2-7A) using the Invitrogen pENTR Directional TOPO cloning kit, based on the manufacturer's instructions. *GRIK2* cDNA was then sub-cloned in a modified pcDNA-DEST47 expression vector (Figure 2-7B) in which the original 3'GFP-tag was replaced by a c-myc-tag (Glu-Gln-Lys-Leu-Ile-Ser-Glu-Glu-Asp-Leu) followed by a stop codon. The sequence of cloned cDNA was verified by direct sequencing.

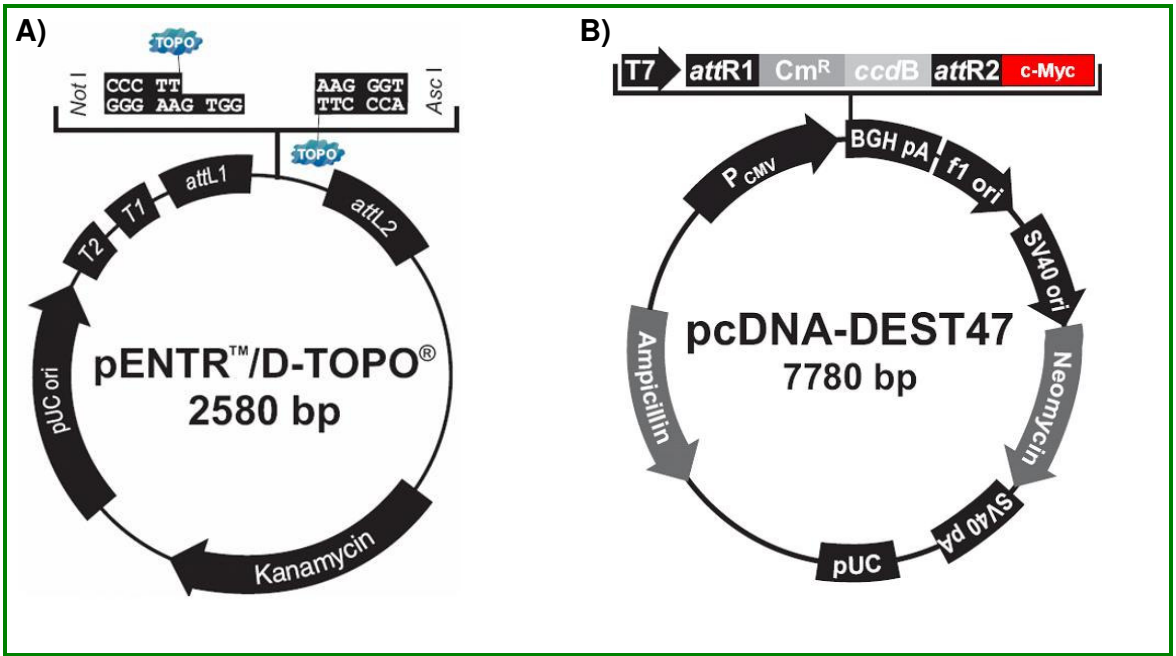

Figure 2-7: Vectors used for cloning *GRIK2* cDNA. A) Entry and B) destination vector

A deletion of GLUR6 exon 7 and 8 was introduced by site-directed mutagenesis, using the Stratagene QuikChange kit (Table 2-5) based on the manufacturer's instructions. The following primers were used: GGT TTG CTG GAT GGA TTT ATG ACG ATT GGA ACG TGG GAT CCA GCC (forward primer) and GGC TGG ATC CCA CGT TCC AAT

CGT CAT AAA TCC ATC CAG CAA ACC (reverse primer). After site-directed mutagenesis, the sequence was confirmed by sequencing.

2.3.2.11. Chemical transformation

100ng of Plasmid DNA were incubated with 250 µl of chemically competent E-Coli TOP10 cells for 30 min on ice. The mixture was then heat shocked at 42°C for 45 sec and chilled on ice for 2 min. The cells were afterwards incubated for 1 h in 1 ml LB medium with vigorous shaking at 37°C before incubating them overnight at 37°C on agar plates containing the appropriate selection antibiotic.

2.3.2.12. Transfection

HEK293 cells were transfected with *GRIK2* wildtype (Wt) or deletion (Δ) constructs for either protein labeling and extraction or immunfluorescence studies. Non-transfected cells (NT) were used as negative controls.

For protein labeling and extraction in a cell surface biotinylation assay, 2 x 10^6 cells were seeded in 75 cm^2 flasks (Table 2-4) one day before transfection. For transfection, 60-80% confluent flasks were used.

The following steps were performed: 83 µl transfection agent DreamFect® were mixed with 500 µl OptiMEM and pre-incubated for 5 min. Purified plasmid DNA (66 µg) was mixed with 500 µl OptiMEM and pre-incubated for 5 min. The mixture of DreamFect®-OptiMEM was then added to Construct-OptiMEM and incubated for at least 20 min. Then the final mixture was added to each flask after replacing the culture medium with fresh medium without antibiotics to reduce the stress condition in the flask as much as possible. 24 h after transfection, the medium was discarded and the cells were washed with sterile room temperature PBS prior to incubating them for another 24-48 h with fresh medium until they reached full confluence.

For immunofluorescence experiments, $2x10^4$ cells were cultured for 24 h in 6-well plates on coverslips coated with poly-lysine (Poly-lysine coating provides an anchored platform for the cells and helps those cells for a better growth).

For transfection purified plasmid DNA (2 µg) and 8 µl DreamFect® were separately mixed with 100 µl OptiMEM and pre-incubated for 5 min, then mixed with each other and incubated for 20 min before adding this total mixture to 2 ml fresh medium. 24 h after transfection, old medium was removed and were cultured for another 24 h with an antibiotic-free medium before they were fixed for immunofluorescence studies.

2.3.3. Protein methods

2.3.3.1. Western blot analysis

Samples, SDS-PAGE and membrane preparation

Sonicated total cell lysate and eluate from biotinylation experiments (see Section 2.3.3.2) were used as samples for Western blotting.

First, a SDS poly-acrylamide gel electrophoresis (SDS-PAGE) with 10% acrylamide gels on a Bio-Rad mini-apparatus (Table 2-3) was performed. The method is called SDS-PAGE because sodium dodecyl sulfate (SDS), a strong anionic detergent, is used to denature the proteins. A discontinuous poly-acrylamide gel consisting of a stacking gel on top of a separating gel was used to separate the denatured proteins according to their molecular weight. The method applied here followed the most commonly used system, the so called Laemmli method (Laemmli 1970).

To prepare the protein samples for SDS-PAGE separation, they were completely denatured by first adding Laemmli protein loading buffer in 1:4 v/v (from a 5x stock of Laemmli protein loading buffer, Table 2-2) and subsequently incubating the mixture at 95°C for 5 minutes. For gel preparation, SDS-PAGE cassettes from Bio-Rad (Table 2-3) were used. Approximately 5 cm of the Cassettes were filled up with liquid separating gel mixture (Table 2-22) and a thin layer of water was slowly added to smoothen the top layer of the separating gel and prevent evaporation. The mixture was then allowed to polymerize (30 min at room temperature).

Table 2-22: Component volumes for SDS-PAGE gels (in ml)		
	10 ml of 10% separating gel	**5 ml stacking gel**
H_2O	4.1	3.075
1.5 M Tris-HCl, pH 8.8	2.5	---
0.5 M Tris-HCl, pH 6.8	---	1.25
20% (w/v) SDS	0.05	0.025
Acrylamide/Bis-acrylamide (30%/0.8% w/v)	3.3	0.67
10% (w/v) APS	0.05	0.025
TEMED	0.005	0.005

After polymerization of the separating gel, the covering water layer was removed and the stacking gel mixture (Table 2-22) poured on top. A 15-well comb was inserted to create loading wells. After polymerization of the stacking gel (30 min at room temperature), the comb was removed slowly without disturbing the wells. The cassette was then vertically inserted into the electrophoresis chamber, filled with electrophoresis running buffer and denatured protein samples were loaded into the wells using a Hamilton syringe (Table 2-3). The apparatus was connected to a constant current source (25 mAmp) for electrophoresis. Migration of the proteins in the gel was judged by visually monitoring the tracking dyes (Bromophenol blue) from the protein-loading buffer. As soon as the front dye reached the end of the separating gel, the electrophoresis was stopped. The gel was removed from the cassette and used to transfer the proteins on a nitrocellulose membrane.

Proteins separated by SDS-PAGE were electro-transferred onto a nitrocellulose membrane by a semi-dry method as follows:

Unfixed gels were incubated at room temperature shortly in a transfer buffer (Table 2-2). Nitrocellulose membranes were first soaked and activated in pure methanol for 1 min. Whatman paper and membranes were then soaked in the same transfer buffer as the gels. In order to make the transfer set, membrane was placed on two layers of Whatman paper on the anode pole of a transfer unit (Schleicher and Schuell) and the

gel was placed on the top of membrane followed by two other Whatman papers on the cathode side. Air bubbles were removed from the whole transfer-set by rolling a glass rod over it. The electro-transfer was done at a constant current of 250 mAmp (for a single gel) for 45 min. Protein transfer from the gel to the membrane was confirmed by staining the membranes with Ponceau Red dye solution (Table 2-2).

Blocking

In order to prevent unspecific binding, have clearer results and eliminate false positive signals, the membranes were incubated with 5% non-fat milk powder dissolved in TBS-T buffer for 30 min at room temperature.

Detection

For GLUR6 detection, blocked membranes were incubated first with the appropriate primary antibody dilution (Table 2-7) in TBST buffer for 1 h at room temperature (or alternatively overnight at 4℃), washed 3 times for 5 min at room temperature with TBST buffer and then incubated with horseradish peroxidase (HRP) conjugated secondary antibody dilution (in TBST buffer) for 1 h at room temperature.

For GAPDH detection, membranes were only incubated with HRP conjugated GAPDH antibody.

Analysis: Chemiluminescence detection

Prior to chemiluminescence analysis, the membranes were washed again 3 times for 5 min at room temperature with TBST. Then equal amounts of enhanced chemiluminescent (ECL) solutions from the ECL kit (Table 2-5) were mixed immediately before applying the mixture to the surface of the membrane. The blot was then covered with a thin plastic foil and exposed to MS Photographic films in

Western blot HyperCassette and developed using a Curix 60 X-ray film-developing machine.

Re-using membranes

In order to probe different proteins, previously probed membranes were stripped by incubating the membrane in the stripping buffer (Table 2-2) for 30 minutes at 50°C. It was then washed with PBST, 3 times (10 min each time) at room temperature before blocking with 5% non-fat milk powder dissolved in TBS-T buffer for 30 min at room temperature and reprobing with a different primary antibody.

2.3.3.2. Cell surface biotinylation assay

In order to check the presence of the GLUR6 wildtype or deletion protein on the cell surface, the proteins were over expressed in HEK293 cells. These cells were then used for a cell surface biotinylation assay using the Pinpoint cell surface protein isolation kit (Table 2-5) according to the manufacturer's instructions.

The isolated surface proteins were separated by SDS-PAGE and investigated by GLUR6 specific Western blot analysis.

2.3.3.3. Immunocytochemistry

HEK293 cells were fixed 24-48 h after transfection with 4% PFA (Table 2-1) for 10 min at room temperature and permeabilized with 0.1% Triton X-100 (in PBS) for 5 min. Subsequently the cells were blocked with 10% normal goat serum (in PBS) for 1 h at room temperature.

The membrane proteins Cadherin and GLUR6 were detected by incubation with the antibodies panCadherin (1:2000 dilution) and Anti-GLUR6/7 (1:2000 dilution) for 1 h respectively.

They were labeled by the secondary antibodies Alexa Fluor® 488 chicken anti-mouse (1:1000 dilution) and Alexa Fluor® 488 chicken anti-rabbit (1:1000 dilution) for 1 h. All incubations were performed at room temperature.

Images were taken on a confocal laser-scanning microscope (Zeiss Axiovert 100 M) with a 63x-objective and analysed with the Zeiss LSM image examiner software.

3. Results

3.1. Linkage analysis

48 families with a minimum of two mentally retarded children were selected for linkage analysis after exclusion of Fragile-X syndrome, large chromosomal aberrations and disorders of fatty, amino or organic acid metabolism.

For these families, whole genome SNP typing using the Human Mapping 10k Array, Version 2 (Kennedy et al. 2003) was performed with DNA from all affected individuals, the parents and, if available, a maximum of two healthy siblings. The genotype data from each family were then used for linkage analysis.

3.1.1. Relationship evaluation based on genotype data

In order to verify the relationships between individuals, the genotyping data were subjected to standard quality control analysis, using GRR (graphical representation of relationship errors; (Abecasis et al. 2001) and PedCheck (O'Connell and Weeks 1998).

GRR was employed to compare the relationship of individuals based on pedigree information with the relationships suggested by the genotype data.

In two families, M167 and M172 (Figure 3-1), decreased allele sharing and increased genotype variability pointed to inconsistencies between the relationships inferred by genotypes and pedigree information, indicating possible sample mix-ups. These could however not be resolved and the families were therefore excluded from further analysis.

In the remaining 46 families with correct verified relationships, the few SNPs that showed Mendelian or non-Mendelian inheritance errors were identified by PedCheck and excluded from linkage analysis (these errors could have occurred due to unspecific hybridization or erroneous base calling).

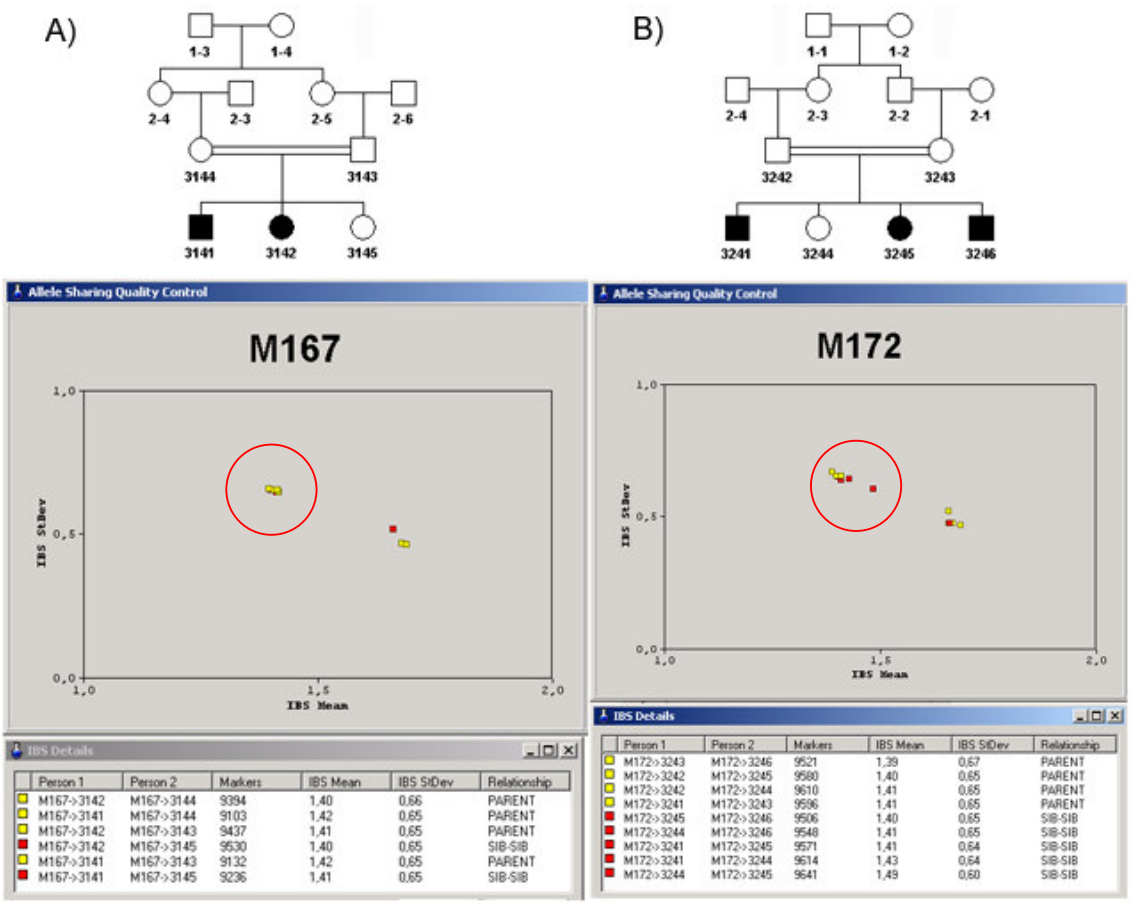

Figure 3-1: Pedigree and GRR software results for the families with data inconsistency: A) M167 and B) M172. Each graph shows the ratio of IBS (identical by state) standard deviation and IBS mean. Individuals with less allele sharing (IBS Mean) and higher variability (IBS StDev) are indicated by red circle. Details of relationships in which expected and observed allele sharing and genotype variability are significantly different are shown below each graph.

In order to use the genotyping data with the linkage analysis software, they were converted into appropriate formats by the ALOHOMORA software (Ruschendorf and Nurnberg 2005). For linkage analysis the programs Merlin (Abecasis et al. 2002) and GeneHunter (Kruglyak et al. 1996) for non-parametric and GeneHunter and Allegro (Gudbjartsson et al. 2000) for parametric multipoint linkage analysis were applied. Haplotypes were determined using GeneHunter software and used to prove homozygosity in the intervals obtained by linkage analysis.

3.1.2. Linkage results

For a given family, intervals were considered as potential sites of the causative mutation for NS-ARMR if the corresponding LOD scores were less than one unit lower than the highest peak observed ("one LOD down" method), and if all affected members were homozygous carriers of the same SNP haplotype. After linkage analysis 5 further families had to be excluded from the study for several reasons:

First, in two cases (M160 and M193) detailed clinical re-evaluation revealed syndromic forms of ARMR (Figure 3-2).

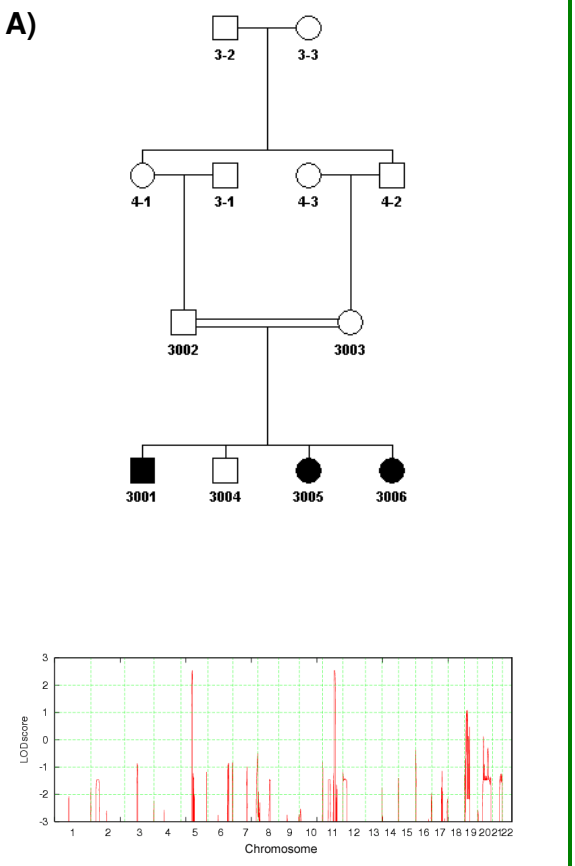

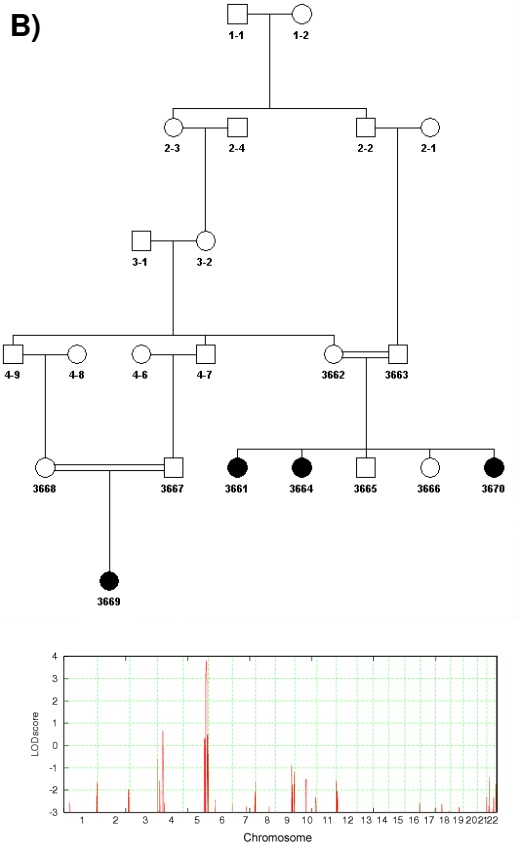

Chromosome	Start	End
Chr05	70940451	75986606
Chr11	79708481	96412402

Chromosome	Start	End
Chr05	170070287	174400961

Figure 3-2: Pedigree and linkage analysis results and detailed interval information for families with syndromic ARMR. Affected members of the family M160 (A) showed congenital cataracts and a history of seizures in addition to MR. In the family M193 (B), hirsutism, oligomenorrhea and obesity were observed in most affected individuals.

Second, two NS-ARMR families (M145 and M155) had to be excluded as no interval could be linked to the phenotype (Figure 3-4).

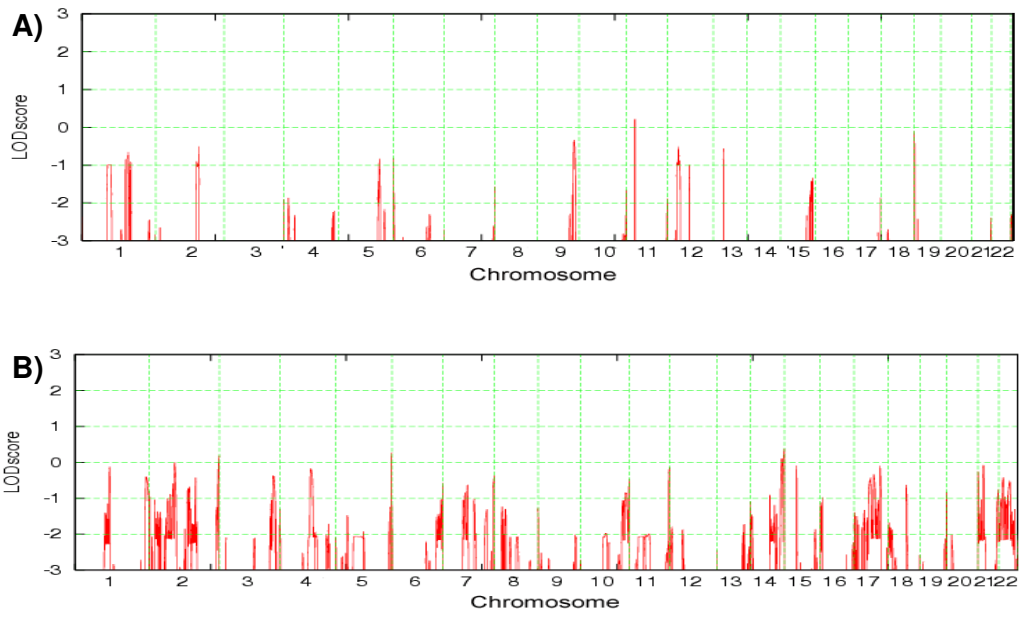

Figure 3-3: parametric linkage analysis results from Allegro software for two families with data inconsistency. The failure to detect a region with the maximum possible LOD-score shows the lack of common homozygous regions between the affected individuals in both families (refer to supplementary data 1 for pedigrees).

Third, one family was excluded due to an exceptionally high degree of consanguinity (Figure 3-4).

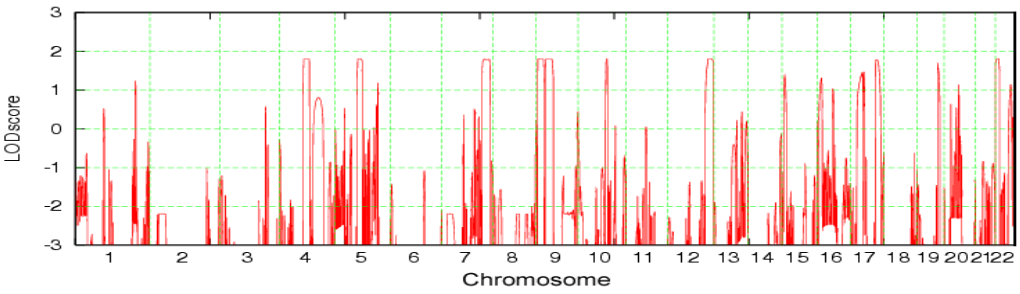

Figure 3-4: Parametric linkage analysis results from Allegro software for a family with high degree of consanguinity. M181 linkage result shows many regions with the maximum possible LOD-score (LOD 1.8 in a first cousin marriage with 2 affected individuals; Refer to supplementary data 1 for pedigree). As these regions include a very large portion of the genome, this family was excluded from further analysis.

For 34 of the remaining 41 families (pedigrees shown in supplementary data B), linkage analysis revealed more than one linkage interval, reflecting the limiting size of most of these families and/or a high degree of consanguinity (Table 3-1).

In first-cousin marriages with two affected children, the minimum size of the families considered in this study, parametric linkage analysis typically resulted in 5–6 intervals, each with the maximally attainable LOD score of 1.8, but in many of them, the number of peaks could be reduced to about 3 by including all available unaffected siblings or other family members. However, in 7 larger families, single linkage intervals with LOD scores above 2 (Figure 3-7 to Figure 3-13) were identified.

To study the genomic distribution of the genomic intervals with linkage to NS-ARMR, and to get a first impression as to the number and localization of genetic defects causing NS-ARMR in the Iranian population, a method that was previously employed to show that genetic defects underlying non-syndromic X-linked MR cluster on proximal Xp (Ropers et al. 2003) was used. The result is presented in Figure 3-5, which shows a curve that resulted from the superposition of weighted linkage intervals from 78 consanguineous families with NS-ARMR including the 41 families from this study.

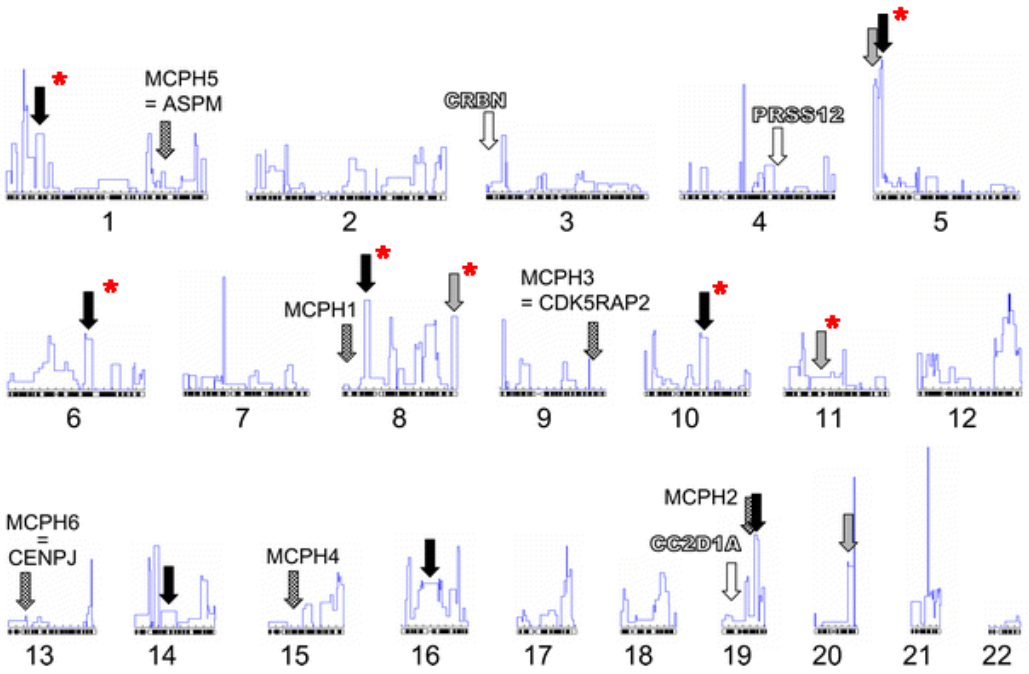

Figure 3-5: Distribution of linkage intervals reveals heterogeneity of NS-ARMR and defines novel MRT loci. Single intervals identified in the families that were part of this study are indicated by asterisks. Black arrows: single intervals with LOD scores >3 (= novel MRT loci), gray arrows: single intervals with LOD scores between 2 and 3. In small families with several co-segregating haplotypes, their cumulative length was used to normalize their weight. For this calculation, linkage intervals were disregarded if their LOD scores were more than 1 unit lower than those of the highest LOD score observed in that family. The surface under the curve is a parameter for the proportion of gene defects mapping to the relevant genome segment. Empty arrows: cloned MRT genes, checkered arrows: loci for ARMR with microcephaly.

The NS-ARMR families with single co-segregating intervals, as exemplified by the interval at the distal end of chromosome 8q, are represented by rectangles of different shape, but identical surface, or 'weight'. It is noteworthy that none of these intervals encompassed previously reported ARMR genes nor loci for autosomal recessive primary microcephaly (Woods et al. 2005).

For families with more than one interval, the lengths of all physical genome intervals (as defined by the distance between the closest SNP markers flanking the

respective haplotypes) co-segregating with NS-ARMR were added up and their total 'weight' was normalized in accordance with the fact that each family represents one single mutation. Thereafter, the weighted linkage intervals from all families including 37 families that were analyzed in another study were graphically superposed. The resulting curve reflects the genomic distribution of the mutations causing NS-ARMR in 78 families. Interval positions and weights for the individual families are listed in Table 3-1.

The surface under the curve, covering a given region of the genome, is a parameter for the proportion of gene defects mapping to the respective genome segment. Given the considerable number and length of linkage intervals in small families, it is not surprising that some of these overlap. Still, it appears that their co-localization on some chromosomes is not completely random. For example, there is apparent clustering of linkage intervals on chromosomes 16 and 19, which may indicate that these regions carry genes that are mutated in more than one family. Interestingly however, none of the previously identified autosomal recessive mental retardation genes map to these mutation hotspots, which suggests that they do not have a major role in NS-ARMR.

Table 3-1: Homozygosity regions identified in all 41 families with non-syndromic autosomal recessive mental retardation.[1]

No.	Family ID	Chr.	Start[2]	End[2]	Length of interval [bp]	SUM	Weight[3]
1	7903104	Chr02	211525939	214796724	3270785	32078165	311,739
		Chr08	70515456	78708089	8192633		
		Chr12	40596176	47435692	6839516		
		Chr15	92397640	100256656	7859016		
		Chr18	1	5916216	5916215		
2	8303095	Chr01	230304802	233625390	3320588	10591217	944,179
		Chr13	106199619	106878224	678605		
		Chr17	68095922	74687946	6592024		
3	8402061	Chr01	75810501	87323731	11513230	26787771	373,305
		Chr08	6780950	13570617	6789667		

Table 3-1: Homozygosity regions identified in all 41 families with non-syndromic autosomal recessive mental retardation.[1]

No.	Family ID	Chr.	Start[2]	End[2]	Length of interval [bp]	SUM	Weight[3]
		Chr08	18875108	20835297	1960189		
		Chr14	78285563	84810248	6524685		
4	M001*	Chr08	139384002	146308819	6924817		1444,081
5	M002	Chr07	131783461	141598180	9814719	83785404	119,353
		Chr11	95870533	99123453	3252920		
		Chr12	23744336	66603891	42859555		
		Chr13	1	24029946	24029945		
		chr17	8903986	12732251	3828265		
6	M022	Chr07	50046933	52496765	2449832	4678707	2137,343
		Chr04	78109292	80338167	2228875		
7	M027	Chr01	84145263	151806474	67661211	125806721	79,487
		Chr03	179677333	189923920	10246587		
		Chr11	71935368	92437739	20502371		
		Chr14	70423192	97819744	27396552		
8	M034	Chr02	164634247	200030451	35396204	65525923	152,611
		Chr03	1	2264798	2264797		
		Chr03	117632275	132780249	15147974		
		Chr09	8167428	11140966	2973538		
		Chr13	103176645	108048350	4871705		
		Chr14	103176645	108048350	4871705		
9	M037	Chr01	24754048	64170564	39416516	102430943	97,627
		Chr03	108991086	114218596	5227510		
		Chr04	131961015	134021275	2060260		
		Chr05	31569098	33101281	1532183		
		Chr08	117872823	134630304	16757481		
		Chr11	59788033	64246729	4458696		

Table 3-1: Homozygosity regions identified in all 41 families with non-syndromic autosomal recessive mental retardation.[1]

No.	Family ID	Chr.	Start[2]	End[2]	Length of interval [bp]	SUM	Weight[3]
		Chr12	100067176	108357441	8290265		
		Chr19	5374643	15353848	9979205		
		Chr19	35770059	50478886	14708827		
10	M053	Chr07	83565801	94343583	10777782	39265935	254,674
		Chr12	18917349	28710301	9792952		
		Chr18	46999467	65694668	18695201		
11	M061	Chr04	178134007	183316114	5182107	14135210	707,453
		Chr11	75633996	78652934	3018938		
		Chr12	1	5934166	5934165		
12	M068	Chr02	28251178	44895495	16644317	87856482	113,822
		Chr05	16045437	52476934	36431497		
		Chr07	90254248	111877650	21623402		
		Chr13	38125547	42483844	4358297		
		Chr17	8811157	17610126	8798969		
13	M090	Chr01	21400651	26043388	4642737	9676207	1033,463
		Chr03	19346584	24380054	5033470		
14	M092	Chr09	2988820	6322901	3334081	8829608	1132,553
		Chr14	18481044	21050680	2569636		
		Chr16	75764770	78690661	2925891		
15	M096*	Chr01	36714137	46061538	9347401	9347401	1069,816
16	M097*	Chr06	95965958	105949023	9983065	9983065	1001,696
17	M100*	Chr08	28724711	35200624	6475913	6475913	1544,184
18	M104	Chr01	1	6605831	6605830	39644592	252,241
		Chr05	110281001	111518927	1237926		
		Chr11	116737522	128936463	12198941		
		Chr14	1	19601896	19601895		

Table 3-1: Homozygosity regions identified in all 41 families with non-syndromic autosomal recessive mental retardation.[1]

No.	Family ID	Chr.	Start[2]	End[2]	Length of interval [bp]	SUM	Weight[3]
19	M122*	Chr11	33940362	75178700	41238338	41238338	242,493
10	M124	Chr04	25524333	33583318	8058985	20258137	493,629
		Chr09	26089466	38288618	12199152		
21	M136	Chr01	189799271	205719248	15919977	150237425	66,561
		Chr05	94403747	145808863	51405116		
		Chr06	141574843	149574490	7999647		
		Chr11	30529083	73776570	43247487		
		Chr11	117605273	134482954	16877681		
		Chr14	74764341	89551858	14787517		
22	M141	Chr05	1677089	17444767	15767678	88427500	113,087
		Chr06	93549023	97375947	3826924		
		Chr19	8829549	56763284	47933735		
		Chr22	25544435	46443598	20899163		
23	M148	Chr01	210055469	214496733	4441264	109820305	91,058
		Chr13	31582126	52306655	20724529		
		Chr14	56451601	88705132	32253531		
		Chr16	26352579	55532856	29180277		
		Chr18	5898215	21618534	15720319		
		Chr18	52024710	59525095	7500385		
24	M158	Chr01	214293299	231082139	16788840	41491523	241,013
		Chr07	23488693	38800278	15311585		
		Chr12	6755671	16146769	9391098		
25	M161	Chr02	234216839	243018229	8801390	62749695	159,363
		Chr05	0	3582185	3582185		
		Chr05	145721638	163503982	17782344		
		Chr15	82004960	96162993	14158033		

Table 3-1: Homozygosity regions identified in all 41 families with non-syndromic autosomal recessive mental retardation.[1]

No.	Family ID	Chr.	Start[2]	End[2]	Length of interval [bp]	SUM	Weight[3]
		Chr16	9561557	27987300	18425743		
26	M168	Chr10	0	2170332	2170332	13105231	763,054
		Chr10	10953080	13302149	2349069		
		Chr14	86475818	95061648	8585830		
27	M170	Chr03	136179026	150835697	14656671	56290036	177,651
		Chr05	10185963	14320936	4134973		
		Chr06	71113159	82327384	11214225		
		Chr09	79048668	97492683	18444015		
		Chr21	35045926	42886078	7840152		
28	M171	Chr02	237648575	243018229	5369654	22869771	437,258
		Chr06	155713132	158457552	2744420		
		Chr21	0	14755697	14755697		
29	M173*	Chr10	71041135	80718414	9677279	9677279	1033,348
30	M175	Chr01	189614266	193962973	4348707	31623306	316,222
		Chr02	229842774	243615958	13773184		
		Chr11	20647459	25145757	4498298		
		Chr21	37972980	46976097	9003117		
31	M176	Chr02	123831874	142199167	18367293	19624579	509,565
		Chr04	78759808	80017094	1257286		
32	M178	Chr02	204616975	218456105	13839130	16948905	590,009
		Chr05	7715816	10825591	3109775		
33	M179	Chr02	47025603	50673438	3647835	12510847	799,306
		Chr08	92694714	101557726	8863012		
34	M180	Chr02	65801963	71318110	5516147	97914031	102,13
		Chr03	2910083	19346584	16436501		
		Chr05	164996462	173734018	8737556		

Table 3-1: Homozygosity regions identified in all 41 families with non-syndromic autosomal recessive mental retardation.[1]

No.	Family ID	Chr.	Start[2]	End[2]	Length of interval [bp]	SUM	Weight[3]
		Chr06	168107667	170975699	2868032		
		Chr13	21910480	23584523	1674043		
		Chr14	21719153	23876069	2156916		
		Chr16	27303962	78123542	50819580		
		Chr17	0	9705256	9705256		
35	M182	Chr07	8138585	16686998	8548413	37894291	263,892
		Chr11	20044296	32437935	12393639		
		Chr14	95229257	105311216	10081959		
		Chr16	73453779	78918580	5464801		
		Chr20	1	1405480	1405479		
36	M189	Chr06	4507465	53479046	48971581	61615000	162,298
		Chr10	15324589	22530131	7205542		
		Chr10	90656681	96094558	5437877		
37	M192*	Chr05	5144766	10786514	5641748	5641748	1772,5
38	M195	Chr10	10078469	15324589	5246120	31221703	320,29
		Chr10	128756300	135037215	6280915		
		Chr14	34845793	54540461	19694668		
39	M196	Chr02	229842774	234855951	5013177	30499487	327,874
		Chr06	39932610	40849835	917225		
		Chr18	57884652	64124707	6240055		
		Chr19	37946718	56275748	18329030		
40	M197	Chr06	51274732	58379697	7104965	18585748	538,047
		Chr11	22802550	26320392	3517842		
		Chr16	65490838	73453779	7962941		
41	M209	Chr03	63120465	68367673	5247208	39543594	252,885
		Chr09	2973774	7087991	4114217		

Table 3-1: Homozygosity regions identified in all 41 families with non-syndromic autosomal recessive mental retardation.[1]

No.	Family ID	Chr.	Start[2]	End[2]	Length of interval [bp]	SUM	Weight[3]
		Chr10	55676573	60884005	5207432		
		Chr12	107308599	116464605	9156006		
		Chr13	100777273	106849230	6071957		
		Chr17	64820537	68000315	3179778		
		Chr21	40246973	43200832	2953859		
		Chr21	43200832	46813969	3613137		

[1] Intervals with LOD scores less than 1 unit lower than the highest peak have been selected and haplotype compatibility for all regions has been proved. [2]Physical position according to NCBI genome build 36.1. [3] 10000/S with the S being the sum of physical lengths of all intervals in the family (equal for all intervals in a given family).

*Families with single linkage interval.

3.1.3. New Mental retardation (MRT) loci

In the 7 families with single autosomal linkage intervals (Figure 3-6, Table 3-2) the patients were clinically re-evaluated, in order to confirm the absence of additional clinical features and thus their non-syndromic status.

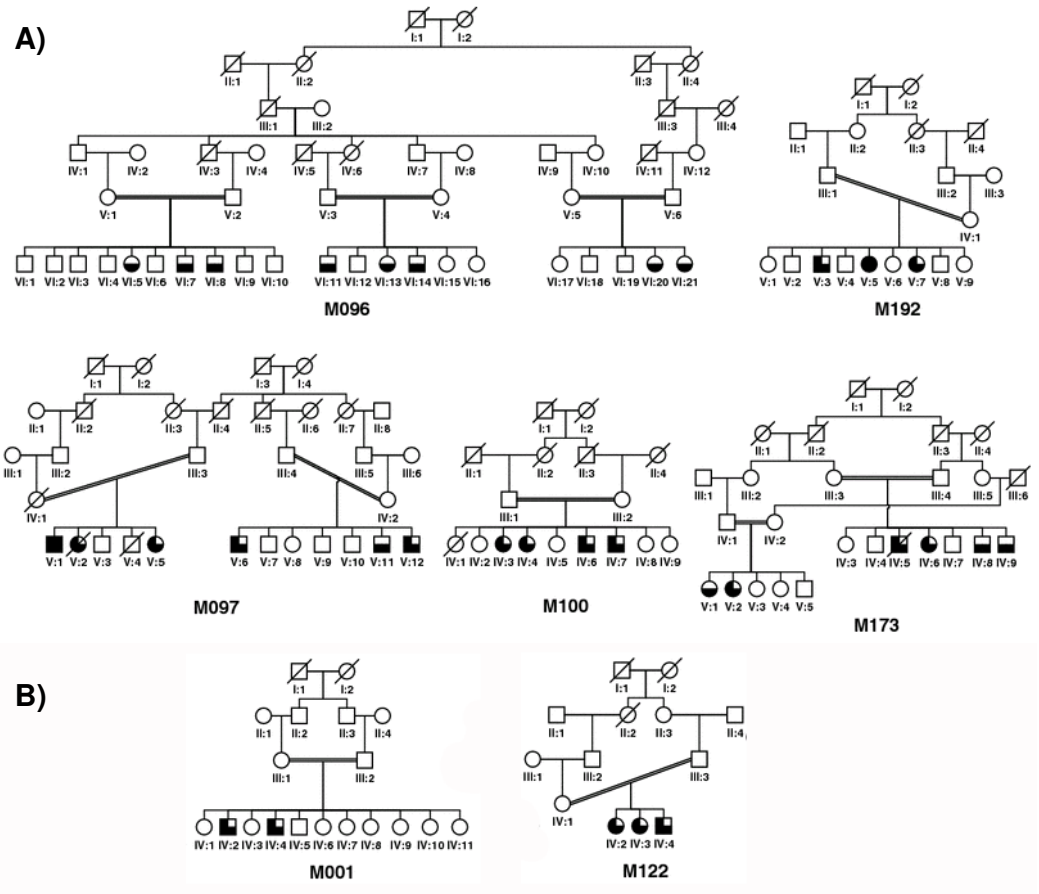

Figure 3-6: Analyzed pedigrees and degree of mental retardation for the families with single linkage interval. A) MRT and B) putative MRT families. The shown pedigrees are simplified but show the complete number of family members in the patient generation at the time of sample collection. Filled symbols indicate severe MR, three-quarter-filled symbols depict moderate MR and half-filled symbols mild MR.

Five of these linkage intervals had LOD scores above 3 (Morton 1998). They were thus considered as novel gene loci for NS-ARMR (Figure 3-6A,Table 3-2A) and named “Mental Retardation 4 to 8” (MRT4–8). This was done in accordance with the

nomenclature used for previously mapped NS-ARMR loci (OMIM 249500, 607417, 608443) (Molinari et al. 2002; Higgins et al. 2004; Basel-Vanagaite et al. 2006).

In the remaining 2 families (Figure 3-6B) with single linkage intervals, the LOD scores were above 2 but below 3 and thus too low to formally prove that these sites represent additional MRT loci. However these intervals are still likely to contain the causative mutation, as they represent genomic regions that co-segregate with the disease and have the highest LOD score in the respective family.

Table 3-2: Regions of homozygosity in families with single linkage intervals*

Chr.	Start SNP (position in bp)**		End SNP (position in bp)**		Interval [Mbp]	LOD score	Family	MRT No.
A)								
1	rs514262	(36955568)	rs953070	(46403641)	9.4	7.2***	M096	4
5	rs1824938	(5145028)	rs60701	(10786776)	5.6	3.0	M192	5
6	rs2246786	(95965958)	rs720225	(105949023)	10.0	4.3	M097	6
8	rs1113990	(28758718)	rs1534587	(35262498)	6.5	3.3	M100	7
10	rs1599711	(71041135)	rs942793	(80718164)	9.7	5.0***	M173	8
B)								
8	rs968652	(139482128)	qter	(146274826)	6.8	2.0	M001	
11	rs939038	(33932629)	rs644361	(75130040)	41.2	2.7	M122	

***All intervals are defined by the closest flanking recombinant SNP markers **Markers flanking regions of homozygosity that are shared by all patients of families with a single linkage interval. Physical positions are based on the May 2004 genome assembly. ***Result of split-pedigree-analysis (GeneHunter software)**

The results of linkage analysis and the haplotypes of the 7 families with single linkage intervals are shown in Figures 3-7 to 3-13. Parametric ("LOD-score") and non-parametric ("NPL") LOD scores as calculated by the Allegro and Merlin software are provided in genome-wide linkage plots for the analyzed families. The shown haplotypes were drawn by Haplopainter software using haplotypes inferred by the GeneHunter and Merlin software.

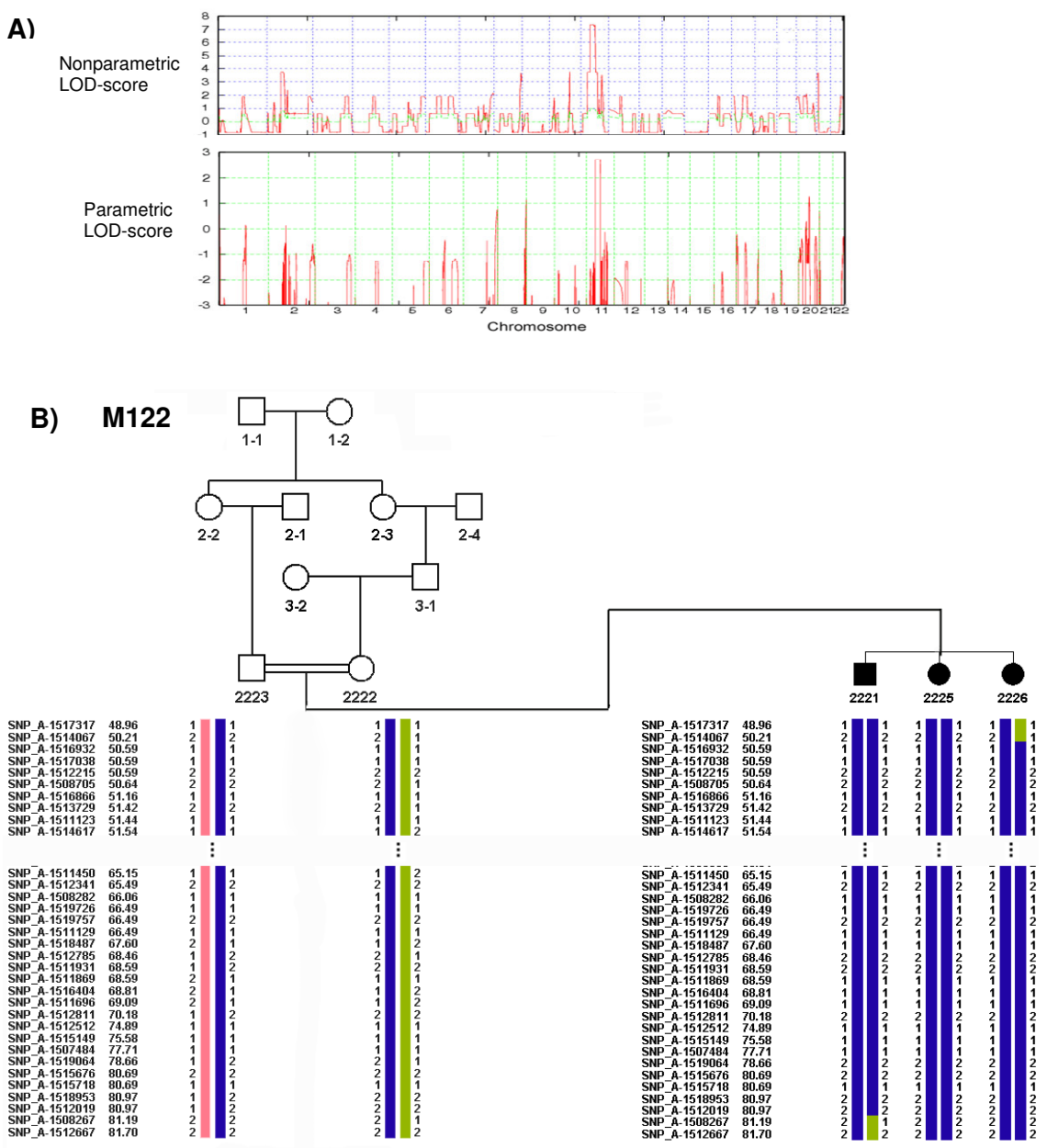

Figure 3-7: Family M122. (A) Whole genome parametric (Allegro) and non-parametric (Merlin) linkage results (B) The haplotype of the only linkage interval based on the "one LOD down" method.

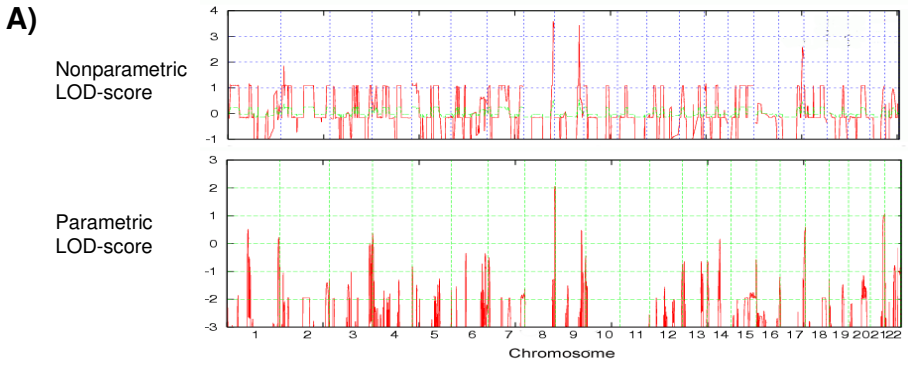

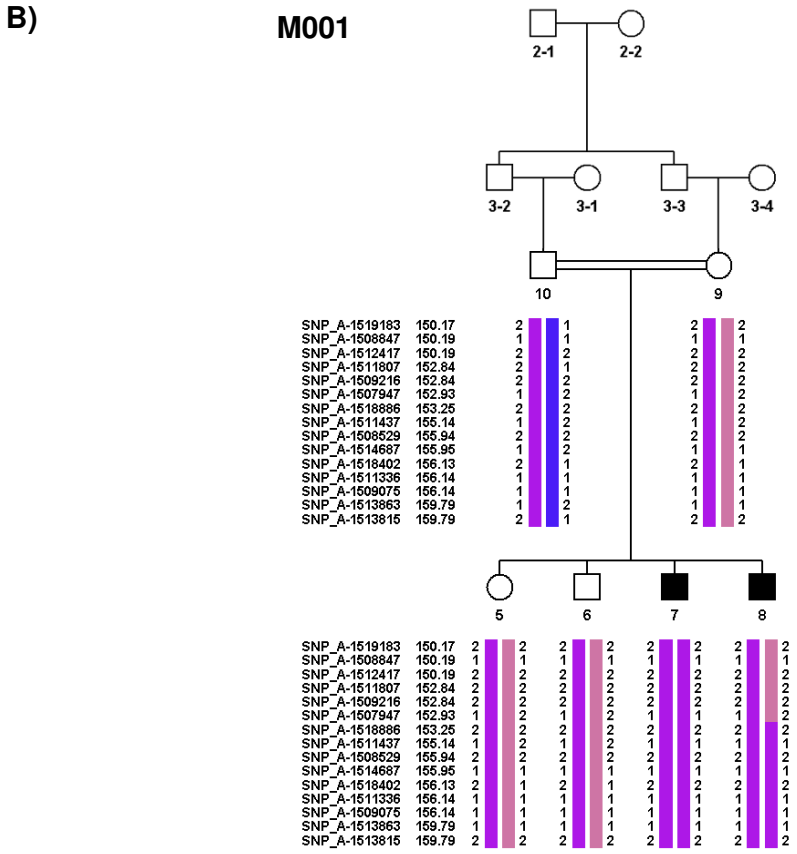

Figure 3-8: Family M001. (A) Whole genome parametric (Allegro) and non-parametric (Merlin) linkage results (B) The haplotype of the only linkage interval based on "one LOD down" method.

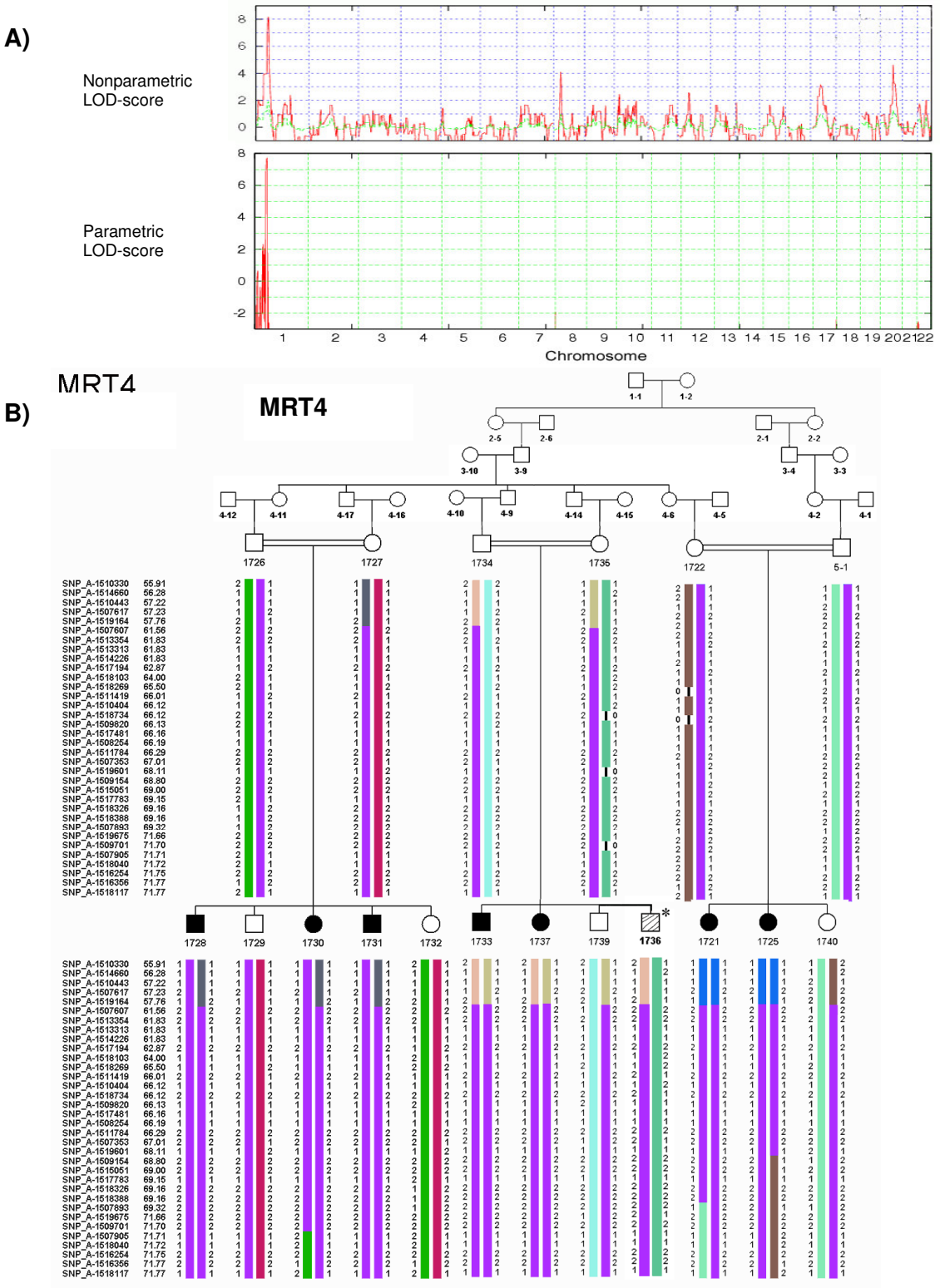

Figure 3-9: Family M096. (A) Whole genome parametric (Allegro) (B) Non-parametric (Merlin) linkage results and the haplotype of MRT4 locus.

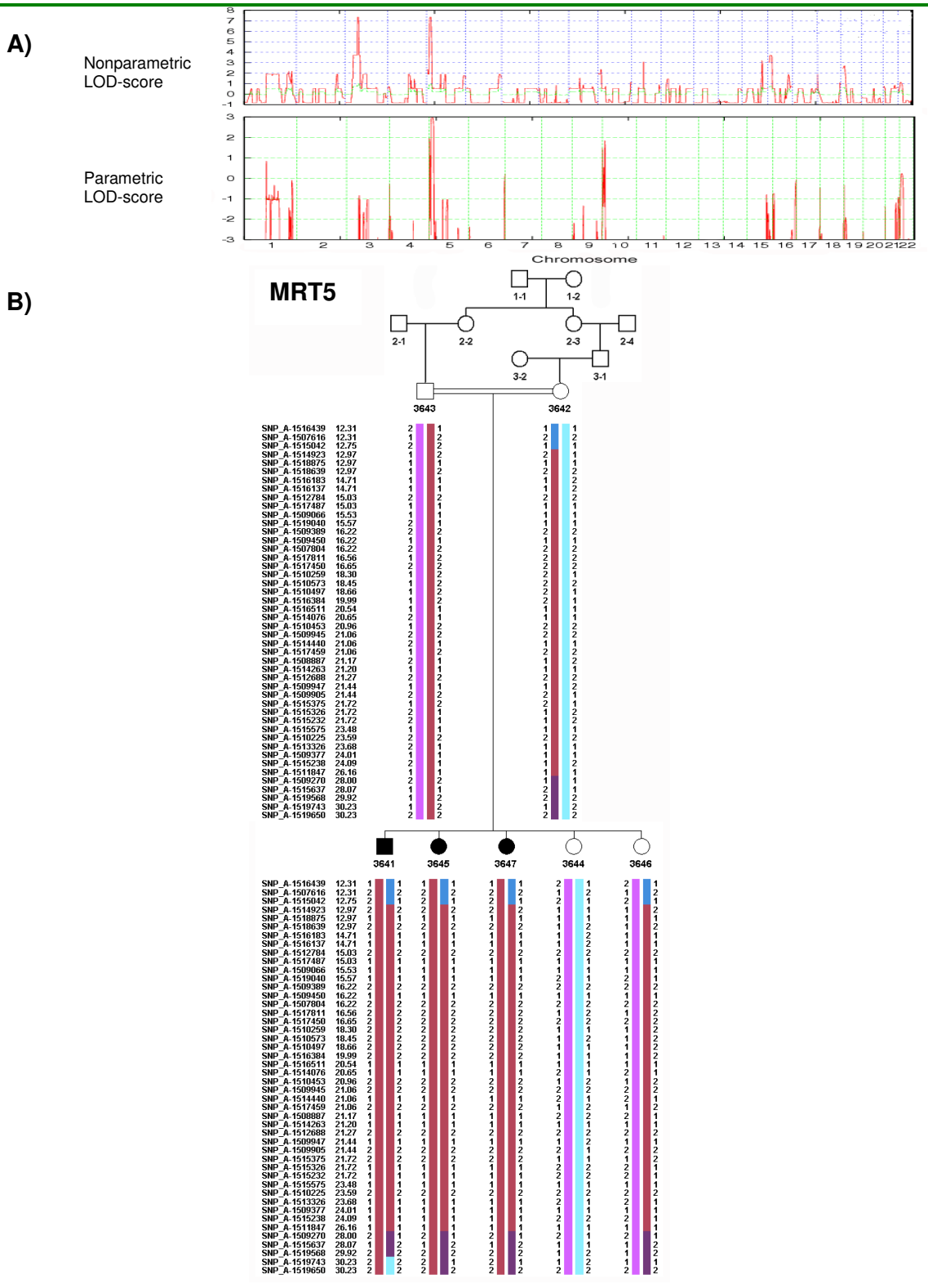

Figure 3-10: Family M192. (A) Whole genome parametric (Allegro) (B) Non-parametric (Merlin) linkage results and the haplotype of MRT5 locus.

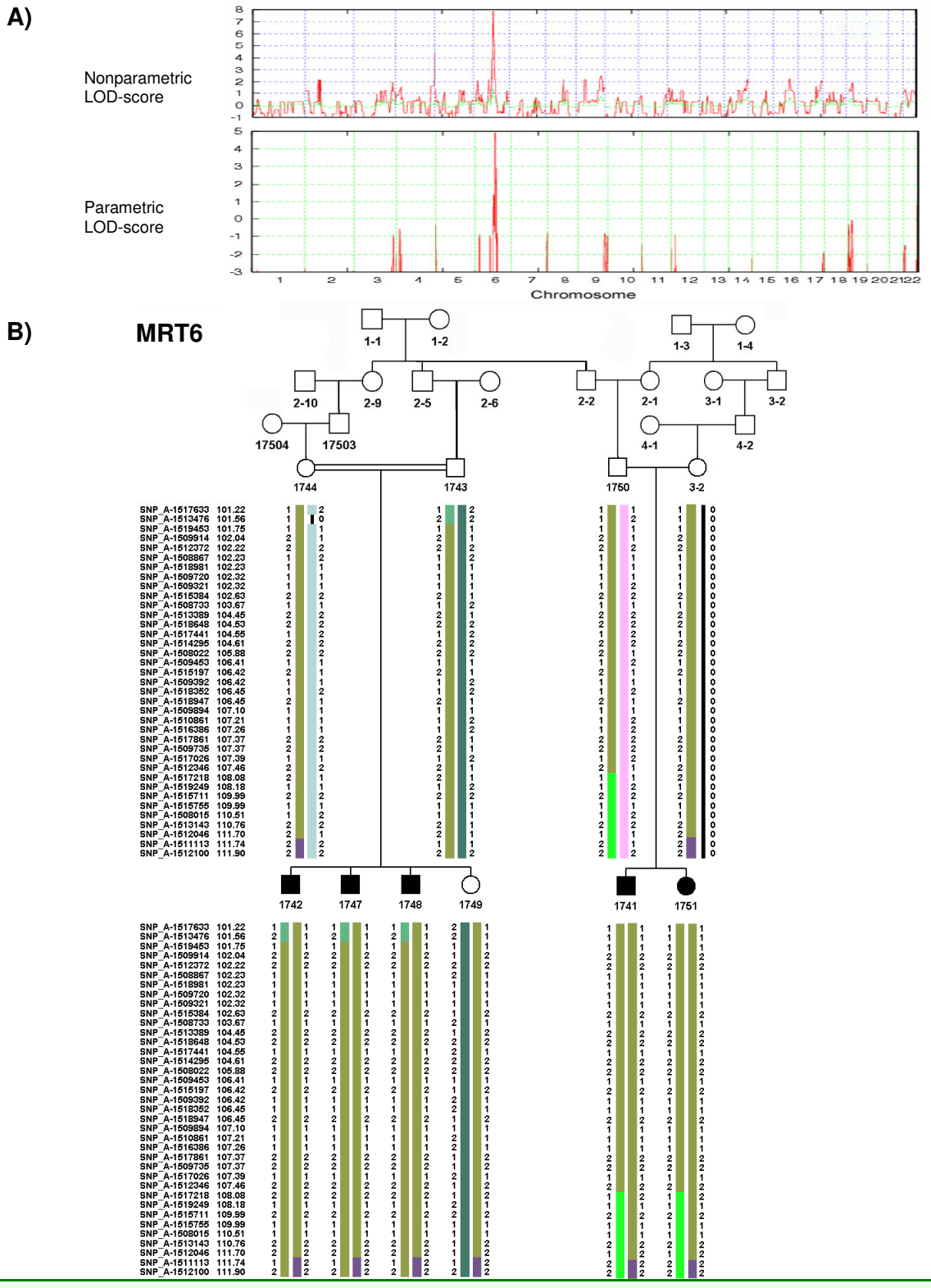

Figure 3-11: Family M097. (A) Whole genome parametric (Allegro) (B) Non-parametric (Merlin) linkage results and the haplotype of MRT6 locus (Detailed family structure in supplementary data D).

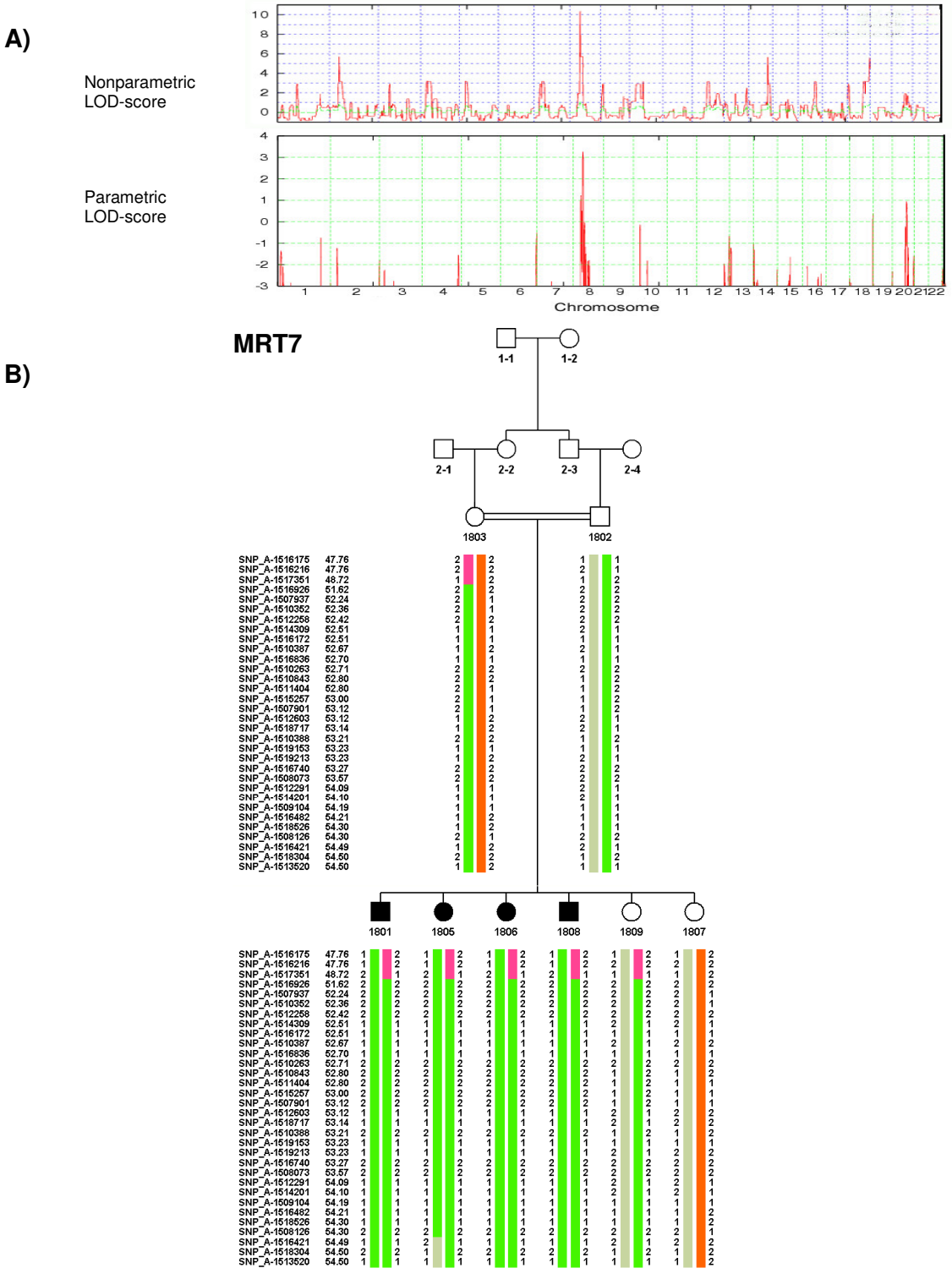

Figure 3-12: Family M100. (A) Whole genome parametric (Allegro) (B) Non-parametric (Merlin) linkage results and the haplotype of MRT7 locus.

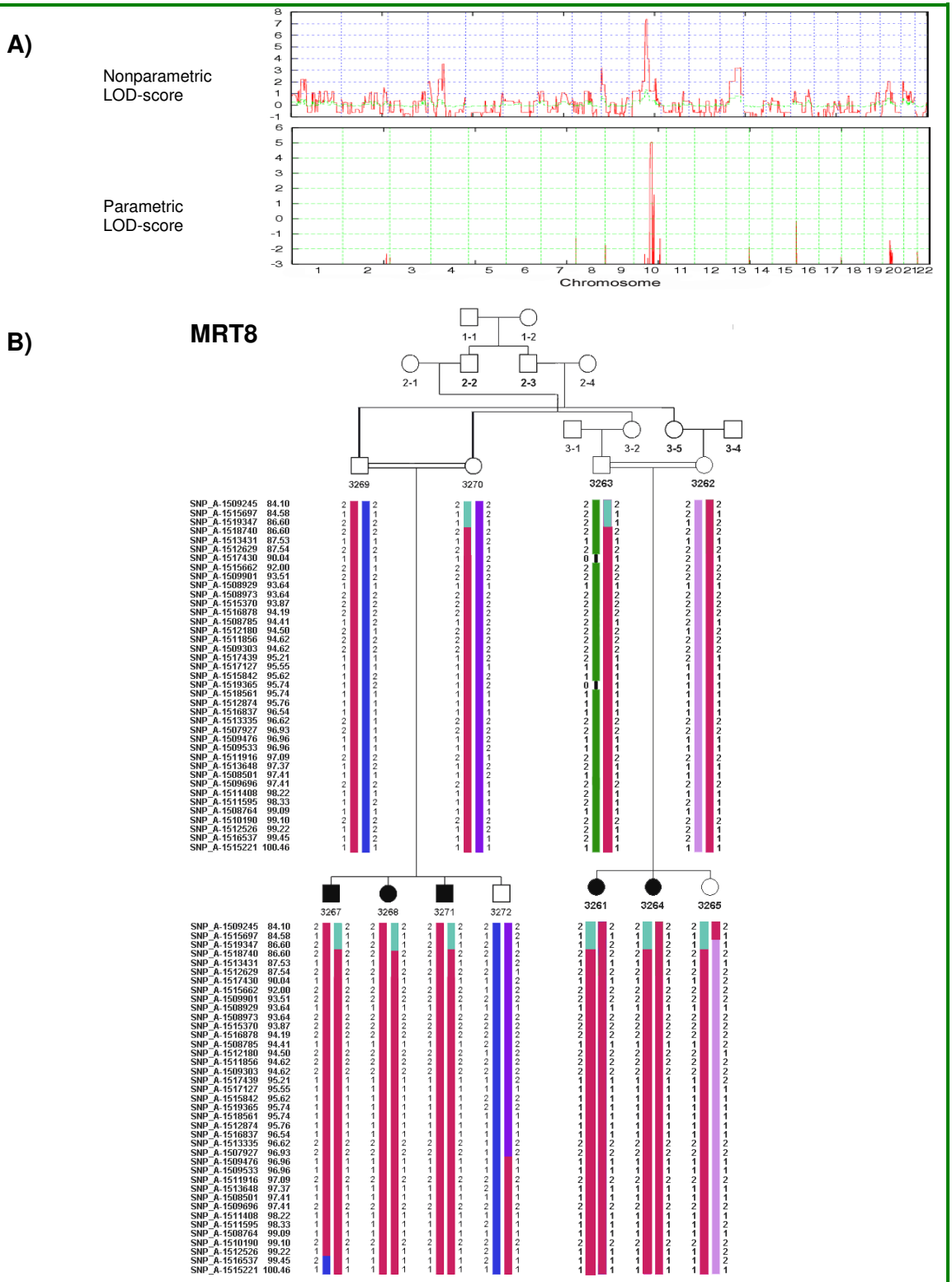

Figure 3-13: Family M173. (A) Whole genome parametric (Allegro) (B) Non-parametric (Merlin) linkage results and the haplotype of MRT8 locus.

3.2. Mutation screening in MRT loci

Prior to mutation screening of coding exons and exon-intron boundaries, genes in the MRT5 (Figure 3-10), MRT6 (Figure 3-11) and MRT7 (Figure 3-12) intervals as well as the only linkage intervals of families M001 (Figure 3-8) and M193 (syndromic ARMR, Figure 3-2B) were ranked according to their expression patterns and functional relevance in the central nervous system. Table 3-3 shows the genes for which mutation screening was performed.

Table 3-3: Candidate ARMR genes screened for mutation.

Family	Locus	Genes
M192	MRT5	*SEMA5A, ADCY2, ADAMTS16, MARCH6*
M097	MRT6*	*GRIK2, CCNC, COQ3, GPR145, GPR63, KIAA1900 (KLHL32), POU3F2, SIM1*
M100	MRT7	*NRG1, DUSP4, PURG, RBM13, DUSP26, FUT10*
M001	-----	*GRINA, ARC*
M193	-----	*STC2, GABRP*

* See supplementary data C for additional information.

This screen did not lead to the identification of disease causing mutations in families M192 (MRT5), M100 (MRT7), M001 and M193. In contrast, the failure to amplify exons 7 and 8 of *GRIK2* gene in patients from family M097 (MRT6) indicated the presence of a genomic deletion in these individuals (Figure 3-14).

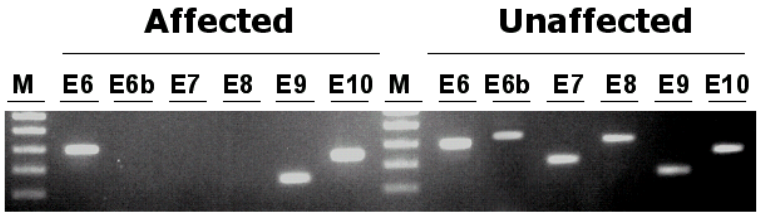

Figure 3-14: PCR amplification of exon 6-exon 10 from the *GRIK2* gene in one affected and one unaffected M097 family member. E6-E10: Amplicons pertaining to exons 6-10 (E6b: a provisional exon between exons 6 & 7, M: Size marker). For primer sequences see supplementary data A.

3.3. Genomic deletion in the *GRIK2* gene

GRIK2 is one of more than 20 annotated genes (Figure 3-15) in the 9.98 Mb of MRT6, located on chromosome 6q16.1-q21 (Supplementary data C).

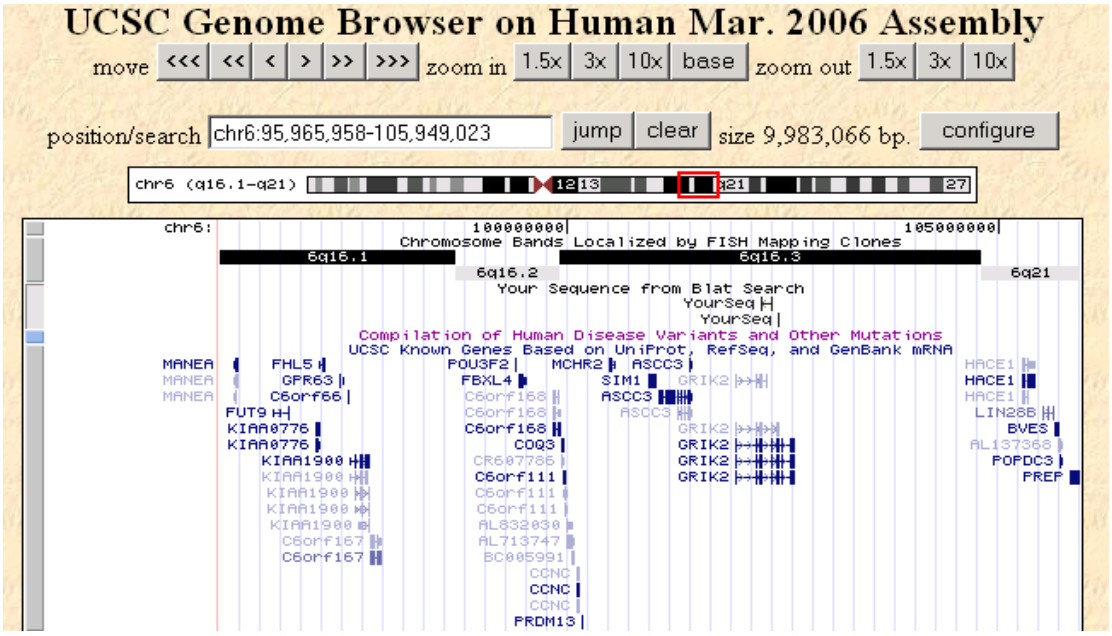

Figure 3-15: UCSC genome browser view of the MRT6 locus.

GRIK2 (Glutamate receptor, ionotropic, Kainate 2) encodes a subunit of kainate induced glutamate receptors (KARs). Glutamate receptors mediate the majority of excitatory neurotransmission in the brain. They are involved in excitatory and inhibitory neurotransmission in central nervous system and have a role in activity dependent synaptogenesis during development, synaptic plasticity and long-term potentiation. *GRIK2* is highly expressed in the brain especially in the cerebellum and cerebral cortex (Bahn et al. 1994).

The deletion found in *GRIK2* was determined to encompass ~120 kb, as shown by PCR-amplification of short DNA segments tiling initially proposed deletion borders. This approach was based on the assumption that the deletion borders were located between the last amplicons that could not be amplified and the first ones that could.

However, it turned out to be impossible to obtain a deletion spanning PCR product when using various combinations of primer target sequences from introns 6 and 8 that were not deleted in the patients (Figure 3-16).

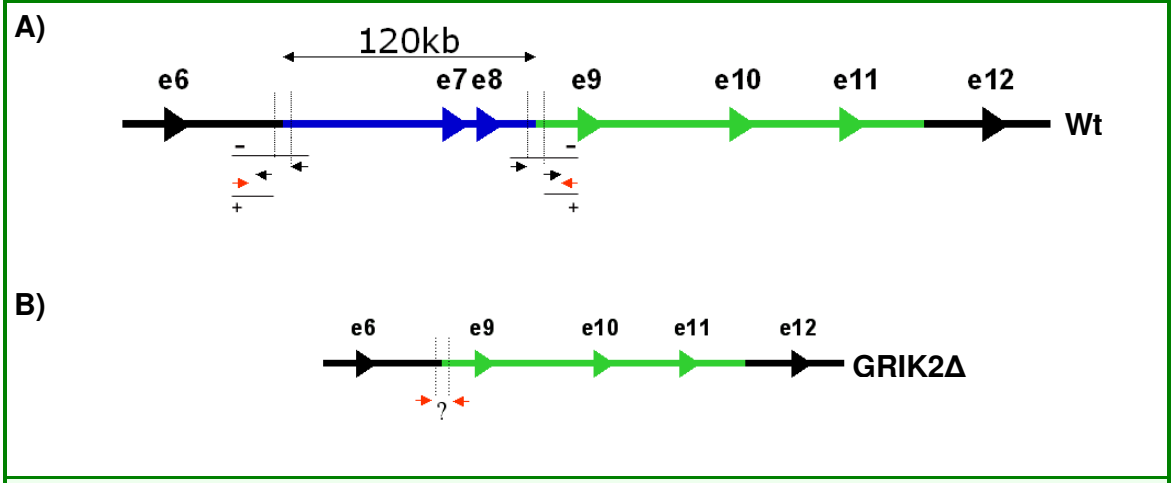

Figure 3-16: Schematic representation of *GRIK2* exons 6-12. A) Wild-type (Wt) and B) mutant *GRIK2* with the deletion found in MRT6 patients (*GRIK2*Δ). Exons and introns are represented by arrowheads and lines respectively. Dotted lines show the approximate position of the deletion borders. Small arrows show the primers used for border determination. The respective amplicons are indicated by lines of differing length. "+" indicates pcr-products that were successfully amplified, "-" shows which amplicons could not be obtained. Red arrows mark primers that were used for deletion spanning PCR but did not yield an amplicon.

As EBV transformed cell lines were available from all patients and two of their healthy siblings, we then explored the possibility of detecting a *GRIK2* mRNA transcript in these cells.

We performed a northern blot analysis to evaluate the level of wild-type *GRIK2* transcript in 5 healthy control lymphoblastoid cell lines as compared to total RNA from fetal brain. However, while the *GRIK2* transcript could be detected in fetal brain total RNA using a 600 bp radioactive probe, it was not possible to detect it in control lymphoblastoid cell lines, which indicated that the level of *GRIK2* expression in lymphoblastoid cell lines is extremely low and thus beyond the detection limit of our Northern blot analysis.

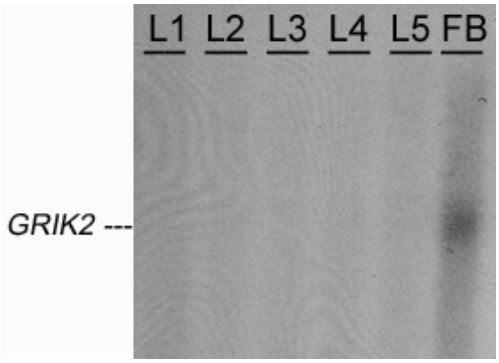

Figure 3-17: Northern blot analysis of 5 lymphoblastoid cell line total RNA (L1-L5) and fetal brain mRNA (FB) with a 597 bp P^{32}-labeled probe. A *GRIK2* transcript could be detected in fetal brain mRNA but not in lymphoblastoid cell lines.

Therefore, in order to be able to perform functional studies concerning the gene product of *GRIK2* without exons 7 and 8 (*GRIK2*Δ), we engineered a deletion construct from fetal brain RNA in a pcDNA-DEST47 expression vector (Figure 2-7B), where the original 3'GFP-tag was replaced by a c-myc-tag (Glu-Gln-Lys-Leu-Ile-Ser-Glu-Glu-Asp-Leu) followed by a stop codon.

3.3.1. Functional characterization of the gene product of *GRIK2*, lacking exons 7 and 8 (GLUR6Δ)

Loss of exons 7 and 8 in the *GRIK2* gene results in the formation of a GLUR6 protein with an in-frame deletion of 84 amino acids between aa317 and aa402, close to the first ligand-binding domain (S1) in the extracellular N-terminal region (GLUR6Δ; Figure 3-18).

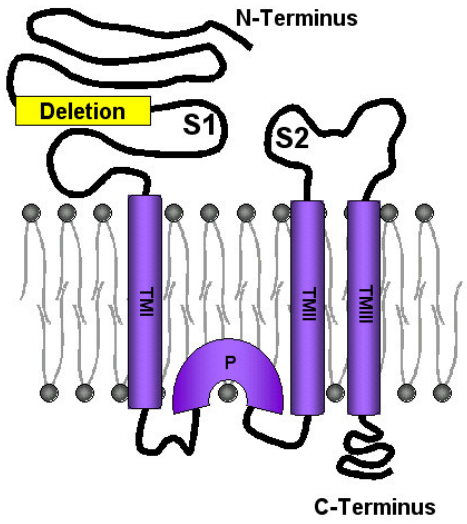

Figure 3-18: Schematic view of the GLUR6 protein structure and the position of the deletion. The deleted domain is shown by a yellow bar. S1 & S2 form the ligand-binding pocket. TM: Transmembrane domain. P: Pore forming domain.

Even though all the functional domains of the predicted protein are unaffected by a deletion of exons 7 and 8, it might still have an effect on the ligand binding properties of the resulting protein through its close proximity to the ligand binding structures. However, as it has been shown that GLUR6 structure is also important for its appropriate localization to the cell surface, with the integrity of the N-terminus and the C-terminus being important for its trafficking to the membrane (Jaskolski et al. 2004), the first question to ask was whether the defective protein would still be able to reach the cell surface. We therefore performed immunocytochemistry experiments and a cell surface protein biotinylation test to verify whether the deletion protein was able to pass the cytoplasmic checkpoints on its way to the plasma membrane.

The results of the immunocytochemistry studies showed clear co-localization of both wild-type GLUR6 as well as GLUR6Δ with the endogenous membrane protein, Cadherin in HEK293 cells transfected with the wild type or *GRIK2*Δ constructs (Figure 3-19).

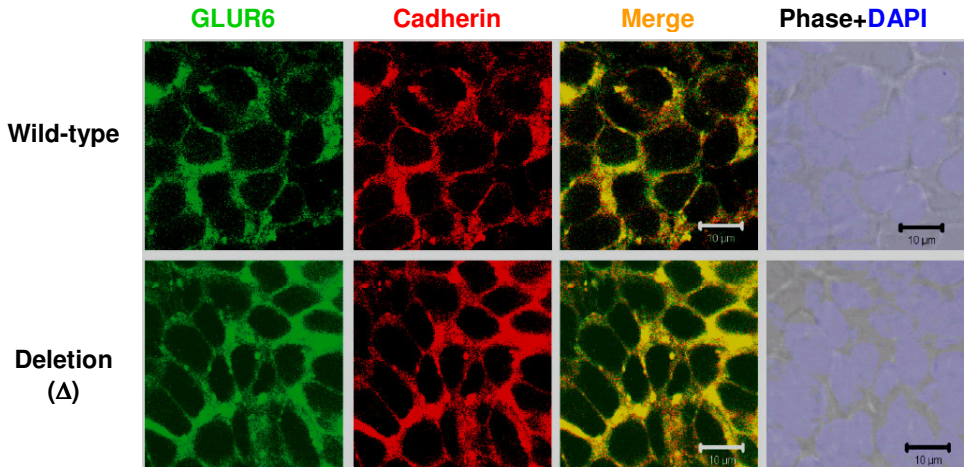

Figure 3-19: Immunocytochemistry studies in HEK293 cells transfected with *GRIK2* wild-type and Deletion (Δ) expression vectors and stained with Anti-GLUR6/7 (green) and Anti-Cadherin (red) antibodies. The results show co-localization of GLUR6 and Cadherin (used as plasma membrane marker).

The biotinylation experiments confirmed that these cells had considerable amounts of GLUR6 protein in the plasma membrane (Figure 3-20), as both GLUR6-Wt and GLUR6Δ were detected in the plasma membrane protein fraction. The cytoplasmic protein GAPDH could not be detected in the plasma membrane fraction, ruling out a possible contamination of the membrane fraction with cytoplasmic proteins (Figure 3-20).

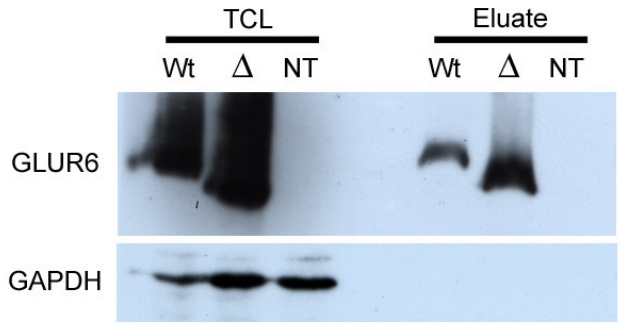

Figure 3-20: GLUR6Δ is present on the Plasma Membrane of transfected HEK293 cells. Both GLUR6-Wt/Δ are present in the membrane protein fraction (Eluate). TCL: total cell lysate. NT: untransfected cells

3.3.2. Further characterization of the genomic *GRIK2* mutation by Southern blot and I-PCR experiments

In parallel with the investigation of the cellular localization of GLUR6 and GLUR6Δ, PCR experiments were performed with various primer combinations to define the borders of the putative deletion of exons 7 and 8, but none of these led to the amplification of a junction-fragment. We therefore investigated the 5' region of the putative deletion in all available family members by Southern blot analysis. To detect the 5' border of the deletion, a 802 bp probe was used. The expected fragment size corresponding to a *GRIK2* allele lacking exons 7 and 8 was 1.5kb, still we identified a 6.5kb band in carriers of the mutant allele (Figure 3-21), which pointed to the presence of a more complex genomic rearrangement.

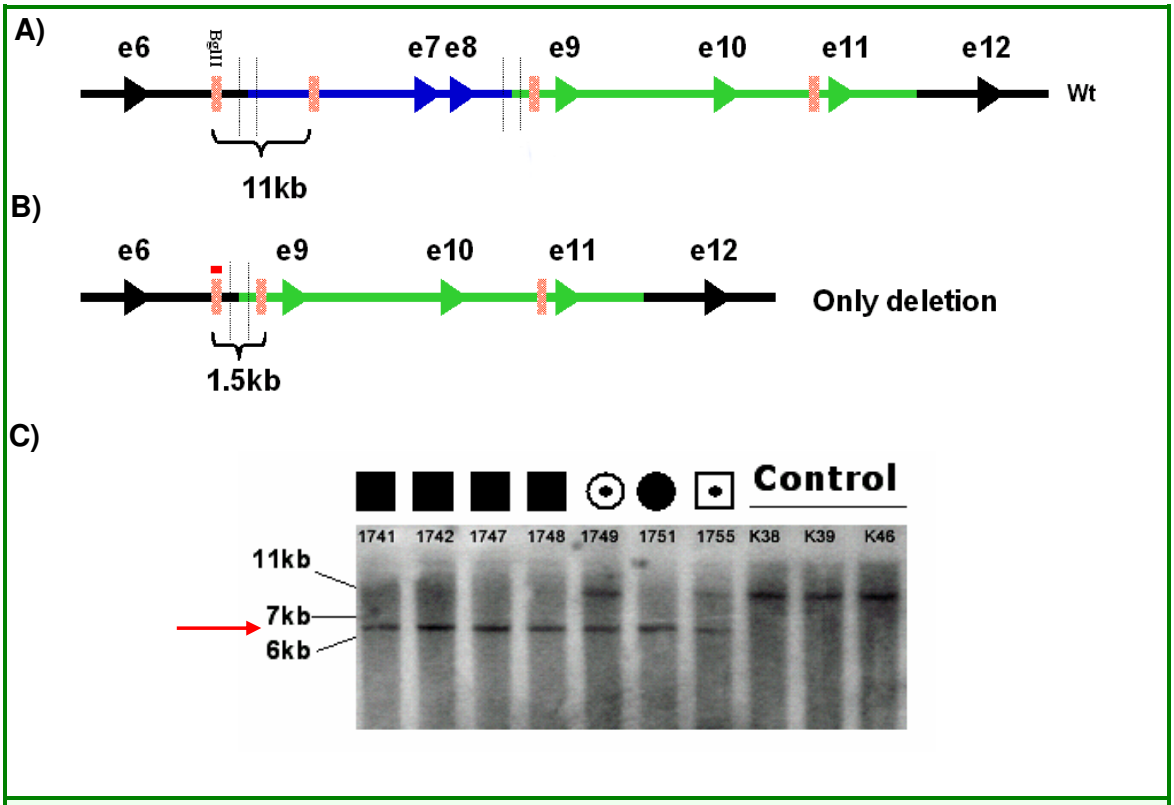

Figure 3-21: *Bgl*II Southern blot with probe specific for intron 6 of *GRIK2*: Schematic view of A) *GRIK2*-Wt and B) *GRIK2*Δ, with *Bgl*II restriction sites. Arrowheads and lines depict exons and introns respectively. Restriction sites are indicated with pink rectangles. The red bar in B) marks the position of the Southern blot probe. Dotted lines show the approximate position of the deletion borders. C) Southern blot results from patient, deletion carrier and control DNA. Instead of the expected 1.5kb band in deletion carriers, a 6.5kb band was observed (red arrow). The wild-type allele is detected as an 11kb band.

Therefore, aiming for the aberrant fragment detected by Southern blot, we performed an I-PCR experiment followed by cloning and sequencing of the relevant amplicon (Figure 3-22). This confirmed the deletion of exon 7 and 8 by uncovering a sequence junction between remnants of intron 6 and 8. This junction fragment was joined to a sequence fragment belonging to intron 11 in reverse orientation (Figure 3-23). Based on these results we proposed that the mutation comprises an inversion of about 80kb including exons 9,10 and 11 in combination with a 120kb deletion encompassing exons 7 and 8.

Figure 3-22: Inverse-PCR strategy and results. A) Schematic view of the proposed *GRIK2* mutant allele based on Southern blot results. Arrowheads and lines depict the exons and introns respectively. Restriction sites are indicated with pink rectangles. The irregular red line shows the unknown sequence detected by Southern blotting. Dotted lines show the approximate position of the deletion borders. B) The ~6.5kb band in *GRIK2* intron 6 specific Southern blots could be amplified in three affected and one carrier individual but not in the healthy control DNA (arrow).

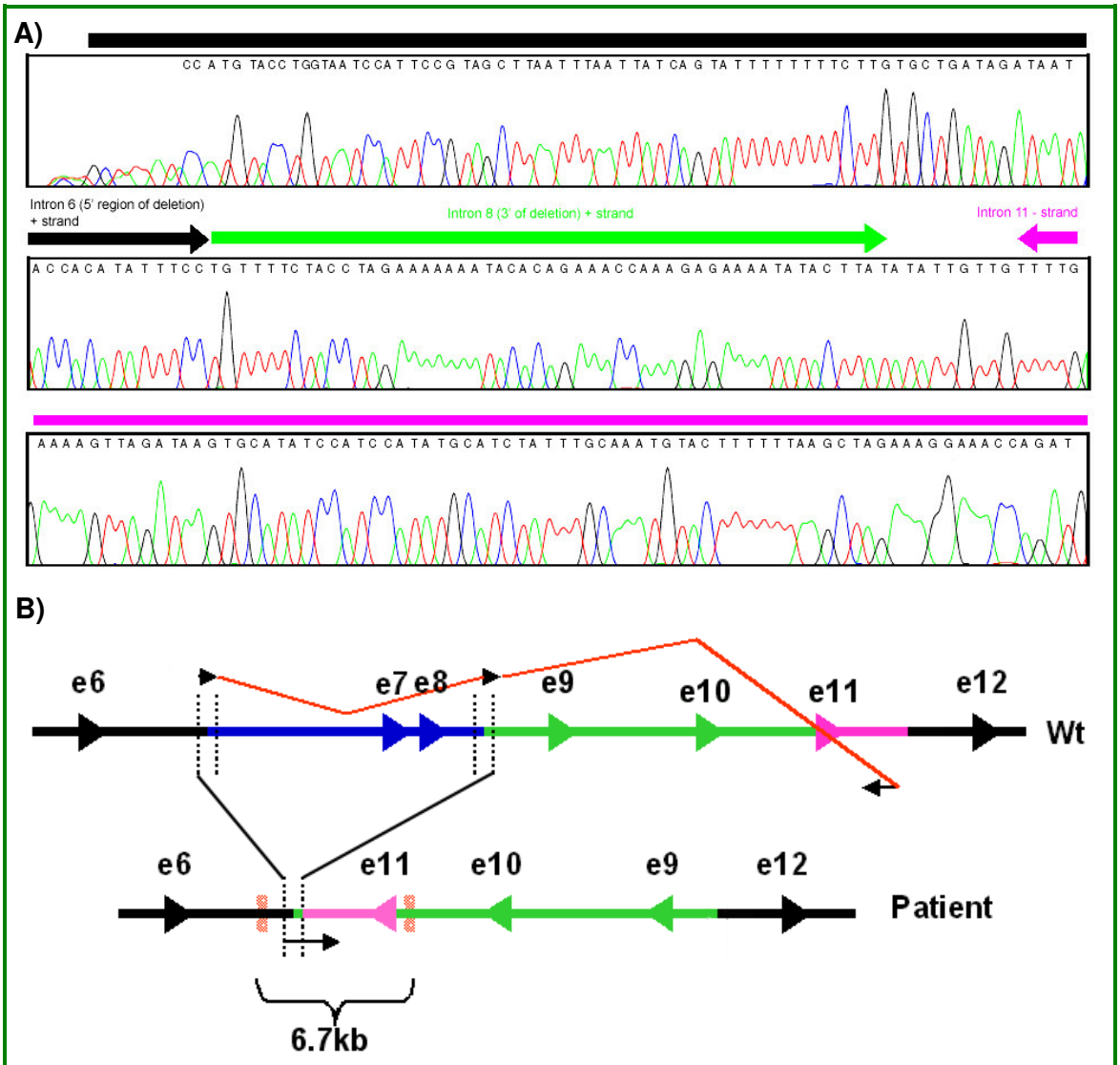

Figure 3-23: Sequencing result of the Inverse-PCR product. A) Chromatogram of the Inverse-PCR sequence showing the deletion borders (The junction between black and green arrows) connected to a reversely oriented fragment of intron 11 (The junction between green and pink arrow). B) Schematic deletion-inversion as model proposed by Inverse-PCR results: Wild type (Wt) and mutant (Patient) *GRIK2* genomic structure is shown. Arrowheads and lines depict the exons and introns respectively. *Bgl*II Restriction sites are indicated by pink rectangles. Red lines indicate the junction between intron 6, intron 8 and intron 11. Dotted lines show the approximate position of the deletion borders. The black arrow under the mutant allele indicates the mutant genomic region whose sequence is shown in A).

In order to test this hypothesis, we then attempted to determine the full extent of the mutation by searching for the 3' border of the mutation. For this purpose, we first

performed tiled PCRs of amplicons in intron 11. This led to the identification of an 18.7 kb deletion downstream of the previously assumed inversion border (Figure 3-24).

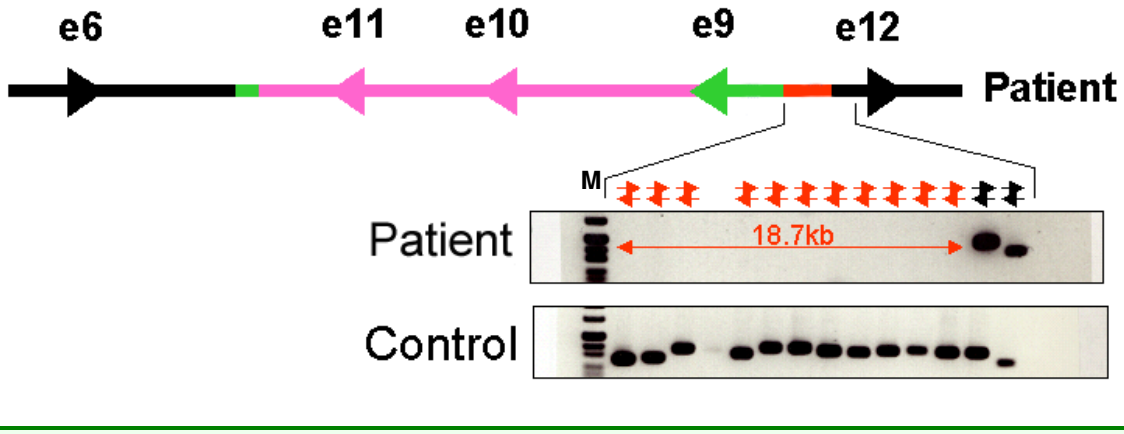

Figure 3-24: *GRIK2* Intron 11 deletion. An approximately 18.7 kb part of intron 11 could not be amplified from patient DNA. Arrowheads and lines depict the exons and introns respectively. The red line indicates the intron 11 deletion. Red arrows indicate the amplicons, which could not be amplified from patient DNA. Black arrows show the regions, which could be amplified in both controls and patients.

We then perfomed a Southern blot (using a 930 bp probe amplified from the 3' end of the inversion in intron 8, Figure 3-25B) and a border-spanning PCR (Figure 3-25A and C). Subsequent sequencing of the junction fragment allowed us to determine the exact sequence of the 3' border of the inversion (Figure 3-25D). The full extent of the mutation is depicted in Figure 3-26.

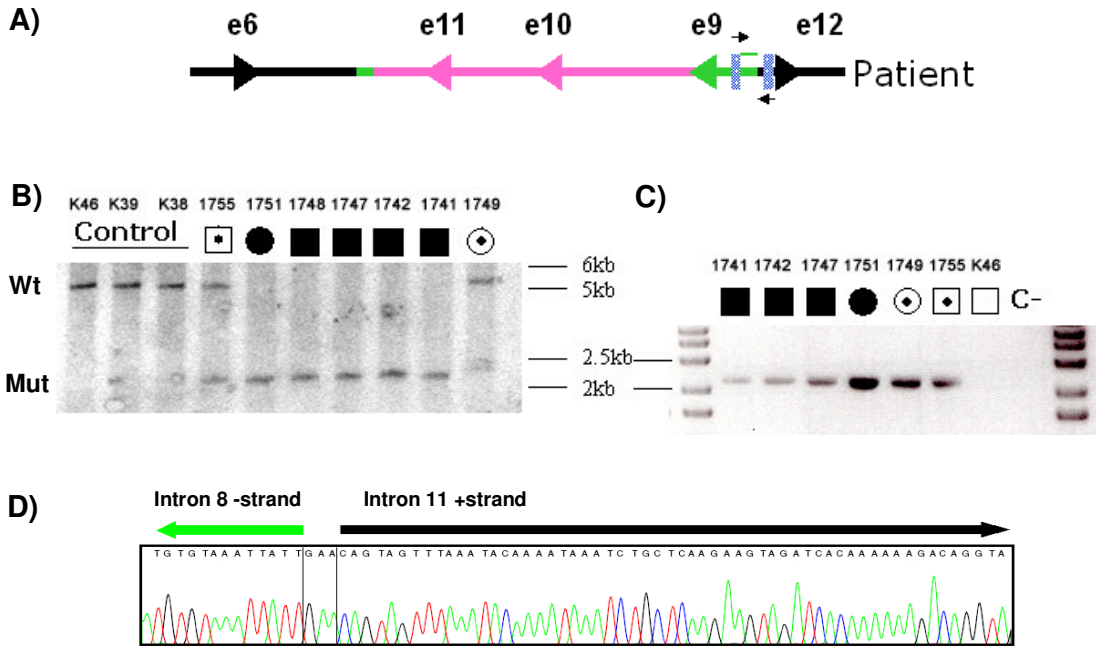

Figure 3-25: 3' border of the *GRIK2* mutation. A) Schematic view of the proposed *GRIK2* mutant allele with deletion-inversion mutation. A green bar marks the position of the Southern blot probe; *EcoR*IV restriction sites are indicated by blue rectangles. Arrows show primers for border spanning PCR. B) Southern blot results for the 3' border of the *GRIK2* mutation showing wild-type (Wt) and mutant (Mut) bands. C) Agarose gel electrophoresis of 3' border spanning PCR amplicon. D) Sequence of the 3' border spanning PCR amplicon showing a junction between intron 11 and reversely oriented intron 8 (Junction between black and green arrows).

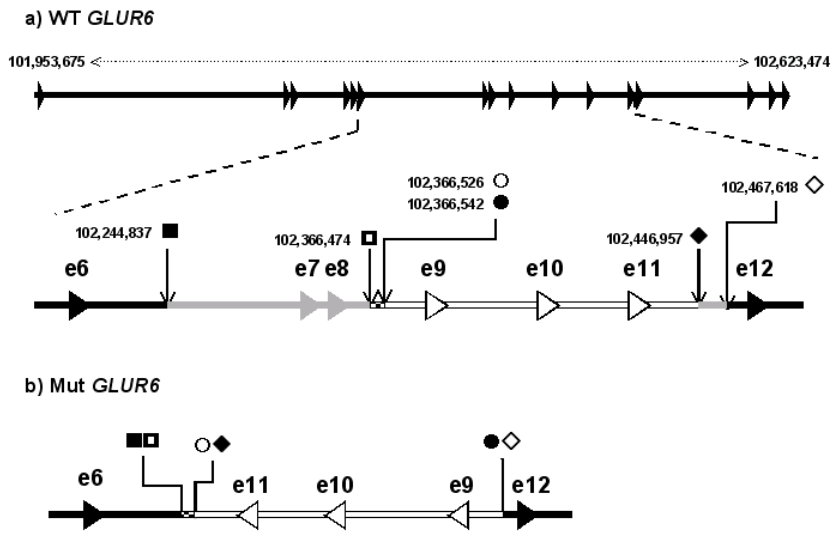

Figure 3-26: Genomic mutation in *GRIK2*: A) Schematic representation of the *GRIK2* wild-type allele. Physical coordinates (↔) of *GRIK2* are given according to NCBI build 36.1. Numbered arrowheads depict exons. Black shading indicates unaffected sequence, deleted regions are shaded in grey, and the inversion is marked in white. A checkered pattern marks the uninverted sequence fragment 5' of the deletion of exon 7 and 8. Squares, circles and diamonds mark the positions of the deletion and inversion borders. b) Schematic representation of the *GRIK2* mutant allele.

3.3.3. The *GRIK2* deletion is not a common polymorphism

In order to rule out the possibility that the change found in *GRIK2* might be a common polymorphism, DNA from a panel of 172 individuals holding university degrees was also screened by Southern blotting (Figure 3-21C). None of these controls carried the *GRIK2* deletion, not even in the heterozygous state. (see supplementary data F). Moreover, the mutation was not found in 390 individuals from a random population sample (healthy blood donors) that were screened by a deletion spanning PCR, using a primer located in the 53 bp sequence between the deletion and inversion.

3.3.4. *GRIK2* expression in lymphoblastoid cell lines of patients

With a deletion encompassing exons 7 and 8 in addition to an inversion comprising exons 9, 10 and 11, the predicted transcript should have a junction between exon 6 and exon 12.

In order to investigate the expression of mutant *GRIK2* in our family, cDNA from EBV-transformed lymphoblastoid cell lines (LBCs) of all available patients and healthy siblings was generated. This cDNA was used to perform PCRs with different combinations of forward primers from exon 6 and reverse primers from exons 12, 13 and 14. While RT-PCRs using exon 6 primers in combination with exon 12 and 13 primers did not lead to a consistent pattern of amplification from patient cDNA, a combination of primers from exons 6 and 14 resulted in an aberrant fragment in the homozygous and heterozygous carriers of the mutation (Figure 3-27A). The sequence of this amplicon showed a junction between exon 6 and exon 14 (E6-E14), pointing to a transcript that has not been reported as a splice variant of *GRIK2* so far (for more information about *GRIK2* splice variants please see supplementary data E). As compared to the transcript expected from the deletion/inversion, this corresponds to a transcript that translates into a GLUR6 protein, which in addition to S1, M1 and M2 also lacks the M3 transmembrane domain (Figure 3-27B). All other differentially spliced transcripts detected include a premature stop codon due to changes in the open reading frame, which lead to mRNA degradation by non-sense mediated decay. (Amrani et al. 2006). These transcripts are either the result of a junction between known GLUR6 exons (number 3), or aberrantly spliced unknown exon-like sturctures (number 4,5) created by the inversion (Figure 3-27A).

A)

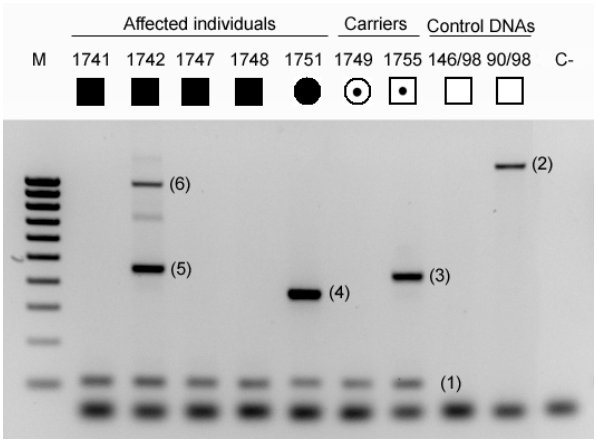

B)

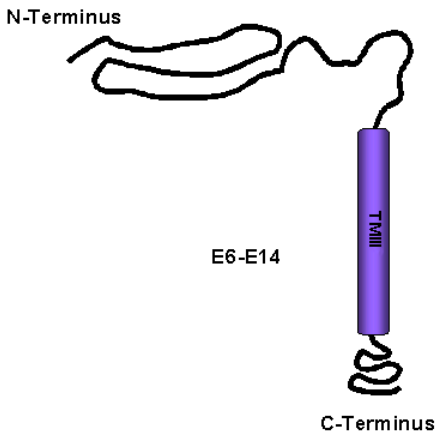

Figure 3-27: Evaluation of the GLUR6 transcript in the patient and control lymphoblastoid cells. A) Results of RT-PCR on the cDNA of patients, carriers and healthy controls lymphoblastoid cell line. The sequence of above observed bands show the transcript exon (E) content as follows: (1): E6-E14, (2): E6-E7-E8-E9-E10-E11-E13-E14, (3): E6-E12-E13-E14, (4): E6-E12b-E13-E14, (5): E6-I9R-E13-E14, (6): E6-E9-E10-E11-E12-E13-E14 (result of contamination with E7-8 deletion vector). B) Schematic view of the protein coded by the E6-E14 transcript.

4. Discussion

4.1. Homozygosity mapping in 48 families with NS-ARMR

Homozygosity mapping is a powerful strategy to localize and identify gene defects underlying autosomal recessive disorders (Lander and Botstein 1987), but this approach depends on the availability of large consanguineous families. Such families are common in Iran, where close to 40% of all children are born to consanguineous parents and 70% of the population is below the age of 30, which reflects large family sizes. As part of a collaborative effort to identify the molecular causes of NS-ARMR in a systematic fashion, we have recruited a cohort of unrelated Iranian families with NS-ARMR, which is by far the largest of its kind.

As gene mapping is an error-prone process, pre-linkage analysis control steps were employed to reduce error probabilities, which are to a great extent due to sample mix-ups and genotyping errors. However, not all of such mistakes can be prevented by these control methods. In 2 families, M145 and M155 (Figure 3-4) linkage analysis did not reveal any candidate interval. One of the possible reasons for this problem is mis-diagnosis. If, for example, a patient is mis-diagnosed as healthy individual, the linkage results can be greatly distorted because putative candidate haplotypes might be disregarded as they are then falsely assigned to an unaffected individual. Proper diagnosis is particularly crucial in mild forms of non-syndromic MR, where it is not easy to distinguish patients from healthy relatives whose mental abilities might appear to be low due to a lack of proper education. It is also a difficult issue when environmental and peri-natal causes of MR have to be considered.

Another problem that can affect the outcome of linkage analysis is the effect of high degree of consanguinity. High degree of consanguinity in some families in our cohort reduced the informative markers from 30-35% (expected) to 20-22% (observed) which was in line with previous studies implying that prolonged parental inbreeding leads to ~5% increase in the background level of homozygosity compared to predictions by simple models of consanguinity (Woods et al. 2005). This high degree of homozygosity increases the false-positive rate in homozygosity mapping and is

not always favourable. An example is family M181 (See Figure 3-5) in which more than 8 homozygous intervals were observed. Because these regions represent a large portion of the genome in which candidate gene selection is confined simply by the number of genes included, the result of linkage analysis in this family was excluded from overall comparison of results.

Our study of the remaining 41 families led to the identification of 5 new MRT loci and 2 putative loci with LOD scores between 2 and 3. A parallel study of additional 39 NS-ARMR families in our research group resulted in the identification of 3 additional MRT loci and 2 further single intervals with LOD scores between 2 and 3 (MRT9-11, Black and grey arrows without asterisks in figure 3-2). The fact that none of the three previously identified MRT genes or the 8 (plus 4) linkage intervals defined by this study coincide, strongly argues against the existence of a single frequent genetic cause of ARMR in the Iranian population. The same seems to be true for the published loci for primary microcephaly: mutations in these genes do not seem to contribute significantly to NS-ARMR (Garshasbi et al. 2006), although it has been shown that they do not necessarily lead to massive head size reduction (Trimborn et al. 2005; Garshasbi et al. 2006). Even though we observed an accumulation of linkage intervals in some parts of the genome such as the regions on chromosome 16 and 19 in which several families have at least one linkage interval overlapping an MRT locus (see Figure 3-5), no common mutation could so far be identified in these regions (Moheb et al., personal communication). Taken together, these findings suggest that NS-ARMR is at least as heterogeneous as NSXLMR, for which more than 30 different etiologically relevant genes are known to date (Chiurazzi et al. 2008), and that many more families will have to be investigated before firm statements can be made about the frequency and genomic distribution of NS-ARMR genes. For these future studies the focus should lie on large families, as those have a high probability of yielding small linkage intervals with high LOD scores.

To shed light on the nature and function of the novel MRT genes, mutation screening of functional and positional candidate genes has to be carried out. According to the ENSEMBL database, the 5 plus 2 newly identified MRT intervals contain more than 500 brain-expressed genes with a wide spectrum of different functions. Several of these belong to gene families that play a role in cognition, or

have previously been implicated in the aetiology of mental handicaps. A prominent example are glutamate receptors, which are known to play a central role in the brain, and it was particularly interesting that two members of the *GRIK* family (glutamate receptor, ionotropic, Kainate) map to novel MRT loci: *GRIK2* to MRT 6 (Chr. 6) and *GRIK3* to MRT 4 (Chr. 1). While we were able to identify a complex deletion-inversion mutation in the *GRIK2* gene, the coding sequence of *GRIK3* did not contain any damaging changes. This however is not surprising, considering the fact that the number of functionally interesting candidate genes mapping to these intervals is very large, and the search for the causative mutations is complicated by the fact that they are not necessarily located in the protein coding regions. The latter seems to apply at least to some of the smaller intervals, where mutation screening of all coding sequences and exon-intron boundaries is already approaching completion, and where the search may have to be extended to evolutionarily conserved non-coding sequences in order to find changes in the cis regulatory elements or newly created splice sites. Other approaches might help in these cases. For example, verification of the expression level of the MRT genes in patients in comparison to healthy individuals is such an alternative method. Although this approach is limited to the genes expressed in lymphoblastoid cell lines or skin fibroblasts, the only source of material available from the patients in this cohort. Another way to tackle the problem of finding disease causing mutations is the employment of novel sequencing techniques. These new multiplex sequencing-by-synthesis technologies are revolutionizing resequencing and will remove various obstacles that impair the systematic elucidation of genetic disorders. High-throughput, low-cost sequencing will greatly facilitate the search for causative mutations in large physical or genetic intervals defined by linkage studies and it will be economically feasible to screen entire genes, including introns, UTRs, and promoter regions, which are likely to harbour previously undetected pathogenetic variations (Ropers 2007).

4.2. The first *GRIK2* mutation in a family with NSARMR

The complex deletion-inversion mutation we identified in the *GRIK2* gene encompasses an in-frame deletion of exons 7 and 8 and inversion comprising exons 9, 10 and 11. All borders of the mutation we found are flanked by repetitive elements and low complexity regions as shown in Figure 4-1. But it is not clear, whether these relatively short elements can be considered to have been instrumental in causing the mutation.

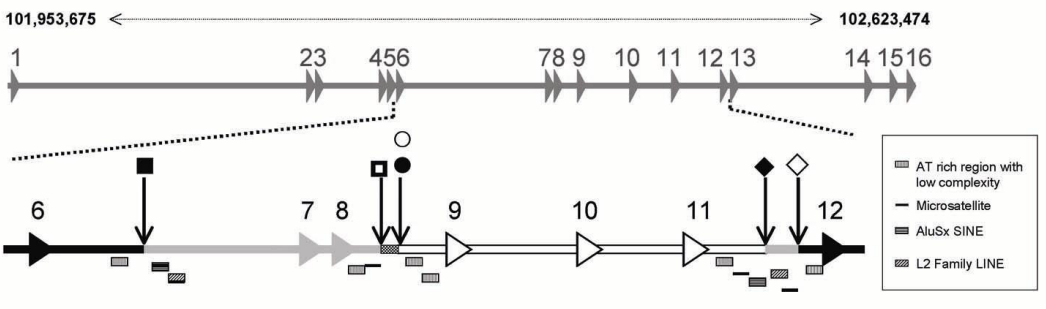

Figure 4-1: Genomic mutation in *GRIK2* and the position of the repetitive elements surrounding the mutation borders. Schematic representation of the *GRIK2* wildtype allele. Physical coordinates (↔) of *GRIK2* are given according to NCBI build 36.1. Exons are depicted by numbered arrowheads. Black shading indicates unaffected sequence, deleted regions are shaded in grey, the inversion is marked in white. A checkered pattern marks the uninverted sequence fragment 5' of the deletion of exon 7 and 8. Squares, circles and diamonds mark the positions of the deletion and inversion borders. Rectangular symbols below the schematic of *GRIK2* mark the locations of low sequence complexity regions or repetitive elements.

As the mutation borders are exactly the same in both branches of the family, it seems to be identical by descent, i.e. derived from the same common ancestor (who should be at least one generation older than the ancestors depicted in the pedigree of the family, Figure 3-11). The fact that a 53 bp segment from intron 8 in correct orientation separates deletion and inversion, suggests that deletion and inversion event could have happened separately. However, the occurrence of two rare events in such close proximity seems to be less probable than a single mutation event, unless one assumes that one event induced the other by destabilizing the sequence

integrity in this position. But which scenario is true cannot be answered by the data we have. Investigations of additional NS-ARMR patients who are distant relatives of our patients might shed more light on this question.

As the mutation is a complex and large deletion-inversion encompassing more than 200 kb we asked the question whether it might be part of an even larger chromosomal rearrangement in the genome of the patient.. To answer this question, submegabase resolution array CGH was performed in collaboration with the group of Dr. Ullmann at the Max Planck Institute for Molecular Genetics in Berlin. The results confirm that the deletion co-segregates with MR in all patients of this family (Figure 4-2), and exclude other co-segregating submicroscopic deletions or duplications. These findings corroborate our conclusion that the observed *GRIK2* mutation is solely responsible for the phenotype of the patient.

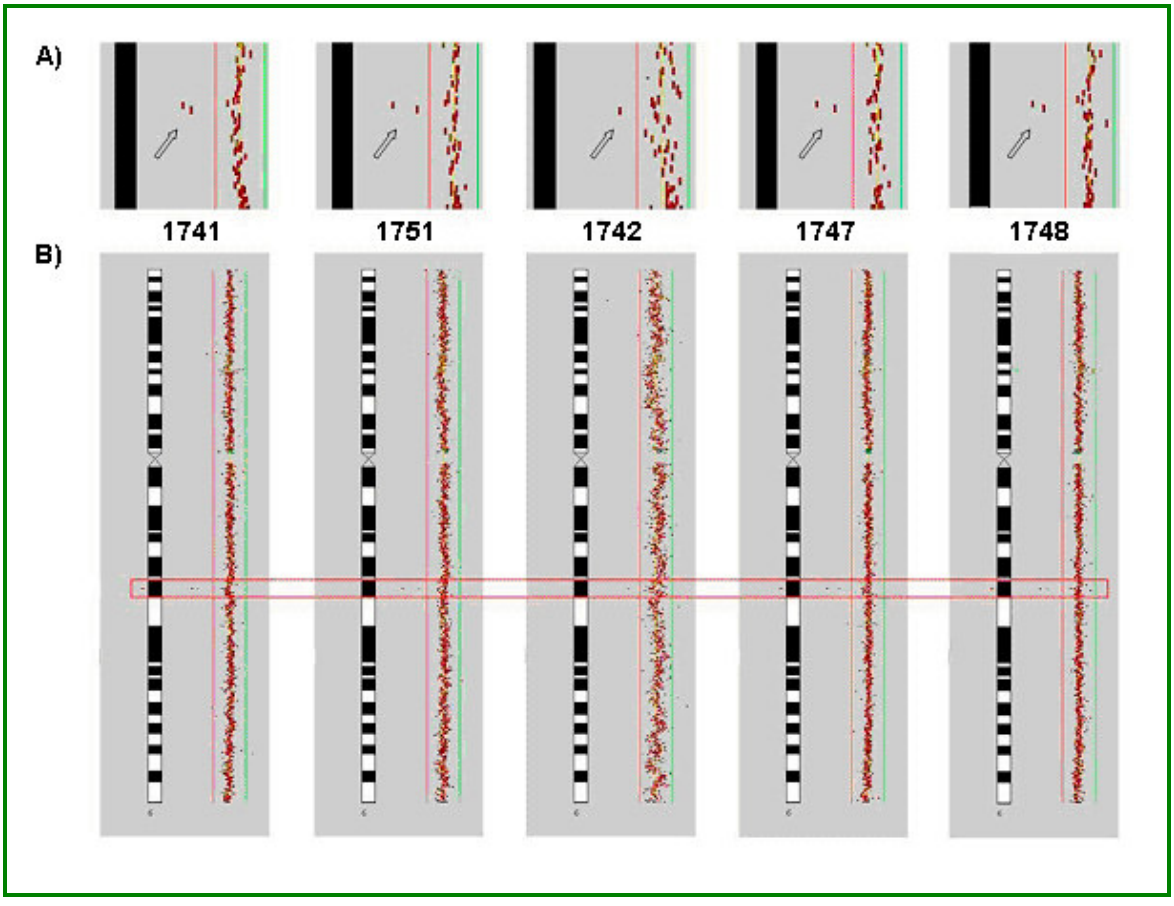

Figure 4-2: Array CGH results from MR patients. The experiments were carried out as previously described (Erdogan et al. 2006). Red and green bars indicate the log2-ratio thresholds -0.3 (loss) and 0.3 (gain), respectively. A homozygous deletion of 6q16.3 was the only aberration that co-segregated with the disease, being present in all affected and absent in all unaffected probands tested. A) Zoom-in of patient 6q16.3, demonstrating a deletion of two BAC clones (RP11-226C08 and RP11-543M18; indicated by arrow) encompassing *GRIK2* (due to lower hybridization quality in 1742 only one BAC represents the DNA copy number loss). B) Overall view of chromosome 6 in the corresponding cases. A red rectangle highlights the region depicted in A).

Additional evidence that the mutation is causative is provided by the absence of the mutation in 1124 chromosomes from 562 healthy individuals, a control cohort that was composed of healthy Iranian as well as German individuals to reduce the effect of population specific polymorphisms.

4.3. Impairment of GLUR6 channel function as cause of MR

As our initial mutation screening results only showed the absence of exons 7 and 8, our first approach to study GLUR6 function in our MR patients was to produce a *GRIK2* cDNA clone lacking these two exons and to investigate it in HEK 293 cells, which do not show endogenous *GRIK2* expression. The deletion of exons 7 and 8 leads to the loss of 84 amino acids between aa317 and aa402 close to the first ligand-binding domain (S1) in the extracellular N-terminal region of GLUR6 (Figure 4-3,a-a). In our experiments we compared the deletion construct with a wild type construct in order to find out whether the deletion construct would still be able to reach the cell membrane and if so, whether it would still be capable of forming functional ion channels.

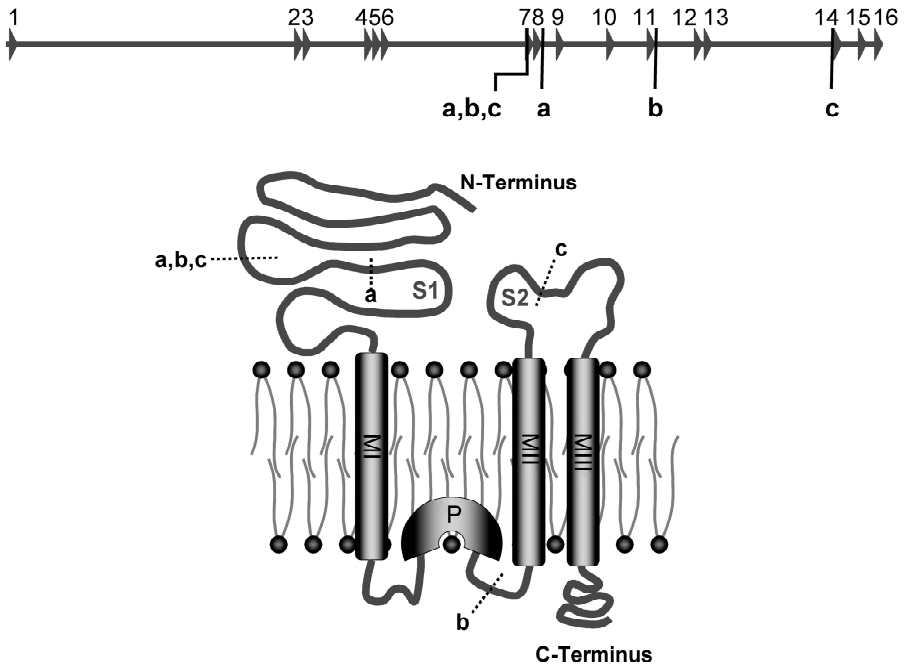

Figure 4-3: Impact of *GRIK2* mutation on GLUR6 protein structure. Shown is a schematic representation of the *GRIK2* wild-type allele and a cartoon of a GLUR6 monomer. MI–MIII = transmembrane domains; P = pore loop. Letters indicate the start and end of different alterations in the genomic sequence and their corresponding impact on the resulting protein. a = deletion of exons 7 and 8; b = complete genomic rearrangement, as observed in patients with MR; c = region lacking in the putative transcript with a junction between exons 6 and 14.

Using a biotinylation assay and immunocytochemistry experiments we could show that both the wildtype as well as the deletion protein localize to the cell surface. This indicated that the deletion does not prevent the protein from passing the relevant checkpoints in the endoplasmatic reticulum.

In order to investigate whether the deletion protein was still able to form functional ion channels we started a collaboration with Prof. Dr. Dietmar Schmitz and Benjamin Rost (Neuroscience Research center, Charite Universitaetsmedizin, Berlin) who performed electrophysiological experiments on HEK293 cells transfected with either *GRIK2* wildtype or deletion construct (GLUR6Δ). Whole cell patch clamp assays revealed that GLUR6Δ completely lost the ability to conduct ions when activated by

kainate (Figure 4-4A) or glutamate (not shown), independent of agonist dosage (Figure 4-4B).

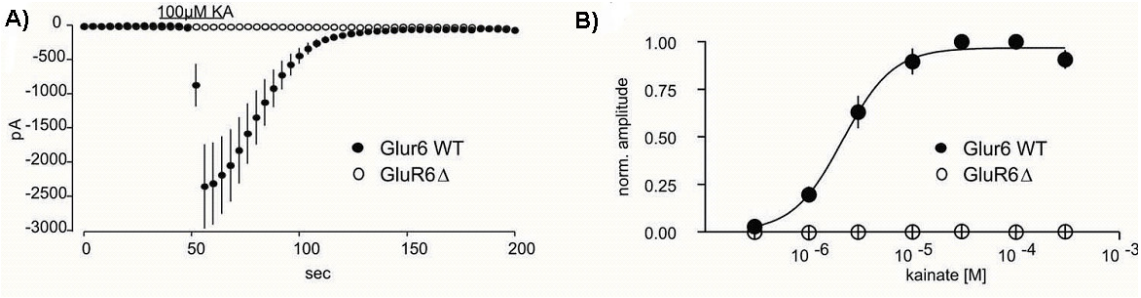

Figure 4-4: Loss of function in GLUR6Δ: A) Mean (GLUR6-WT: n = 8; GLUR6Δ: n = 9) currents evoked by 100 µM Kainate. B) Dose-response curve for Kainate, normalized to response in 100 µM Kainate. Error bars represent standard error of the mean (GLUR6-WT: n = 6 to 8 per reading point; GLUR6Δ: n = 3 to 9 per reading point). HEK293 cells were co-transfected with either GLUR6-WT or GLUR6Δ plasmid in combination with a green fluorescent transfection marker (1.8 µg cDNA encoding wild type *GRIK2* or *GRIK2*Δ plus 0.2 µg pEGFP-N1-vector, BD Biosciences Clonetech) using the tranfection reagent Fugene (Roche). For whole cell patch clamp r*EcoR*dings, cells were detached with 1 mM EDTA in cold PBS, 24 or 48 h post transfection, transferred to Poly-D-lysin coated coverslips and allowed to settle for at least 4 h. The r*EcoR*dings were performed using an intracellular solution containing 130 mM CsCl, 9.4 mM NaCl, 1 mM $MgCl_2$, 0.2 mM GTP, 10 mM EGTA and 10 mM HEPES (pH adjusted to 7.3 with CsOH). The cells were superfused with HEPES-buffered solution (140 mM NaCl, 2.4 mM KCl, 10 mM Glucose, 10 mM HEPES, 2.5 mM $CaCl_2$ and 1.3 mM $MgCl_2$; pH adjusted to 7.3 with NaOH) and treated for 5 minutes with 200 µg/ml Concanavalin A (ConA) in glucose free extracellular solution immediately before r*EcoR*dings, in order to prevent lectin aggregation. Cells were voltage clamped at –60 mV, using an Axoclamp 700A. R*EcoR*dings were digitized with 5 kHz and analysed online using IGOR Pro (Wavemetrics). All r*EcoR*dings were performed at room temperature.

Furthermore, in order to exclude the possibility of altered receptor desensitization, a fast application system (Adesnik et al. 2005) was used for performing whole-cell patch clamp experiments without ConA. Again, a complete loss of function of GLUR6Δ as compared to wild-type GLUR6 channels was observed (Figure 4-5).

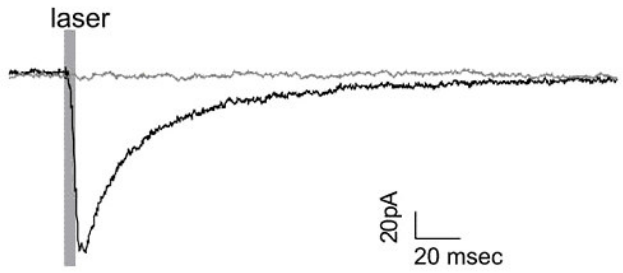

Figure 4-5: Loss of function in GLUR6Δ: Cells expressing WT *GLUR6* show photolytically evoked glutamate responses without prior incubation in ConA (black) whereas *GLUR6*Δ expressing cells show no currents after fast glutamate application (grey). Each trace represents the mean of 5 successive sweeps. 40 µM MNI-caged-glutamate (Tocris) was perfused continuously on the cells in a volume of 10 ml. A 355nm UV laser beam (DPSL-355-1W laser, Rapp Optics) was coupled via a 200 µm quartz fibre optic into a spot illumination adaptor (Rapp Optics), mounted in the epifluorescence path of an Olympus BX51WI microscope (equipped with a laser beam splitter and a 420 nm long pass emitter, both from AHF Analysetechnik) and focused with a 60x water-objective (numerical aperture 0.9; Olympus) onto a spot approximately 40 µm in diameter. The holding current was constant during washing of the caged glutamate.

Taken together, these findings strongly suggested that a deletion of exons 7 and 8 was already sufficient to abolish GLUR6 ion channel activity in carriers.

Still, at the same time our inability to amplify a deletion spanning junction fragment from patient DNA necessitated further experiments to precisely characterize the structure of the mutation. This led to the identification of the more complex rearrangement, comprising not only a deletion of exons 7 and 8, but also an inversion encompassing exons 9, 10 and 11. While the deletion of exons 7 and 8 is in-frame and followed by a short stretch of DNA belonging to intron 8, the complete rearrangement is not in frame any more. It therefore results not only in the removal of S1, TMI and P domains of the protein but also in a premature stop codon in the first part of exon 12 (Figure 4-3), which turns it into a typical substrate for nonsense mediated mRNA decay (NMD) (Amrani et al. 2006).

Our failure to detect endogenous *GRIK2* transcripts by Northern blot analysis indicated that *GRIK2* expression in lymphoblastoid cell lines (which were the only available source of material from the patients) is very low. However, by applying drastic RT-PCR conditions (i.e. 50 PCR cycles or re-PCR) we were able to observe sequences from several aberrant transcripts in RNA from patient lymphoblasts. These showed junctions between exon 6 and 12, exon 6 and 13 or exon 6 in combination with intron 9 and exon 13. All these sequences result in a premature stop codon in the sequence part immediately succeeding exon 6. In one case where an intron 9 sequence in reverse orientation was observed (Figure 3-27A, band No. 5), this was due to the fact that in reverse orientation intron 9 contains an exon like structure which could be spliced in as a consequence of the inversion. The only transcript, which shows an in-frame deletion, had a junction between exon 6 and exon 14 (Figure 3-27B). This transcript however lacks the coding sequences for both ligand-binding domains (S1 and S2), the first two transmembrane domains and the pore forming loop domain leading to an even larger protein defect than what was predicted from the genomic DNA.

Based on this evidence, and according to the fact that lack of exons 7 and 8 alone was sufficient to abolish GLUR6 channel function, it is obvious that homozygous carriers of the observed mutation cannot form functional GLUR6- containing ion channels, which in turn causes the observed MR phenotype.

So far, *GRIK2* is the first ion channel that has been causally implicated in MR. In the context of the evoked current, the response of AMPARs to glutamate is much more intensive than that of KARs (see figure 1-5A). This is interesting, because it might indicate that KARs are fine modulators of the evoked currents and that therefore, their inactivation is not lethal but leads to more subtle cognitive impairment.It is of note, however, that our findings seem to be at variance with the phenotype of *GRIK2* knockout mice. Sensorimotor tests including walk initiation, limb posture, visual placement, bridge crossing, negative geotaxis and muscle strength have not shown any specific changes in GLUR6$^{-/-}$ mice. A rotarod test has shown no change in sensorimotor learning in GLUR6$^{-/-}$ mice and therefore no obvious deficit has been attributable to cerebellar function in GLUR6$^{-/-}$ mice. Although GLUR6$^{-/-}$ mice have

been less active than the wildtype, in the Morris water maze test learning ability has been comparable between wild-type and knockout mice (Mulle et al. 1998).

The only abnormality reported in mice was a significant reduction in both contextual and auditory fear memory at early (1 and 3 days) as well as later (1 and 2 weeks) time points after fear conditioning in the *GRIK2* knockout mice (Ko et al. 2005). In the light of our findings, a detailed re-evaluation of the genotype-phenotype correlation in *GRIK2*$^{-/-}$ mice will be necessary.

4.4. Additional GLUR6 functions that might be involved in the aetiology of MR

As we observed a transcript containing a junction between exon 6 and 14 in patient lymphoblasts which does not have a premature stop codon and could thus still be translated into protein, it might be interesting to ask whether there are other functional aspects of GLUR6 that can still be influenced by such a protein fragment.

Indeed it has been found that C-terminal trafficking determinants in the GLUR6 KAR subunit are responsible for the efficient targeting of homomeric KARs to the plasma membrane (Yan et al. 2004). Electrophysiological r*EcoR*dings and confocal immunofluorescence have shown that robust surface expression of GLUR6 receptors is dependent on a minimal motif composed predominantly of basic residues in the medial portion of the C-terminal tail as well as a cysteine residue shown to be a substrate for palmitoylation (Pickering et al. 1995). This basic domain, which is a critical component for forward trafficking of the GLUR6 subunit and therefore represents an important determinant of KAR function, would be present in a protein lacking exons 7-13. Although this aberrant protein cannot form functional channels, its surface localization might be of great importance because of the following reasons:

In addition to an involvement in canonical ion flux signalling pathways, KARs have functions in a noncanonical signalling pathway (Figure 4-6) that links KARs to G-protein activation, which in turn might regulate voltage-dependent Ca^{2+} channels

(Rodriguez-Moreno and Lerma 1998; Rozas et al. 2003). It is not well known how canonical and noncanonical signalling pathways are related (Lerma 2006), but GLUR6 and KA2 subunits are involved in both processes (Melyan et al. 2004; Fisahn et al. 2005).

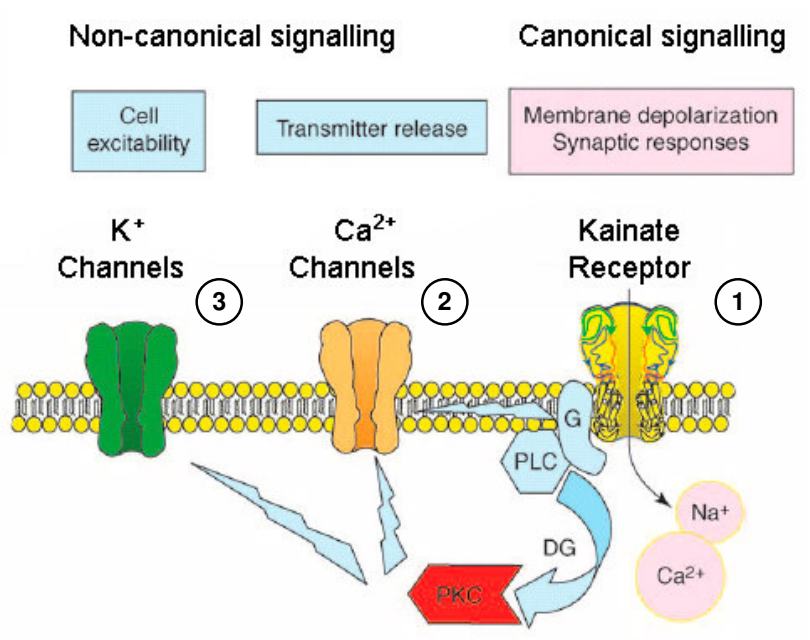

Figure 4-6: Dual signalling by KARs. KARs can form cationic ion channels (the canonical pathway), through which, upon activation, they depolarize the membrane (1). However, they can also act as part of a noncanonical signalling pathway involving the activation of a pertussis toxin-sensitive G protein (G). As a consequence, phospholipase C (PLC) is also activated, leading to the activation of Protein Kinase C (PKC), probably by the increase in diacylglycerol (DG). This second-messenger system could inhibit Ca^{2+} channels and intracellular Ca^{2+} signal ($[Ca^{2+}]_i$) (Rozas et al. 2003). This action might lead to the modulation of transmitter release (2). The activation of PKC could produce the inhibition of the Ca^{2+}-dependent K^+ current responsible for the repolarization of the membrane after repetitive firing (slow afterhyperpolarizing current [I_{sAHP}]) (Melyan et al. 2004). The inhibition of such a current by KARs drastically increases membrane excitability (3); (Figure edited from (Lerma 2006).

Noncanonical signalling leads to an inward Ca^{2+}-activated K^+ current (slow after hyperpolarizing current: I_{sAHP}) and does not rely on the activation of a KAR-mediated current. Experiments showing that the modulation of I_{sAHP} is significantly decreased in GLUR6 and KA2 knockout mice have established a specific involvement of

GLUR6 in this signalling pathway. What is more, I_{sAHP} modulation is supposed to be mediated by G-proteins and it has been shown that it is the KA2 subunit in GLUR6/KA2 complexes which establishes the conexion with e.g. $G\alpha_{9/11}$ (Ruiz et al. 2005) while KA2 membrane localization in turn depends on GLUR6. So altogether, as the non-canonical signalling pathway of GLUR6 might be KA2 dependent and KA2 surface expression is GLUR6 dependent, the existence of a fragmented GLUR6 protein with intact N- and C-terminus might still promote KA2 surface localization and subsequently sustain the function of the non-canonical KAR signalling pathway. If this were true, it would mean that it is indeed the impairment of canonical signalling that leads to MR in our patients.

In addition, a defect in the non-canonical signalling pathway could be a plausible explanation for the cognitive impairment of homozygous *GRIK2* mutation carriers. This is illustrated by the fact that several XLMR genes code for proteins involved in G-Protein mediated intracellular signalling: *OPHN1*, *ARHGEF6*, *PAK3*, and *GDI1*. *OPHN1* (oligophrenin) is a Rho-GTPase-activating protein (Billuart et al. 1998), whereas ARHGEF6, also called aPIX, belongs to the group of guanine nucleotide exchange factors (GEF) for Rho-GTPases (Kutsche et al. 2000). *PAK3* (p21 activated kinase 3) is a downstream effector of Rho-GTPases, like Rac and Cdc42 (Allen et al. 1998). The GDP dissociation inhibitor *GDI1* controls the activity of GTPases like *Rab3a*, by maintaining *Rab3a* in the inactive GDP-bound form (D'Adamo et al. 1998).

So further studies should include the investigation of pathway specific effects e.g. by an approach that allows to block each of the two KAR signalling pathways individually in a cell or animal model. Furthermore, as $GLUR6^{-/-}$ and $KA2^{-/-}$ mice are already available, a phenotype comparison between the two could be a first step towards finding out in which way the two KAR signalling pathways can play a role in the aetiology of MR.

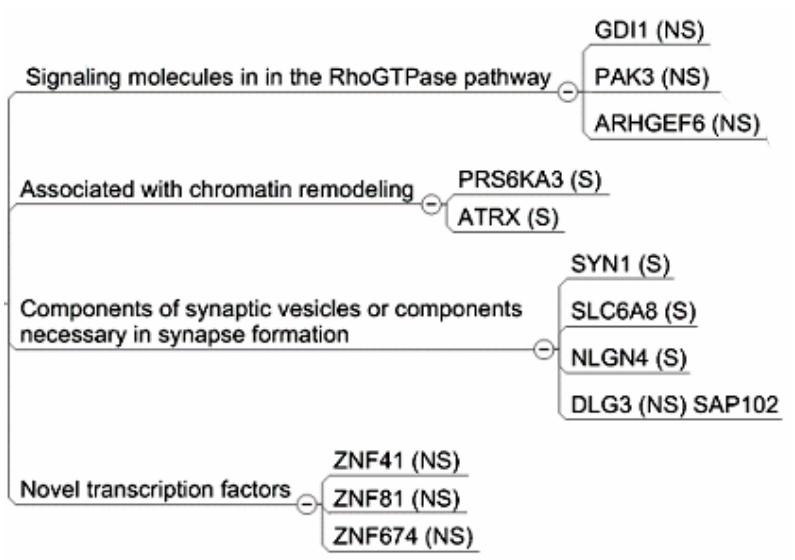

Figure 4-7: Classification of XLMR genes. S: Syndromic, NS: Non-syndromic (Raymond and Tarpey 2006).

4.5. Role of GLUR6 in synapse formation and structure

At the cellular level, it is conceivable that defective GLUR6 could also have structural effects. Indeed, GLUR6 has been found to be involved in profilin II–mediated interactions with actin, (Coussen et al. 2005; Wechsler and Teichberg 1998) through which it might contribute to the stabilization of dendritic spine morphology (Ackermann and Matus 2003) and normal neuritogenesis (da Silva et al. 2003). Further studies of this aspect of GLUR6 function in model organisms will be particularly interesting, because abnormal morphogenesis of dendritic spines is observed in a variety of MR disorders, such as fragile X syndrome (MIM 300624) (Grossman et al. 2006).

Finally, another avenue to be explored might be the investigation of a putative impact of GLUK6 deficiency on synaptic plasticity. In this context, it is of note that GLUK6 also seems to interact with synapse-associated protein 102 (SAP102)(Garcia et al. 1998) for which mutations in the coding gene (DLG3) were found in families with severe X-linked MR (Tarpey et al. 2004).

By identifying *GRIK2* as a novel NS-ARMR gene, we provide strong evidence that functional integrity of this ionotropic glutamate receptor might be a sine qua non for normal human brain function. Given the unclear phenotype of *GRIK2*-deficient mice, this study also indicates that genotype-phenotype studies in man are indispensable for identifying the genes that play a role in complex behavioral traits. Finally, we expect that our results will stimulate research into the role of other KARs in cognition and behavior. *GRIK2* is the first gene for NS-ARMR with a known function in the CNS. Its identification is part of an ongoing systematic effort to unravel the molecular causes of recessive MR, which will shed more light on the function of the human brain in health and disease.

5. ACKNOWLEDGEMENTS

I owe my deepest thanks to my parents -Mr. Nader Motazacker and Mrs. Forouzandeh Ostadrahimi- and my sisters -Shadi and Shiva-, for their everlasting support and encouragement during all these years.

I am thankful to my Grandparents –Mr. Ahmad Ostadrahimi and Mrs. Esmat Jenab (PBUH)-, my uncle, aunt and cousin –Mr. Ezzatollah Ostadrahimi, Mrs Aghdas Ostadrahimi and Zahra- for their encouragement and support.

Special thanks to Mr. Tavassoli, high-school Biology teacher who helped me feel the excitement of the Biology by interesting discussions at the end of my high-school biology courses.

Many thanks to Susanne Freier not only for her scientific support in the cell culture facility of MPIMG but also for all generous help and support I got from her (and Mr. Siegfried Freier) during my stay in Germany.

I would like to thank Prof. Dr. Hans-Hilger Ropers and Prof. Dr. Hossein Najmabadi for establishment of the scientific framework in which I did my Ph.D., supervision of my work and for their support and guidance throughout this study.

I am grateful to Dr. Andreas W. Kuss, my group leader for his advices during my PhD thesis and his support and critical comments on my thesis.

I would like to thank Dr. Lars R. Jensen for his comments, fruitful discussions and practical help in the lab.

Special thanks to Masoud Garshasbi, my old friend for the great time I had with him before and during Ph.D. period and for the numerous life lessons I learned from him direct or indirectly.

Many thanks to Dr. Chandan Goswami and Vanessa Suckow for the support in immunocytochemistry and the protein related experiments.

Many thanks to Prof. Dr. Schmitz and Benjamin Rost at the Neuroscience Research Center (NWFZ) - Charité Berlin not only for the collaboration in GLUR6 electrophysiological studies but also for the fruitful discussions and comments as well as permission to attend their “Thursday meetings” which helped me a lot in understanding the functions of GLUR6 protein.

I’m very grateful to my colleagues in the familial cognitive disorders group for the friendly atmosphere. Many thanks to Bettina Lipkowitz, Katharina Albers, Chen Wei, Lia A. Moheb, Sahar Esmaeeli, Johanna Waltzak, Bartek Budney, Achim Salamon, Marianne Schlicht, Georg Lienke, Marion Amende and Melanie Wendehack.

I would like to thank my Iranian colleagues at the Genetics Research Center, University of social welfare and rehabilitation sciences in Iran who did most of the clinical and cytogenetic pre-screening in the patients: I would like to thank Dr. Farkhondeh Behjati, Dr. Kimia Kahrizi, Dr. Yousef Shafeghati, Prof. Dr. Molavi, Ms. Susan Banihashemi, Ms. Saghar Ghasemi and Ms. Sedigheh Abedini.

I would like to thank Prof. Dr. Guerters and Dr. O. Blankenstein for mass-spectrometry experiments performed at the Institute for Experimental Pediatric Endocrinology in Charite Universitaetmedizin, Berlin, Germany.

Our “Mensa-Consortium” provided a nice opportunity to talk to my friends about work and life related issues everyday. I would like to thank my dear friends Joyce So, Beatris Aranda, Olivier Hagens, Artur Muradyan, Johanna Aigner, Djan, Swen Krause for everyday walk toward Mensa and scientific as well as daily discussions.

During my Ph.D. I got help and support from many other people. I would like to thank Dr. Vera Kalscheuer, Dr. Andreas Tzschach, Dr. Reinhard Ullmann, Corinna Menzel, Nils Rademacher, Dr. Luciana Musante and Stella Kunde.

I acknowledge the financial support of the Max Planck Society and Iranian Molecular Medicine network.

Finally, I want to express my deep appreciation to my wife, Maryam, not only for the comments on this manuscript but also for her continuous love, care and sweetness which has made my life full of happiness and motivation.

6. References

AAMR (2005). Definition of mental retardation, American Association on Mental Retardation.

Abecasis, G. R., Cherny, S. S., Cookson, W. O. and Cardon, L. R. (2001). "GRR: graphical representation of relationship errors." Bioinformatics 17(8): 742-3.

Abecasis, G. R., Cherny, S. S., Cookson, W. O. and Cardon, L. R. (2002). "Merlin--rapid analysis of dense genetic maps using sparse gene flow trees." Nat Genet 30(1): 97-101.

Ackermann, M. and Matus, A. (2003). "Activity-induced targeting of profilin and stabilization of dendritic spine morphology." Nat Neurosci 6(11): 1194-200.

Adesnik, H., Nicoll, R. A. and England, P. M. (2005). "Photoinactivation of native AMPA receptors reveals their real-time trafficking." Neuron 48(6): 977-85.

Agrawal, S. G. and Evans, R. H. (1986). "The primary afferent depolarizing action of kainate in the rat." Br J Pharmacol 87(2): 345-55.

Ali, A. B. (2003). "Involvement of post-synaptic kainate receptors during synaptic transmission between unitary connections in rat neocortex." Eur J Neurosci 17(11): 2344-50.

Allen, K. M., Gleeson, J. G., Bagrodia, S., Partington, M. W., MacMillan, J. C., Cerione, R. A., Mulley, J. C. and Walsh, C. A. (1998). "PAK3 mutation in nonsyndromic X-linked mental retardation." Nat Genet 20(1): 25-30.

Amrani, N., Sachs, M. S. and Jacobson, A. (2006). "Early nonsense: mRNA decay solves a translational problem." Nat Rev Mol Cell Biol 7(6): 415-25.

Andresen, J. M., Gayan, J., Cherny, S. S., Brocklebank, D., Alkorta-Aranburu, G., Addis, E. A., Cardon, L. R., Housman, D. E. and Wexler, N. S. (2007). "Replication of twelve association studies for Huntington's disease residual age of onset in large Venezuelan kindreds." J Med Genet 44(1): 44-50.

APA (1994). Diagnostic and Statistical Manual of Mental Disorders IV (ed 4). Washington, DC American Phsychiatric Association.

Arning, L., Kraus, P. H., Valentin, S., Saft, C., Andrich, J. and Epplen, J. T. (2005). "NR2A and NR2B receptor gene variations modify age at onset in Huntington disease." Neurogenetics 6(1): 25-8.

Bah, J., Quach, H., Ebstein, R. P., Segman, R. H., Melke, J., Jamain, S., Rietschel, M., Modai, I., Kanas, K., Karni, O., Lerer, B., Gourion, D., Krebs, M. O., Etain, B., Schurhoff, F., Szoke, A., Leboyer, M. and Bourgeron, T. (2004). "Maternal transmission disequilibrium of the glutamate receptor GRIK2 in schizophrenia." Neuroreport 15(12): 1987-91.

Bahn, S., Volk, B. and Wisden, W. (1994). "Kainate receptor gene expression in the developing rat brain." J Neurosci 14(9): 5525-47.

Bahring, R., Bowie, D., Benveniste, M. and Mayer, M. L. (1997). "Permeation and block of rat GluR6 glutamate receptor channels by internal and external polyamines." J Physiol 502 (Pt 3): 575-89.

Baptista, J., Prigmore, E., Gribble, S. M., Jacobs, P. A., Carter, N. P. and Crolla, J. A. (2005). "Molecular cytogenetic analyses of breakpoints in apparently balanced reciprocal translocations carried by phenotypically normal individuals." Eur J Hum Genet 13(11): 1205-12.

Barbon, A., Vallini, I. and Barlati, S. (2001). "Genomic organization of the human GRIK2 gene and evidence for multiple splicing variants." Gene 274(1-2): 187-97.

Basel-Vanagaite, L., Attia, R., Yahav, M., Ferland, R. J., Anteki, L., Walsh, C. A., Olender, T., Straussberg, R., Magal, N., Taub, E., Drasinover, V., Alkelai, A., Bercovich, D., Rechavi, G., Simon, A. J. and Shohat, M. (2006). "The CC2D1A, a member of a new gene family with C2 domains, is involved in autosomal recessive non-syndromic mental retardation." J Med Genet 43(3): 203-10.

Ben-Ari, Y. and Cossart, R. (2000). "Kainate, a double agent that generates seizures: two decades of progress." Trends Neurosci 23(11): 580-7.

Bettler, B. and Mulle, C. (1995). "Review: neurotransmitter receptors. II. AMPA and kainate receptors." Neuropharmacology 34(2): 123-39.

Billuart, P., Bienvenu, T., Ronce, N., des Portes, V., Vinet, M. C., Zemni, R., Roest Crollius, H., Carrie, A., Fauchereau, F., Cherry, M., Briault, S., Hamel, B., Fryns, J. P., Beldjord, C., Kahn, A., Moraine, C. and Chelly, J. (1998). "Oligophrenin-1 encodes a rhoGAP protein involved in X-linked mental retardation." Nature 392(6679): 923-6.

Bowie, D. and Mayer, M. L. (1995). "Inward rectification of both AMPA and kainate subtype glutamate receptors generated by polyamine-mediated ion channel block." Neuron 15(2): 453-62.

Brezun, J. M. and Daszuta, A. (1999). "Depletion in serotonin decreases neurogenesis in the dentate gyrus and the subventricular zone of adult rats." Neuroscience 89(4): 999-1002.

Buhot, M. C., Martin, S. and Segu, L. (2000). "Role of serotonin in memory impairment." Ann Med 32(3): 210-21.

Bureau, I., Bischoff, S., Heinemann, S. F. and Mulle, C. (1999). "Kainate receptor-mediated responses in the CA1 field of wild-type and GluR6-deficient mice." J Neurosci 19(2): 653-63.

Bureau, I., Dieudonne, S., Coussen, F. and Mulle, C. (2000). "Kainate receptor-mediated synaptic currents in cerebellar Golgi cells are not shaped by diffusion of glutamate." Proc Natl Acad Sci U S A 97(12): 6838-43.

Burgoyne, R. D. and Weiss, J. L. (2001). "The neuronal calcium sensor family of Ca2+-binding proteins." Biochem J 353(Pt 1): 1-12.

Burnashev, N., Zhou, Z., Neher, E. and Sakmann, B. (1995). "Fractional calcium currents through recombinant GluR channels of the NMDA, AMPA and kainate receptor subtypes." J Physiol 485 (Pt 2): 403-18.

Cannella, M., Gellera, C., Maglione, V., Giallonardo, P., Cislaghi, G., Muglia, M., Quattrone, A., Pierelli, F., Di Donato, S. and Squitieri, F. (2004). "The gender effect in juvenile Huntington disease patients of Italian origin." Am J Med Genet B Neuropsychiatr Genet 125(1): 92-8.

Cao, Q., Martinez, M., Zhang, J., Sanders, A. R., Badner, J. A., Cravchik, A., Markey, C. J., Beshah, E., Guroff, J. J., Maxwell, M. E., Kazuba, D. M., Whiten, R., Goldin, L. R., Gershon, E. S. and Gejman, P. V. (1997). "Suggestive evidence for a schizophrenia susceptibility locus on chromosome 6q and a confirmation in an independent series of pedigrees." Genomics 43(1): 1-8.

Carrie, A., Jun, L., Bienvenu, T., Vinet, M. C., McDonell, N., Couvert, P., Zemni, R., Cardona, A., Van Buggenhout, G., Frints, S., Hamel, B., Moraine, C., Ropers, H. H., Strom, T., Howell, G. R., Whittaker, A., Ross, M. T., Kahn, A., Fryns, J. P., Beldjord, C., Marynen, P. and Chelly, J. (1999). "A new member of the IL-1 receptor family highly expressed in hippocampus and involved in X-linked mental retardation." Nat Genet 23(1): 25-31.

Casassus, G. and Mulle, C. (2002). "Functional characterization of kainate receptors in the mouse nucleus accumbens." Neuropharmacology 42(5): 603-11.

Castillo, P. E., Malenka, R. C. and Nicoll, R. A. (1997). "Kainate receptors mediate a slow postsynaptic current in hippocampal CA3 neurons." Nature 388(6638): 182-6.

Chace, D. H., Kalas, T. A. and Naylor, E. W. (2003). "Use of tandem mass spectrometry for multianalyte screening of dried blood specimens from newborns." Clin Chem 49(11): 1797-817.

Chaib, H., Place, C., Salem, N., Dode, C., Chardenoux, S., Weissenbach, J., el Zir, E., Loiselet, J. and Petit, C. (1996). "Mapping of DFNB12, a gene for a non-syndromal autosomal recessive deafness, to chromosome 10q21-22." Hum Mol Genet 5(7): 1061-4.

Chattopadhyay, B., Ghosh, S., Gangopadhyay, P. K., Das, S. K., Roy, T., Sinha, K. K., Jha, D. K., Mukherjee, S. C., Chakraborty, A., Singhal, B. S., Bhattacharya, A. K. and Bhattacharyya, N. P. (2003). "Modulation of age at onset in Huntington's disease and spinocerebellar ataxia type 2 patients originated from eastern India." Neurosci Lett 345(2): 93-6.

Chen, A. C., Kalsi, G., Brynjolfsson, J., Sigmundsson, T., Curtis, D., Butler, R., Read, T., Murphy, P., Petursson, H., Barnard, E. A. and Gurling, H. M. (1996). "Lack of evidence for close linkage of the glutamate GluR6 receptor gene with schizophrenia." Am J Psychiatry 153(12): 1634-6.

Chergui, K., Bouron, A., Normand, E. and Mulle, C. (2000). "Functional GluR6 kainate receptors in the striatum: indirect downregulation of synaptic transmission." J Neurosci 20(6): 2175-82.

Chittajallu, R., Braithwaite, S. P., Clarke, V. R. and Henley, J. M. (1999). "Kainate receptors: subunits, synaptic localization and function." Trends Pharmacol Sci 20(1): 26-35.

Chiurazzi, P., Schwartz, C. E., Gecz, J. and Neri, G. (2008). "XLMR genes: update 2007." Eur J Hum Genet.

Christensen, J. K., Paternain, A. V., Selak, S., Ahring, P. K. and Lerma, J. (2004). "A mosaic of functional kainate receptors in hippocampal interneurons." J Neurosci 24(41): 8986-93.

Contractor, A., Sailer, A. W., Darstein, M., Maron, C., Xu, J., Swanson, G. T. and Heinemann, S. F. (2003). "Loss of kainate receptor-mediated heterosynaptic facilitation of mossy-fiber synapses in KA2-/- mice." J Neurosci 23(2): 422-9.

Contractor, A., Swanson, G. and Heinemann, S. F. (2001). "Kainate receptors are involved in short- and long-term plasticity at mossy fiber synapses in the hippocampus." Neuron 29(1): 209-16.

Cossart, R., Esclapez, M., Hirsch, J. C., Bernard, C. and Ben-Ari, Y. (1998). "GluR5 kainate receptor activation in interneurons increases tonic inhibition of pyramidal cells." Nat Neurosci 1(6): 470-8.

Coussen, F., Normand, E., Marchal, C., Costet, P., Choquet, D., Lambert, M., Mege, R. M. and Mulle, C. (2002). "Recruitment of the kainate receptor subunit glutamate receptor 6 by cadherin/catenin complexes." J Neurosci 22(15): 6426-36.

Coussen, F., Perrais, D., Jaskolski, F., Sachidhanandam, S., Normand, E., Bockaert, J., Marin, P. and Mulle, C. (2005). "Co-assembly of two GluR6 kainate receptor splice variants within a functional protein complex." Neuron 47(4): 555-66.

Crawford, D. C., Acuna, J. M. and Sherman, S. L. (2001). "FMR1 and the fragile X syndrome: human genome epidemiology review." Genet Med 3(5): 359-71.

Cui, C. and Mayer, M. L. (1999). "Heteromeric kainate receptors formed by the coassembly of GluR5, GluR6, and GluR7." J Neurosci 19(19): 8281-91.

D'Adamo, P., Menegon, A., Lo Nigro, C., Grasso, M., Gulisano, M., Tamanini, F., Bienvenu, T., Gedeon, A. K., Oostra, B., Wu, S. K., Tandon, A., Valtorta, F., Balch, W. E., Chelly, J. and Toniolo, D. (1998). "Mutations in GDI1 are responsible for X-linked non-specific mental retardation." Nat Genet 19(2): 134-9.

da Silva, L. P., Ciocca Mde, L. and Furlong, E. B. (2003). "[Evaluation of the AOAC 985.29 enzimic gravimetric method for determination of dietary fiber in oat and corn grains]." Arch Latinoam Nutr 53(4): 393-9.

Delorme, R., Krebs, M. O., Chabane, N., Roy, I., Millet, B., Mouren-Simeoni, M. C., Maier, W., Bourgeron, T. and Leboyer, M. (2004). "Frequency and transmission of glutamate receptors GRIK2 and GRIK3 polymorphisms in patients with obsessive compulsive disorder." Neuroreport 15(4): 699-702.

DeVries, S. H. and Schwartz, E. A. (1999). "Kainate receptors mediate synaptic transmission between cones and 'Off' bipolar cells in a mammalian retina." Nature 397(6715): 157-60.

Dingledine, R., Borges, K., Bowie, D. and Traynelis, S. F. (1999). "The glutamate receptor ion channels." Pharmacol Rev 51(1): 7-61.

Eder, M., Becker, K., Rammes, G., Schierloh, A., Azad, S. C., Zieglgansberger, W. and Dodt, H. U. (2003). "Distribution and properties of functional postsynaptic kainate receptors on neocortical layer V pyramidal neurons." J Neurosci 23(16): 6660-70.

Egebjerg, J., Bettler, B., Hermans-Borgmeyer, I. and Heinemann, S. (1991). "Cloning of a cDNA for a glutamate receptor subunit activated by kainate but not AMPA." Nature 351(6329): 745-8.

Erdogan, F., Chen, W., Kirchhoff, M., Kalscheuer, V. M., Hultschig, C., Muller, I., Schulz, R., Menzel, C., Bryndorf, T., Ropers, H. H. and Ullmann, R. (2006). "Impact of low copy repeats on the generation of balanced and unbalanced chromosomal aberrations in mental retardation." Cytogenet Genome Res 115(3-4): 247-53.

European X-linked mental retardation consortuim. (2005). "XLMR genes database update." from http://xlmr.interfree.it/home.htm.

Feigin, A. and Zgaljardic, D. (2002). "Recent advances in Huntington's disease: implications for experimental therapeutics." Curr Opin Neurol 15(4): 483-9.

Fisahn, A., Heinemann, S. F. and McBain, C. J. (2005). "The kainate receptor subunit GluR6 mediates metabotropic regulation of the slow and medium AHP currents in mouse hippocampal neurones." J Physiol 562(Pt 1): 199-203.

Fisahn, J., Herde, O., Willmitzer, L. and Pena-Cortes, H. (2004). "Analysis of the transient increase in cytosolic Ca2+ during the action potential of higher plants with high temporal resolution: requirement of Ca2+ transients for induction of jasmonic acid biosynthesis and PINII gene expression." Plant Cell Physiol 45(4): 456-9.

Fleck, M. W., Cornell, E. and Mah, S. J. (2003). "Amino-acid residues involved in glutamate receptor 6 kainate receptor gating and desensitization." J Neurosci 23(4): 1219-27.

Frerking, M., Malenka, R. C. and Nicoll, R. A. (1998). "Synaptic activation of kainate receptors on hippocampal interneurons." Nat Neurosci 1(6): 479-86.

Frerking, M. and Nicoll, R. A. (2000). "Synaptic kainate receptors." Curr Opin Neurobiol 10(3): 342-51.

Freude, K., Hoffmann, K., Jensen, L. R., Delatycki, M. B., des Portes, V., Moser, B., Hamel, B., van Bokhoven, H., Moraine, C., Fryns, J. P., Chelly, J., Gecz, J., Lenzner, S., Kalscheuer, V. M. and Ropers, H. H. (2004). "Mutations in the FTSJ1 gene coding for a novel S-adenosylmethionine-binding protein cause nonsyndromic X-linked mental retardation." Am J Hum Genet 75(2): 305-9.

Friesema, E. C., Grueters, A., Biebermann, H., Krude, H., von Moers, A., Reeser, M., Barrett, T. G., Mancilla, E. E., Svensson, J., Kester, M. H., Kuiper, G. G., Balkassmi, S., Uitterlinden, A. G., Koehrle, J., Rodien, P., Halestrap, A. P. and Visser, T. J. (2004). "Association between mutations in a thyroid hormone transporter and severe X-linked psychomotor retardation." Lancet 364(9443): 1435-7.

Frints, S. G., Froyen, G., Marynen, P. and Fryns, J. P. (2002). "X-linked mental retardation: vanishing boundaries between non-specific (MRX) and syndromic (MRXS) forms." Clin Genet 62(6): 423-32.

Garcia, C. C., Blair, H. J., Seager, M., Coulthard, A., Tennant, S., Buddles, M., Curtis, A. and Goodship, J. A. (2004). "Identification of a mutation in synapsin I, a synaptic vesicle protein, in a family with epilepsy." J Med Genet 41(3): 183-6.

Garcia, E. P., Mehta, S., Blair, L. A., Wells, D. G., Shang, J., Fukushima, T., Fallon, J. R., Garner, C. C. and Marshall, J. (1998). "SAP90 binds and clusters kainate receptors causing incomplete desensitization." Neuron 21(4): 727-39.

Garshasbi, M., Motazacker, M. M., Kahrizi, K., Behjati, F., Abedini, S. S., Nieh, S. E., Firouzabadi, S. G., Becker, C., Ruschendorf, F., Nurnberg, P., Tzschach, A., Vazifehmand, R., Erdogan, F., Ullmann, R., Lenzner, S., Kuss, A. W., Ropers, H. H. and Najmabadi, H. (2006). "SNP array-based homozygosity mapping reveals MCPH1 deletion in family with autosomal recessive mental retardation and mild microcephaly." Hum Genet 118(6): 708-15.

Gecz, J. (2000). "The FMR2 gene, FRAXE and non-specific X-linked mental retardation: clinical and molecular aspects." Ann Hum Genet 64(Pt 2): 95-106.

Gregor, P., O'Hara, B. F., Yang, X. and Uhl, G. R. (1993). "Expression and novel subunit isoforms of glutamate receptor genes GluR5 and GluR6." Neuroreport 4(12): 1343-6.

Grossman, A. W., Aldridge, G. M., Weiler, I. J. and Greenough, W. T. (2006). "Local protein synthesis and spine morphogenesis: Fragile X syndrome and beyond." J Neurosci 26(27): 7151-5.

Gudbjartsson, D. F., Jonasson, K., Frigge, M. L. and Kong, A. (2000). "Allegro, a new computer program for multipoint linkage analysis." Nat Genet 25(1): 12-3.

Guerrini, R., Shanahan, J. L., Carrozzo, R., Bonanni, P., Higgs, D. R. and Gibbons, R. J. (2000). "A nonsense mutation of the ATRX gene causing mild mental retardation and epilepsy." Ann Neurol 47(1): 117-21.

Henze, D. A., Urban, N. N. and Barrionuevo, G. (2000). "The multifarious hippocampal mossy fiber pathway: a review." Neuroscience 98(3): 407-27.

Herb, A., Burnashev, N., Werner, P., Sakmann, B., Wisden, W. and Seeburg, P. H. (1992). "The KA-2 subunit of excitatory amino acid receptors shows widespread expression in brain and forms ion channels with distantly related subunits." Neuron 8(4): 775-85.

Higgins, J. J., Pucilowska, J., Lombardi, R. Q. and Rooney, J. P. (2004). "A mutation in a novel ATP-dependent Lon protease gene in a kindred with mild mental retardation." Neurology 63(10): 1927-31.

Hirbec, H., Francis, J. C., Lauri, S. E., Braithwaite, S. P., Coussen, F., Mulle, C., Dev, K. K., Coutinho, V., Meyer, G., Isaac, J. T., Collingridge, G. L. and Henley, J. M. (2003). "Rapid and differential regulation of AMPA and kainate receptors at hippocampal mossy fibre synapses by PICK1 and GRIP." Neuron 37(4): 625-38.

Hollmann, M. and Heinemann, S. (1994). "Cloned glutamate receptors." Annu Rev Neurosci 17: 31-108.

Houwen, R. H., Baharloo, S., Blankenship, K., Raeymaekers, P., Juyn, J., Sandkuijl, L. A. and Freimer, N. B. (1994). "Genome screening by searching for shared segments: mapping a gene for benign recurrent intrahepatic cholestasis." Nat Genet 8(4): 380-6.

Howe, J. R. (1996). "Homomeric and heteromeric ion channels formed from the kainate-type subunits GluR6 and KA2 have very small, but different, unitary conductances." J Neurophysiol 76(1): 510-9.

Huang, Y. H., Dykes-Hoberg, M., Tanaka, K., Rothstein, J. D. and Bergles, D. E. (2004). "Climbing fiber activation of EAAT4 transporters and kainate receptors in cerebellar Purkinje cells." J Neurosci 24(1): 103-11.

Huettner, J. E. (1990). "Glutamate receptor channels in rat DRG neurons: activation by kainate and quisqualate and blockade of desensitization by Con A." Neuron 5(3): 255-66.

Huettner, J. E., Kerchner, G. A. and Zhuo, M. (2002). "Glutamate and the presynaptic control of spinal sensory transmission." Neuroscientist 8(2): 89-92.

Jamain, S., Betancur, C., Quach, H., Philippe, A., Fellous, M., Giros, B., Gillberg, C., Leboyer, M. and Bourgeron, T. (2002). "Linkage and association of the glutamate receptor 6 gene with autism." Mol Psychiatry 7(3): 302-10.

Jamain, S., Quach, H., Betancur, C., Rastam, M., Colineaux, C., Gillberg, I. C., Soderstrom, H., Giros, B., Leboyer, M., Gillberg, C. and Bourgeron, T. (2003). "Mutations of the X-linked genes encoding neuroligins NLGN3 and NLGN4 are associated with autism." Nat Genet 34(1): 27-9.

Jaskolski, F., Coussen, F. and Mulle, C. (2005). "Subcellular localization and trafficking of kainate receptors." Trends Pharmacol Sci 26(1): 20-6.

Jaskolski, F., Coussen, F., Nagarajan, N., Normand, E., Rosenmund, C. and Mulle, C. (2004). "Subunit composition and alternative splicing regulate membrane delivery of kainate receptors." J Neurosci 24(10): 2506-15.

Jaskolski, F., Normand, E., Mulle, C. and Coussen, F. (2005). "Differential trafficking of GluR7 kainate receptor subunit splice variants." J Biol Chem 280(24): 22968-76.

Jensen, L. R., Amende, M., Gurok, U., Moser, B., Gimmel, V., Tzschach, A., Janecke, A. R., Tariverdian, G., Chelly, J., Fryns, J. P., Van Esch, H., Kleefstra, T., Hamel, B., Moraine, C., Gecz, J., Turner, G., Reinhardt, R., Kalscheuer, V. M., Ropers, H. H. and Lenzner, S. (2005). "Mutations in the JARID1C gene, which is involved in transcriptional regulation and chromatin remodeling, cause X-linked mental retardation." Am J Hum Genet 76(2): 227-36.

Jo, S., Lee, K. H., Song, S., Jung, Y. K. and Park, C. S. (2005). "Identification and functional characterization of cereblon as a binding protein for large-conductance calcium-activated potassium channel in rat brain." J Neurochem 94(5): 1212-24.

Jonas, P. and Monyer, H. (1999). Ionotropic Glutamate Receptors in the CNS, Springer.

Kalscheuer, V. M., Freude, K., Musante, L., Jensen, L. R., Yntema, H. G., Gecz, J., Sefiani, A., Hoffmann, K., Moser, B., Haas, S., Gurok, U., Haesler, S., Aranda, B., Nshedjan, A., Tzschach, A., Hartmann, N., Roloff, T. C., Shoichet, S., Hagens, O., Tao, J., Van Bokhoven, H., Turner, G., Chelly, J., Moraine, C., Fryns, J. P., Nuber, U., Hoeltzenbein, M., Scharff, C., Scherthan, H., Lenzner, S., Hamel, B. C., Schweiger, S. and Ropers, H. H. (2003). "Mutations in the polyglutamine binding protein 1 gene cause X-linked mental retardation." Nat Genet 35(4): 313-5.

Kaufmann, C. A., Suarez, B., Malaspina, D., Pepple, J., Svrakic, D., Markel, P. D., Meyer, J., Zambuto, C. T., Schmitt, K., Matise, T. C., Harkavy Friedman, J. M., Hampe, C., Lee, H., Shore, D., Wynne, D., Faraone, S. V., Tsuang, M. T. and Cloninger, C. R. (1998). "NIMH

Genetics Initiative Millenium Schizophrenia Consortium: linkage analysis of African-American pedigrees." Am J Med Genet 81(4): 282-9.

Kennedy, G. C., Matsuzaki, H., Dong, S., Liu, W. M., Huang, J., Liu, G., Su, X., Cao, M., Chen, W., Zhang, J., Liu, W., Yang, G., Di, X., Ryder, T., He, Z., Surti, U., Phillips, M. S., Boyce-Jacino, M. T., Fodor, S. P. and Jones, K. W. (2003). "Large-scale genotyping of complex DNA." Nat Biotechnol 21(10): 1233-7.

Kerr, B., Turner, G., Mulley, J., Gedeon, A. and Partington, M. (1991). "Non-specific X linked mental retardation." J Med Genet 28(6): 378-82.

Kidd, F. L. and Isaac, J. T. (1999). "Developmental and activity-dependent regulation of kainate receptors at thalamocortical synapses." Nature 400(6744): 569-73.

Klauck, S. M., Felder, B., Kolb-Kokocinski, A., Schuster, C., Chiocchetti, A., Schupp, I., Wellenreuther, R., Schmotzer, G., Poustka, F., Breitenbach-Koller, L. and Poustka, A. (2006). "Mutations in the ribosomal protein gene RPL10 suggest a novel modulating disease mechanism for autism." Mol Psychiatry 11(12): 1073-84.

Klauck, S. M., Lindsay, S., Beyer, K. S., Splitt, M., Burn, J. and Poustka, A. (2002). "A mutation hot spot for nonspecific X-linked mental retardation in the MECP2 gene causes the PPM-X syndrome." Am J Hum Genet 70(4): 1034-7.

Kleefstra, T., Yntema, H. G., Oudakker, A. R., Banning, M. J., Kalscheuer, V. M., Chelly, J., Moraine, C., Ropers, H. H., Fryns, J. P., Janssen, I. M., Sistermans, E. A., Nillesen, W. N., de Vries, L. B., Hamel, B. C. and van Bokhoven, H. (2004). "Zinc finger 81 (ZNF81) mutations associated with X-linked mental retardation." J Med Genet 41(5): 394-9.

Ko, S., Zhao, M. G., Toyoda, H., Qiu, C. S. and Zhuo, M. (2005). "Altered behavioral responses to noxious stimuli and fear in glutamate receptor 5 (GluR5)- or GluR6-deficient mice." J Neurosci 25(4): 977-84.

Kohler, M., Burnashev, N., Sakmann, B. and Seeburg, P. H. (1993). "Determinants of Ca2+ permeability in both TM1 and TM2 of high affinity kainate receptor channels: diversity by RNA editing." Neuron 10(3): 491-500.

Kruglyak, L., Daly, M. J., Reeve-Daly, M. P. and Lander, E. S. (1996). "Parametric and nonparametric linkage analysis: a unified multipoint approach." Am J Hum Genet 58(6): 1347-63.

Kullmann, D. M. (2001). "Presynaptic kainate receptors in the hippocampus: slowly emerging from obscurity." Neuron 32(4): 561-4.

Kutsche, K., Yntema, H., Brandt, A., Jantke, I., Nothwang, H. G., Orth, U., Boavida, M. G., David, D., Chelly, J., Fryns, J. P., Moraine, C., Ropers, H. H., Hamel, B. C., van Bokhoven, H. and Gal, A. (2000). "Mutations in ARHGEF6, encoding a guanine nucleotide exchange factor for Rho GTPases, in patients with X-linked mental retardation." Nat Genet 26(2): 247-50.

Laemmli, U. K. (1970). "Cleavage of structural proteins during the assembly of the head of bacteriophage T4." Nature 227(5259): 680-5.

Lander, E. S. and Botstein, D. (1987). "Homozygosity mapping: a way to map human recessive traits with the DNA of inbred children." Science 236(4808): 1567-70.

Lebel, R. R., May, M., Pouls, S., Lubs, H. A., Stevenson, R. E. and Schwartz, C. E. (2002). "Non-syndromic X-linked mental retardation associated with a missense mutation (P312L) in the FGD1 gene." Clin Genet 61(2): 139-45.

Lejeune, J., Turpin, R. and Gautier, M. (1959). "[Chromosomic diagnosis of mongolism.]." Arch Fr Pediatr 16: 962-3.

Leonard, H. and Wen, X. (2002). "The epidemiology of mental retardation: challenges and opportunities in the new millennium." Ment Retard Dev Disabil Res Rev 8(3): 117-34.

Lerma, J. (2003). "Roles and rules of kainate receptors in synaptic transmission." Nat Rev Neurosci 4(6): 481-95.

Lerma, J. (2006). "Kainate receptor physiology." Curr Opin Pharmacol 6(1): 89-97.

Lerma, J., Paternain, A. V., Rodriguez-Moreno, A. and Lopez-Garcia, J. C. (2001). "Molecular physiology of kainate receptors." Physiol Rev 81(3): 971-98.

Li, H. and Rogawski, M. A. (1998). "GluR5 kainate receptor mediated synaptic transmission in rat basolateral amygdala in vitro." Neuropharmacology 37(10-11): 1279-86.

Li, P., Wilding, T. J., Kim, S. J., Calejesan, A. A., Huettner, J. E. and Zhuo, M. (1999). "Kainate-receptor-mediated sensory synaptic transmission in mammalian spinal cord." Nature 397(6715): 161-4.

Li, S. and Stys, P. K. (2001). "Na(+)-K(+)-ATPase inhibition and depolarization induce glutamate release via reverse Na(+)-dependent transport in spinal cord white matter." Neuroscience 107(4): 675-83.

London, E. D. and Coyle, J. T. (1979). "Specific binding of [3H]kainic acid to receptor sites in rat brain." Mol Pharmacol 15(3): 492-505.

Lugtenberg, D., Hamel, B., Van Bokhoven, H. and Brouwer, A. (2006). "Strategies for present and future mental retardation." Futuremedicine 1(6): 775-785.

Lugtenberg, D., Yntema, H. G., Banning, M. J., Oudakker, A. R., Firth, H. V., Willatt, L., Raynaud, M., Kleefstra, T., Fryns, J. P., Ropers, H. H., Chelly, J., Moraine, C., Gecz, J., Reeuwijk, J., Nabuurs, S. B., de Vries, B. B., Hamel, B. C., de Brouwer, A. P. and Bokhoven, H. (2006). "ZNF674: A New Kruppel-Associated Box-Containing Zinc-Finger Gene Involved in Nonsyndromic X-Linked Mental Retardation." Am J Hum Genet 78(2): 265-78.

MacDonald, M. E., Vonsattel, J. P., Shrinidhi, J., Couropmitree, N. N., Cupples, L. A., Bird, E. D., Gusella, J. F. and Myers, R. H. (1999). "Evidence for the GluR6 gene associated with younger onset age of Huntington's disease." Neurology 53(6): 1330-2.

Mah, S. J., Cornell, E., Mitchell, N. A. and Fleck, M. W. (2005). "Glutamate receptor trafficking: endoplasmic reticulum quality control involves ligand binding and receptor function." J Neurosci 25(9): 2215-25.

Martin, J. P. and Bell, J. (1943). "A pedigree of mental defect showing sex-linkage." J Neurol Psychiat 6: 154.

Martin, S. and Henley, J. M. (2004). "Activity-dependent endocytic sorting of kainate receptors to recycling or degradation pathways." Embo J 23(24): 4749-59.

Martinez, M., Goldin, L. R., Cao, Q., Zhang, J., Sanders, A. R., Nancarrow, D. J., Taylor, J. M., Levinson, D. F., Kirby, A., Crowe, R. R., Andreasen, N. C., Black, D. W., Silverman, J. M., Lennon, D. P., Nertney, D. A., Brown, D. M., Mowry, B. J., Gershon, E. S. and Gejman, P. V. (1999). "Follow-up study on a susceptibility locus for schizophrenia on chromosome 6q." Am J Med Genet 88(4): 337-43.

Matsuzaki, H., Loi, H., Dong, S., Tsai, Y. Y., Fang, J., Law, J., Di, X., Liu, W. M., Yang, G., Liu, G., Huang, J., Kennedy, G. C., Ryder, T. B., Marcus, G. A., Walsh, P. S., Shriver, M. D., Puck, J. M., Jones, K. W. and Mei, R. (2004). "Parallel genotyping of over 10,000 SNPs using a one-primer assay on a high-density oligonucleotide array." Genome Res 14(3): 414-25.

Mayer, M. L., Ghosal, A., Dolman, N. P. and Jane, D. E. (2006). "Crystal structures of the kainate receptor GluR5 ligand binding core dimer with novel GluR5-selective antagonists." J Neurosci 26(11): 2852-61.

Mehta, S., Wu, H., Garner, C. C. and Marshall, J. (2001). "Molecular mechanisms regulating the differential association of kainate receptor subunits with SAP90/PSD-95 and SAP97." J Biol Chem 276(19): 16092-9.

Meloni, I., Bruttini, M., Longo, I., Mari, F., Rizzolio, F., D'Adamo, P., Denvriendt, K., Fryns, J. P., Toniolo, D. and Renieri, A. (2000). "A mutation in the rett syndrome gene, MECP2, causes X-linked mental retardation and progressive spasticity in males." Am J Hum Genet 67(4): 982-5.

Meloni, I., Muscettola, M., Raynaud, M., Longo, I., Bruttini, M., Moizard, M. P., Gomot, M., Chelly, J., des Portes, V., Fryns, J. P., Ropers, H. H., Magi, B., Bellan, C., Volpi, N., Yntema, H. G., Lewis, S. E., Schaffer, J. E. and Renieri, A. (2002). "FACL4, encoding fatty acid-CoA ligase 4, is mutated in nonspecific X-linked mental retardation." Nat Genet 30(4): 436-40.

Melyan, Z., Lancaster, B. and Wheal, H. V. (2004). "Metabotropic regulation of intrinsic excitability by synaptic activation of kainate receptors." J Neurosci 24(19): 4530-4.

Merienne, K., Jacquot, S., Pannetier, S., Zeniou, M., Bankier, A., Gecz, J., Mandel, J. L., Mulley, J., Sassone-Corsi, P. and Hanauer, A. (1999). "A missense mutation in RPS6KA3 (RSK2) responsible for non-specific mental retardation." Nat Genet 22(1): 13-4.

Molinari, F., Rio, M., Meskenaite, V., Encha-Razavi, F., Auge, J., Bacq, D., Briault, S., Vekemans, M., Munnich, A., Attie-Bitach, T., Sonderegger, P. and Colleaux, L. (2002). "Truncating neurotrypsin mutation in autosomal recessive nonsyndromic mental retardation." Science 298(5599): 1779-81.

Morton, N. E. (1998). "Significance levels in complex inheritance." Am J Hum Genet 62(3): 690-7.

Motazacker, M. M., Rost, B. R., Hucho, T., Garshasbi, M., Kahrizi, K., Ullmann, R., Abedini, S. S., Nieh, S. E., Amini, S. H., Goswami, C., Tzschach, A., Jensen, L. R., Schmitz, D., Ropers, H. H., Najmabadi, H. and Kuss, A. W. (2007). "A Defect in the Ionotropic Glutamate Receptor 6

Gene (GRIK2) Is Associated with Autosomal Recessive Mental Retardation." Am J Hum Genet 81(4): 792-8.

Mulle, C., Sailer, A., Perez-Otano, I., Dickinson-Anson, H., Castillo, P. E., Bureau, I., Maron, C., Gage, F. H., Mann, J. R., Bettler, B. and Heinemann, S. F. (1998). "Altered synaptic physiology and reduced susceptibility to kainate-induced seizures in GluR6-deficient mice." Nature 392(6676): 601-5.

Mulle, C., Sailer, A., Swanson, G. T., Brana, C., O'Gorman, S., Bettler, B. and Heinemann, S. F. (2000). "Subunit composition of kainate receptors in hippocampal interneurons." Neuron 28(2): 475-84.

Najmabadi, H., Motazacker, M. M., Garshasbi, M., Kahrizi, K., Tzschach, A., Chen, W., Behjati, F., Hadavi, V., Nieh, S. E., Abedini, S. S., Vazifehmand, R., Firouzabadi, S. G., Jamali, P., Falah, M., Seifati, S. M., Gruters, A., Lenzner, S., Jensen, L. R., Ruschendorf, F., Kuss, A. W. and Ropers, H. H. (2006). "Homozygosity mapping in consanguineous families reveals extreme heterogeneity of non-syndromic autosomal recessive mental retardation and identifies 8 novel gene loci." Hum Genet.

Naze, P., Vuillaume, I., Destee, A., Pasquier, F. and Sablonniere, B. (2002). "Mutation analysis and association studies of the ubiquitin carboxy-terminal hydrolase L1 gene in Huntington's disease." Neurosci Lett 328(1): 1-4.

O'Connell, J. R. and Weeks, D. E. (1998). "PedCheck: a program for identification of genotype incompatibilities in linkage analysis." Am J Hum Genet 63(1): 259-66.

Oberle, I., Rousseau, F., Heitz, D., Kretz, C., Devys, D., Hanauer, A., Boue, J., Bertheas, M. F. and Mandel, J. L. (1991). "Instability of a 550-base pair DNA segment and abnormal methylation in fragile X syndrome." Science 252(5010): 1097-102.

Ochman, H., Gerber, A. S. and Hartl, D. L. (1988). "Genetic applications of an inverse polymerase chain reaction." Genetics 120(3): 621-3.

Orrico, A., Lam, C., Galli, L., Dotti, M. T., Hayek, G., Tong, S. F., Poon, P. M., Zappella, M., Federico, A. and Sorrentino, V. (2000). "MECP2 mutation in male patients with non-specific X-linked mental retardation." FEBS Lett 481(3): 285-8.

Ou, X. M., Jafar-Nejad, H., Storring, J. M., Meng, J. H., Lemonde, S. and Albert, P. R. (2000). "Novel dual repressor elements for neuronal cell-specific transcription of the rat 5-HT1A receptor gene." J Biol Chem 275(11): 8161-8.

Ou, X. M., Lemonde, S., Jafar-Nejad, H., Bown, C. D., Goto, A., Rogaeva, A. and Albert, P. R. (2003). "Freud-1: A neuronal calcium-regulated repressor of the 5-HT1A receptor gene." J Neurosci 23(19): 7415-25.

Paternain, A. V., Herrera, M. T., Nieto, M. A. and Lerma, J. (2000). "GluR5 and GluR6 kainate receptor subunits coexist in hippocampal neurons and coassemble to form functional receptors." J Neurosci 20(1): 196-205.

Penrose, L. (1938). "A Clinical and Genetic Study of 1280 Cases of Mental Defect." HMSO, London.

Petrij, F., Giles, R. H., Dauwerse, H. G., Saris, J. J., Hennekam, R. C., Masuno, M., Tommerup, N., van Ommen, G. J., Goodman, R. H., Peters, D. J. and et al. (1995). "Rubinstein-Taybi syndrome caused by mutations in the transcriptional co-activator CBP." Nature 376(6538): 348-51.

Pickering, D. S., Taverna, F. A., Salter, M. W. and Hampson, D. R. (1995). "Palmitoylation of the GluR6 kainate receptor." Proc Natl Acad Sci U S A 92(26): 12090-4.

Pinheiro, P. and Mulle, C. (2006). "Kainate receptors." Cell Tissue Res 326(2): 457-82.

Polder, J. J., Meerding, W. J., Bonneux, L. and van der Maas, P. J. (2002). "Healthcare costs of intellectual disability in the Netherlands: a cost-of-illness perspective." J Intellect Disabil Res 46(Pt 2): 168-78.

Porter, R. H., Eastwood, S. L. and Harrison, P. J. (1997). "Distribution of kainate receptor subunit mRNAs in human hippocampus, neocortex and cerebellum, and bilateral reduction of hippocampal GluR6 and KA2 transcripts in schizophrenia." Brain Res 751(2): 217-31.

Priel, A., Selak, S., Lerma, J. and Stern-Bach, Y. (2006). "Block of kainate receptor desensitization uncovers a key trafficking checkpoint." Neuron 52(6): 1037-46.

Rauch, A., Hoyer, J., Guth, S., Zweier, C., Kraus, C., Becker, C., Zenker, M., Huffmeier, U., Thiel, C., Ruschendorf, F., Nurnberg, P., Reis, A. and Trautmann, U. (2006). "Diagnostic yield of various genetic approaches in patients with unexplained developmental delay or mental retardation." Am J Med Genet A 140(19): 2063-74.

Raymond, F. L. and Tarpey, P. (2006). "The genetics of mental retardation." Hum Mol Genet 15 Spec No 2: R110-6.

Reich, D. E., Cargill, M., Bolk, S., Ireland, J., Sabeti, P. C., Richter, D. J., Lavery, T., Kouyoumjian, R., Farhadian, S. F., Ward, R. and Lander, E. S. (2001). "Linkage disequilibrium in the human genome." Nature 411(6834): 199-204.

Ren, Z., Riley, N. J., Garcia, E. P., Sanders, J. M., Swanson, G. T. and Marshall, J. (2003). "Multiple trafficking signals regulate kainate receptor KA2 subunit surface expression." J Neurosci 23(16): 6608-16.

Ren, Z., Riley, N. J., Needleman, L. A., Sanders, J. M., Swanson, G. T. and Marshall, J. (2003). "Cell surface expression of GluR5 kainate receptors is regulated by an endoplasmic reticulum retention signal." J Biol Chem 278(52): 52700-9.

Rodriguez-Moreno, A. and Lerma, J. (1998). "Kainate receptor modulation of GABA release involves a metabotropic function." Neuron 20(6): 1211-8.

Roeleveld, N., Zielhuis, G. A. and Gabreels, F. (1997). "The prevalence of mental retardation: a critical review of recent literature." Dev Med Child Neurol 39(2): 125-32.

Ropers, H. H. (2006). "X-linked mental retardation: many genes for a complex disorder." Curr Opin Genet Dev 16(3): 260-9.

Ropers, H. H. (2007). "New perspectives for the elucidation of genetic disorders." Am J Hum Genet 81(2): 199-207.

Ropers, H. H. and Hamel, B. C. (2005). "X-linked mental retardation." Nat Rev Genet 6(1): 46-57.

Ropers, H. H., Hoeltzenbein, M., Kalscheuer, V., Yntema, H., Hamel, B., Fryns, J. P., Chelly, J., Partington, M., Gecz, J. and Moraine, C. (2003). "Nonsyndromic X-linked mental retardation: where are the missing mutations?" Trends Genet 19(6): 316-20.

Rozas, J. L., Paternain, A. V. and Lerma, J. (2003). "Noncanonical signaling by ionotropic kainate receptors." Neuron 39(3): 543-53.

Rubinsztein, D. C., Leggo, J., Chiano, M., Dodge, A., Norbury, G., Rosser, E. and Craufurd, D. (1997). "Genotypes at the GluR6 kainate receptor locus are associated with variation in the age of onset of Huntington disease." Proc Natl Acad Sci U S A 94(8): 3872-6.

Ruiz, A., Sachidhanandam, S., Utvik, J. K., Coussen, F. and Mulle, C. (2005). "Distinct subunits in heteromeric kainate receptors mediate ionotropic and metabotropic function at hippocampal mossy fiber synapses." J Neurosci 25(50): 11710-8.

Ruschendorf, F. and Nurnberg, P. (2005). "ALOHOMORA: a tool for linkage analysis using 10K SNP array data." Bioinformatics 21(9): 2123-5.

Salomons, G. S., van Dooren, S. J., Verhoeven, N. M., Cecil, K. M., Ball, W. S., Degrauw, T. J. and Jakobs, C. (2001). "X-linked creatine-transporter gene (SLC6A8) defect: a new creatine-deficiency syndrome." Am J Hum Genet 68(6): 1497-500.

Sander, T., Janz, D., Ramel, C., Ross, C. A., Paschen, W., Hildmann, T., Wienker, T. F., Bianchi, A., Bauer, G., Sailer, U. and et al. (1995). "Refinement of map position of the human GluR6 kainate receptor gene (GRIK2) and lack of association and linkage with idiopathic generalized epilepsies." Neurology 45(9): 1713-20.

Savinainen, A., Garcia, E. P., Dorow, D., Marshall, J. and Liu, Y. F. (2001). "Kainate receptor activation induces mixed lineage kinase-mediated cellular signaling cascades via post-synaptic density protein 95." J Biol Chem 276(14): 11382-6.

Schiffer, H. H., Swanson, G. T. and Heinemann, S. F. (1997). "Rat GluR7 and a carboxy-terminal splice variant, GluR7b, are functional kainate receptor subunits with a low sensitivity to glutamate." Neuron 19(5): 1141-6.

Schmitz, D., Mellor, J., Breustedt, J. and Nicoll, R. A. (2003). "Presynaptic kainate receptors impart an associative property to hippocampal mossy fiber long-term potentiation." Nat Neurosci 6(10): 1058-63.

Schmitz, D., Mellor, J., Frerking, M. and Nicoll, R. A. (2001). "Presynaptic kainate receptors at hippocampal mossy fiber synapses." Proc Natl Acad Sci U S A 98(20): 11003-8.

Shibata, H., Shibata, A., Ninomiya, H., Tashiro, N. and Fukumaki, Y. (2002). "Association study of polymorphisms in the GluR6 kainate receptor gene (GRIK2) with schizophrenia." Psychiatry Res 113(1-2): 59-67.

Shoichet, S. A., Hoffmann, K., Menzel, C., Trautmann, U., Moser, B., Hoeltzenbein, M., Echenne, B., Partington, M., Van Bokhoven, H., Moraine, C., Fryns, J. P., Chelly, J., Rott, H. D., Ropers, H. H. and Kalscheuer, V. M. (2003). "Mutations in the ZNF41 gene are associated with cognitive deficits: identification of a new candidate for X-linked mental retardation." Am J Hum Genet 73(6): 1341-54.

Shuang, M., Liu, J., Jia, M. X., Yang, J. Z., Wu, S. P., Gong, X. H., Ling, Y. S., Ruan, Y., Yang, X. L. and Zhang, D. (2004). "Family-based association study between autism and glutamate receptor 6 gene in Chinese Han trios." Am J Med Genet B Neuropsychiatr Genet 131(1): 48-50.

Slager, R. E., Newton, T. L., Vlangos, C. N., Finucane, B. and Elsea, S. H. (2003). "Mutations in RAI1 associated with Smith-Magenis syndrome." Nat Genet 33(4): 466-8.

Sommer, B., Burnashev, N., Verdoorn, T. A., Keinanen, K., Sakmann, B. and Seeburg, P. H. (1992). "A glutamate receptor channel with high affinity for domoate and kainate." Embo J 11(4): 1651-6.

Stephan, A., Mateos, J. M., Kozlov, S. V., Cinelli, P., Kistler, A. D., Hettwer, S., Rulicke, T., Streit, P., Kunz, B. and Sonderegger, P. (2008). "Neurotrypsin cleaves agrin locally at the synapse." Faseb J.

Strachan, T. and Read, A. P. (2004). Human Molecular Genetics, Chapter 13., Garland Science.

Stromme, P., Mangelsdorf, M. E., Shaw, M. A., Lower, K. M., Lewis, S. M., Bruyere, H., Lutcherath, V., Gedeon, A. K., Wallace, R. H., Scheffer, I. E., Turner, G., Partington, M., Frints, S. G., Fryns, J. P., Sutherland, G. R., Mulley, J. C. and Gecz, J. (2002). "Mutations in the human ortholog of Aristaless cause X-linked mental retardation and epilepsy." Nat Genet 30(4): 441-5.

Strutz-Seebohm, N., Korniychuk, G., Schwarz, R., Baltaev, R., Ureche, O. N., Mack, A. F., Ma, Z. L., Hollmann, M., Lang, F. and Seebohm, G. (2006). "Functional significance of the kainate receptor GluR6(M836I) mutation that is linked to autism." Cell Physiol Biochem 18(4-5): 287-94.

Swanson, G. T., Feldmeyer, D., Kaneda, M. and Cull-Candy, S. G. (1996). "Effect of RNA editing and subunit co-assembly single-channel properties of recombinant kainate receptors." J Physiol 492 (Pt 1): 129-42.

Tarpey, P., Parnau, J., Blow, M., Woffendin, H., Bignell, G., Cox, C., Cox, J., Davies, H., Edkins, S., Holden, S., Korny, A., Mallya, U., Moon, J., O'Meara, S., Parker, A., Stephens, P., Stevens, C., Teague, J., Donnelly, A., Mangelsdorf, M., Mulley, J., Partington, M., Turner, G., Stevenson, R., Schwartz, C., Young, I., Easton, D., Bobrow, M., Futreal, P. A., Stratton, M. R., Gecz, J., Wooster, R. and Raymond, F. L. (2004). "Mutations in the DLG3 gene cause nonsyndromic X-linked mental retardation." Am J Hum Genet 75(2): 318-24.

Tarpey, P. S., Raymond, F. L., Nguyen, L. S., Rodriguez, J., Hackett, A., Vandeleur, L., Smith, R., Shoubridge, C., Edkins, S., Stevens, C., O'Meara, S., Tofts, C., Barthorpe, S., Buck, G., Cole, J., Halliday, K., Hills, K., Jones, D., Mironenko, T., Perry, J., Varian, J., West, S., Widaa, S., Teague, J., Dicks, E., Butler, A., Menzies, A., Richardson, D., Jenkinson, A., Shepherd, R., Raine, K., Moon, J., Luo, Y., Parnau, J., Bhat, S. S., Gardner, A., Corbett, M., Brooks, D., Thomas, P., Parkinson-Lawrence, E., Porteous, M. E., Warner, J. P., Sanderson, T., Pearson, P., Simensen, R. J., Skinner, C., Hoganson, G., Superneau, D., Wooster, R., Bobrow, M., Turner, G., Stevenson, R. E., Schwartz, C. E., Futreal, P. A., Srivastava, A. K., Stratton, M. R.

and Gecz, J. (2007). "Mutations in UPF3B, a member of the nonsense-mediated mRNA decay complex, cause syndromic and nonsyndromic mental retardation." Nat Genet 39(9): 1127-33.

Tarpey, P. S., Stevens, C., Teague, J., Edkins, S., O'Meara, S., Avis, T., Barthorpe, S., Buck, G., Butler, A., Cole, J., Dicks, E., Gray, K., Halliday, K., Harrison, R., Hills, K., Hinton, J., Jones, D., Menzies, A., Mironenko, T., Perry, J., Raine, K., Richardson, D., Shepherd, R., Small, A., Tofts, C., Varian, J., West, S., Widaa, S., Yates, A., Catford, R., Butler, J., Mallya, U., Moon, J., Luo, Y., Dorkins, H., Thompson, D., Easton, D. F., Wooster, R., Bobrow, M., Carpenter, N., Simensen, R. J., Schwartz, C. E., Stevenson, R. E., Turner, G., Partington, M., Gecz, J., Stratton, M. R., Futreal, P. A. and Raymond, F. L. (2006). "Mutations in the gene encoding the Sigma 2 subunit of the adaptor protein 1 complex, AP1S2, cause X-linked mental retardation." Am J Hum Genet 79(6): 1119-24.

Telfeian, A. E., Federoff, H. J., Leone, P., During, M. J. and Williamson, A. (2000). "Overexpression of GluR6 in rat hippocampus produces seizures and spontaneous nonsynaptic bursting in vitro." Neurobiol Dis 7(4): 362-74.

Thiele, H. and Nurnberg, P. (2005). "HaploPainter: a tool for drawing pedigrees with complex haplotypes." Bioinformatics 21(8): 1730-2.

Trimborn, M., Richter, R., Sternberg, N., Gavvovidis, I., Schindler, D., Jackson, A. P., Prott, E. C., Sperling, K., Gillessen-Kaesbach, G. and Neitzel, H. (2005). "The first missense alteration in the MCPH1 gene causes autosomal recessive microcephaly with an extremely mild cellular and clinical phenotype." Hum Mutat 26(5): 496.

Turner, G., Gedeon, A. and Mulley, J. (1994). "X-linked mental retardation with heterozygous expression and macrocephaly: pericentromeric gene localization." Am J Med Genet 51(4): 575-80.

Valluru, L., Xu, J., Zhu, Y., Yan, S., Contractor, A. and Swanson, G. T. (2005). "Ligand binding is a critical requirement for plasma membrane expression of heteromeric kainate receptors." J Biol Chem 280(7): 6085-93.

Vervoort, V. S., Beachem, M. A., Edwards, P. S., Ladd, S., Miller, K. E., de Mollerat, X., Clarkson, K., DuPont, B., Schwartz, C. E., Stevenson, R. E., Boyd, E. and Srivastava, A. K. (2002). "AGTR2 mutations in X-linked mental retardation." Science 296(5577): 2401-3.

Vissel, B., Royle, G. A., Christie, B. R., Schiffer, H. H., Ghetti, A., Tritto, T., Perez-Otano, I., Radcliffe, R. A., Seamans, J., Sejnowski, T., Wehner, J. M., Collins, A. C., O'Gorman, S. and Heinemann, S. F. (2001). "The role of RNA editing of kainate receptors in synaptic plasticity and seizures." Neuron 29(1): 217-27.

Watkins, J. C. and Evans, R. H. (1981). "Excitatory amino acid transmitters." Annu Rev Pharmacol Toxicol 21: 165-204.

Wechsler, A. and Teichberg, V. I. (1998). "Brain spectrin binding to the NMDA receptor is regulated by phosphorylation, calcium and calmodulin." Embo J 17(14): 3931-9.

Wechsler, D. (1981). "Wechsler adult intelligence scalerevised (WAIS-R) manual." The Psychological Corporation, New York, USA.

Werner, P., Voigt, M., Keinanen, K., Wisden, W. and Seeburg, P. H. (1991). "Cloning of a putative high-affinity kainate receptor expressed predominantly in hippocampal CA3 cells." Nature 351(6329): 742-4.

Weston, M. C., Schuck, P., Ghosal, A., Rosenmund, C. and Mayer, M. L. (2006). "Conformational restriction blocks glutamate receptor desensitization." Nat Struct Mol Biol 13(12): 1120-7.

Wilcken, B., Wiley, V., Hammond, J. and Carpenter, K. (2003). "Screening newborns for inborn errors of metabolism by tandem mass spectrometry." N Engl J Med 348(23): 2304-12.

Wilding, T. J. and Huettner, J. E. (2001). "Functional diversity and developmental changes in rat neuronal kainate receptors." J Physiol 532(Pt 2): 411-21.

Wisden, W. and Seeburg, P. H. (1993). "A complex mosaic of high-affinity kainate receptors in rat brain." J Neurosci 13(8): 3582-98.

Woods, C. G., Bond, J. and Enard, W. (2005). "Autosomal recessive primary microcephaly (MCPH): a review of clinical, molecular, and evolutionary findings." Am J Hum Genet 76(5): 717-28.

Wu, L. J., Zhao, M. G., Toyoda, H., Ko, S. W. and Zhuo, M. (2005). "Kainate receptor-mediated synaptic transmission in the adult anterior cingulate cortex." J Neurophysiol 94(3): 1805-13.

Yan, S., Sanders, J. M., Xu, J., Zhu, Y., Contractor, A. and Swanson, G. T. (2004). "A C-terminal determinant of GluR6 kainate receptor trafficking." J Neurosci 24(3): 679-91.

Yan, W., Wilson, C. C. and Haring, J. H. (1997). "Effects of neonatal serotonin depletion on the development of rat dentate granule cells." Brain Res Dev Brain Res 98(2): 177-84.

Yasuno, F., Suhara, T., Nakayama, T., Ichimiya, T., Okubo, Y., Takano, A., Ando, T., Inoue, M., Maeda, J. and Suzuki, K. (2003). "Inhibitory effect of hippocampal 5-HT1A receptors on human explicit memory." Am J Psychiatry 160(2): 334-40.

Yeargin-Allsopp, M., Murphy, C. C., Cordero, J. F., Decoufle, P. and Hollowell, J. G. (1997). "Reported biomedical causes and associated medical conditions for mental retardation among 10-year-old children, metropolitan Atlanta, 1985 to 1987." Dev Med Child Neurol 39(3): 142-9.

Zemni, R., Bienvenu, T., Vinet, M. C., Sefiani, A., Carrie, A., Billuart, P., McDonell, N., Couvert, P., Francis, F., Chafey, P., Fauchereau, F., Friocourt, G., des Portes, V., Cardona, A., Frints, S., Meindl, A., Brandau, O., Ronce, N., Moraine, C., van Bokhoven, H., Ropers, H. H., Sudbrak, R., Kahn, A., Fryns, J. P., Beldjord, C. and Chelly, J. (2000). "A new gene involved in X-linked mental retardation identified by analysis of an X;2 balanced translocation." Nat Genet 24(2): 167-70.

7. Supplementary data

A. Primers

Primers used for *GRIK2* coding sequence amplification and sequencing		
Exon number	**Primer sequence**	**Direction**
5'UTR	GGGCTGTCAGATCGGTTG	Forward
5'UTR	TCGGGTAGAAATGAGGATGC	Reverse
Exon1	AGTGGAAGGTTGTTCCTTGG	Forward
Exon1	AGAGCGAACCGCCTGTTTAC	Reverse
Exon2	ACACGCAAATGCACTTGCAC	Forward
Exon2	CCTAGAAATTTGAATTCCAGGAAAC	Reverse
Exon3	ACACTGGCACCTCTCCTCTC	Forward
Exon3	AAGAACCTGGAATGGGCTTC	Reverse
Exon4	CGTTCTTGGCCGTATCAAAC	Forward
Exon4	AAAAGAAGATCATATTGTAAGTGCAAG	Reverse
Exon5	TTGTAGGTTGATTCTTTATCACATCC	Forward
Exon5	TGTCCTCTCTGATAATAATTTTGGTG	Reverse
Exon6	TTTCAGTAATACATGCCTGTGAAG	Forward
Exon6	TGCATTGTAGCTCTGATATTTTGC	Reverse
Exon7	TTGCAAACCATCTACCACAAG	Forward
Exon7	GGACACTTGCTAGAAAAACCAC	Reverse
Exon8	TCTAGCAATGTAAACTGAAAAGTAATG	Forward
Exon8	CCCTTTATCCTTGAATCCTAATTG	Reverse
Exon9	TTTCTTTTGCAGTACTCTCTACCAC	Forward
Exon9	TGTCCTTTTCTATGCACTTCTGTG	Reverse
Exon10	AAGCAATAATTCTGATGATGAGTTTC	Forward
Exon10	TCAACAAAAGAGTAAACCTTGTAGC	Reverse
Exon11	CATAATCGTTACTGAGGCAATTAAG	Forward
Exon11	GCACCCCATGGAAAATAAAG	Reverse
Exon12	TCTGTCTTTTTGTTTCTTTTGCAG	Forward
Exon12	CACCCCCAGCAAAGAGTG	Reverse

Exon13	GTGATTCCATTCTGCCACTG	Forward
Exon13	TTGTGAATCGAGAGAAGTTTGC	Reverse
Exon14	GCATTATAGGAGCACATGGAAAC	Forward
Exon14	AATGGCATACGTGGACACAC	Reverse
Exon15	TCTGCCCTCCTCTCATCTTG	Forward
Exon15	ATGAATGACATAAGACAATTTAGAGC	Reverse
Exon16	TTTAAATGTCAACGGGATCAAG	Forward
Exon16	TTTATGTGGCACCTGACAGC	Reverse
Exon16b	CATTGTTTCAAGAATTAGAGATGTG	Forward
Exon16b	GAAACCCACGCACTGTGTC	Reverse
Exon16c	TTGATCTTGGACAGTTACAGTTTATG	Forward
Exon16c	AACATTCTGGCTAAATTGTTTGG	Reverse
Exon6b	AATTCCACGATTCCATCCAG	Forward
Exon6b	AGAAACTGTGGGCCAGGTG	Reverse

B. Pedigrees

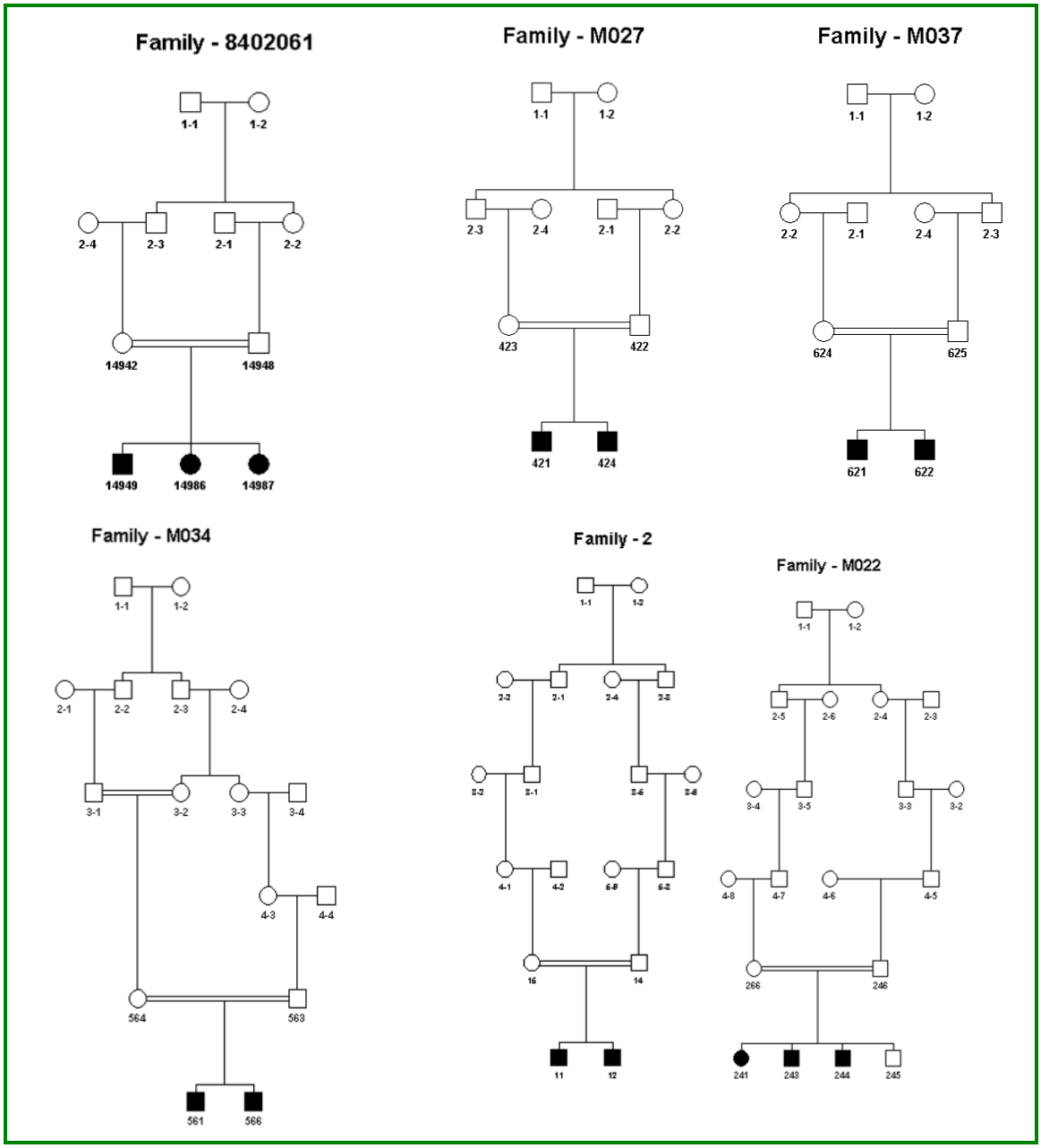
Family - 8402061
1-1
1-2
2-4
2-3
2-1
2-2
14942
14948
14949
14986
14987
Family - M027
1-1
1-2
2-3
2-4
2-1
2-2
423
422
421
424
Family - M037
1-1
1-2
2-2
2-1
2-4
2-3
624
625
621
622
Family - M034
1-1
1-2
2-1
2-2
2-3
2-4
3-1
3-2
3-3
3-4
4-3
4-4
564
563
561
566
Family - 2
1-1
1-2
Family - M022
1-1
1-2
2-5
2-6
2-4
2-3
3-4
3-5
3-3
3-2
4-8
4-7
4-6
4-5
266
246
241
243
244
245

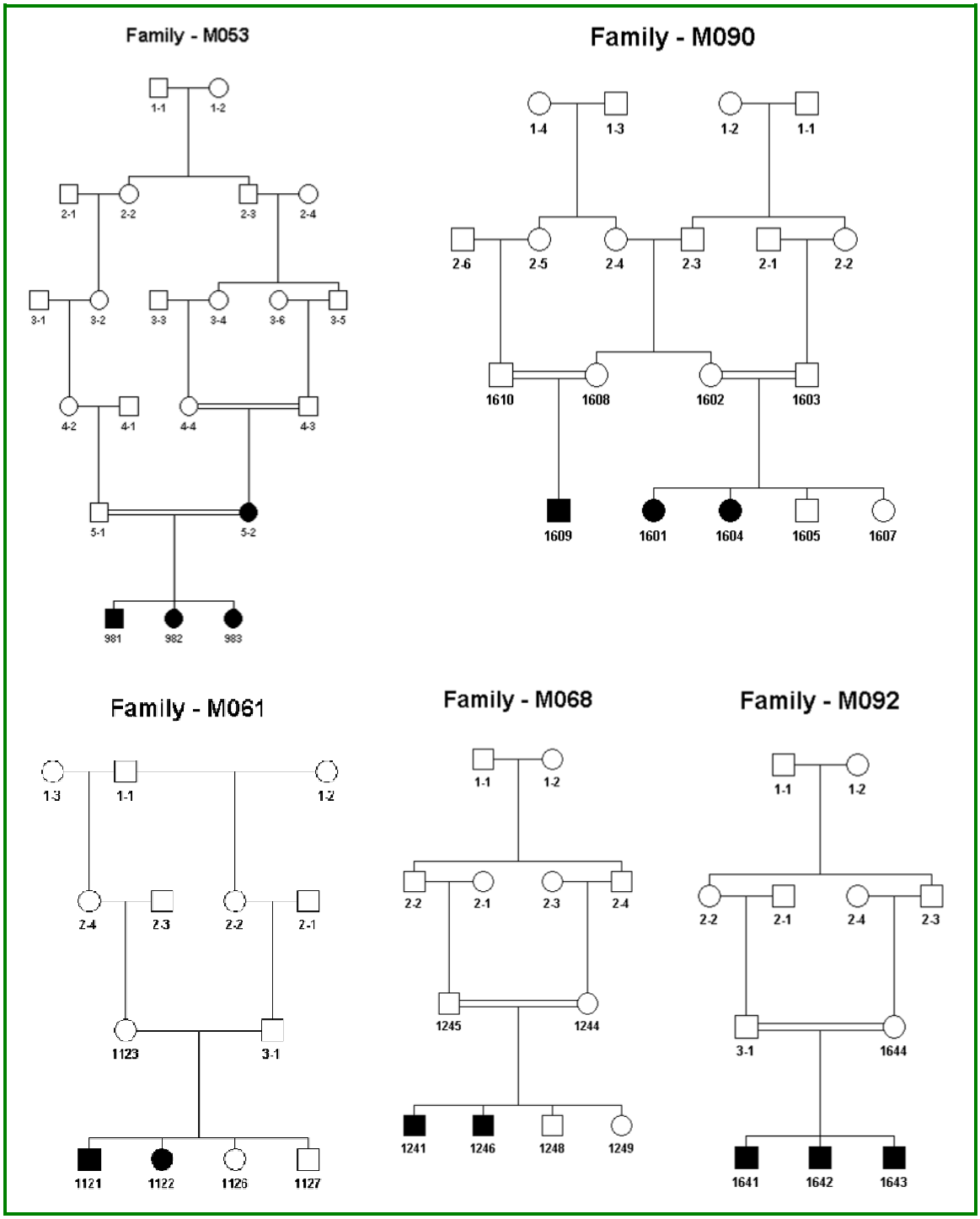
Family - M053
1-1
1-2
2-1
2-2
2-3
2-4
3-1
3-2
3-3
3-4
3-6
3-5
4-2
4-1
4-4
4-3
5-1
5-2
981
982
983
Family - M090
1-4
1-3
1-2
1-1
2-6
2-5
2-4
2-3
2-1
2-2
1610
1608
1602
1603
1609
1601
1604
1605
1607
Family - M061
1-3
1-1
1-2
2-4
2-3
2-2
2-1
1123
3-1
1121
1122
1126
1127
Family - M068
1-1
1-2
2-2
2-1
2-3
2-4
1245
1244
1241
1246
1248
1249
Family - M092
1-1
1-2
2-2
2-1
2-4
2-3
3-1
1644
1641
1642
1643

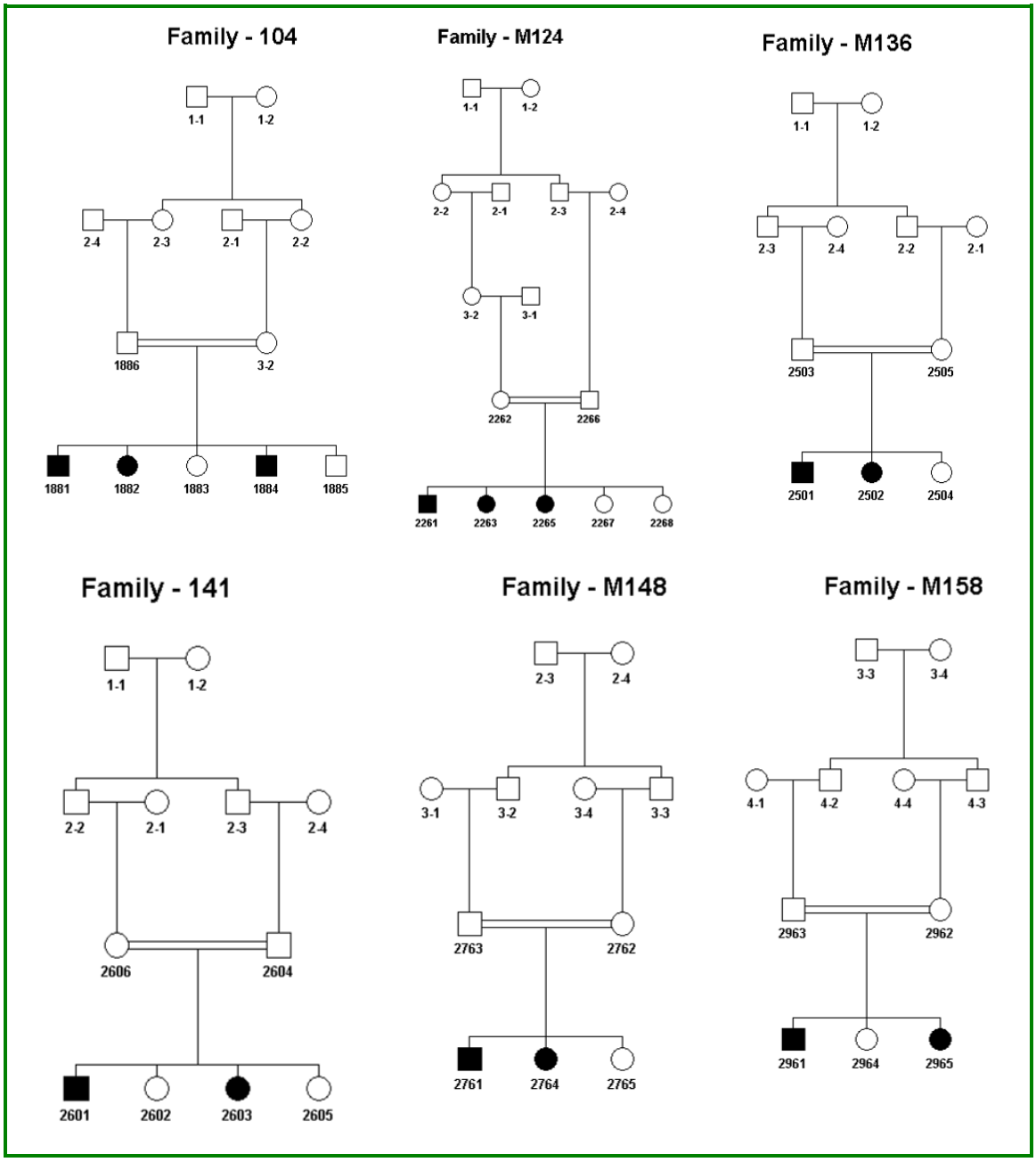
Family - 104
1-1
1-2
2-4
2-3
2-1
2-2
1886
3-2
1881
1882
1883
1884
1885
Family - M124
1-1
1-2
2-2
2-1
2-3
2-4
3-2
3-1
2262
2266
2261
2263
2265
2267
2268
Family - M136
1-1
1-2
2-3
2-4
2-2
2-1
2503
2505
2501
2502
2504
Family - 141
1-1
1-2
2-2
2-1
2-3
2-4
2606
2604
2601
2602
2603
2605
Family - M148
2-3
2-4
3-1
3-2
3-4
3-3
2763
2762
2761
2764
2765
Family - M158
3-3
3-4
4-1
4-2
4-4
4-3
2963
2962
2961
2964
2965

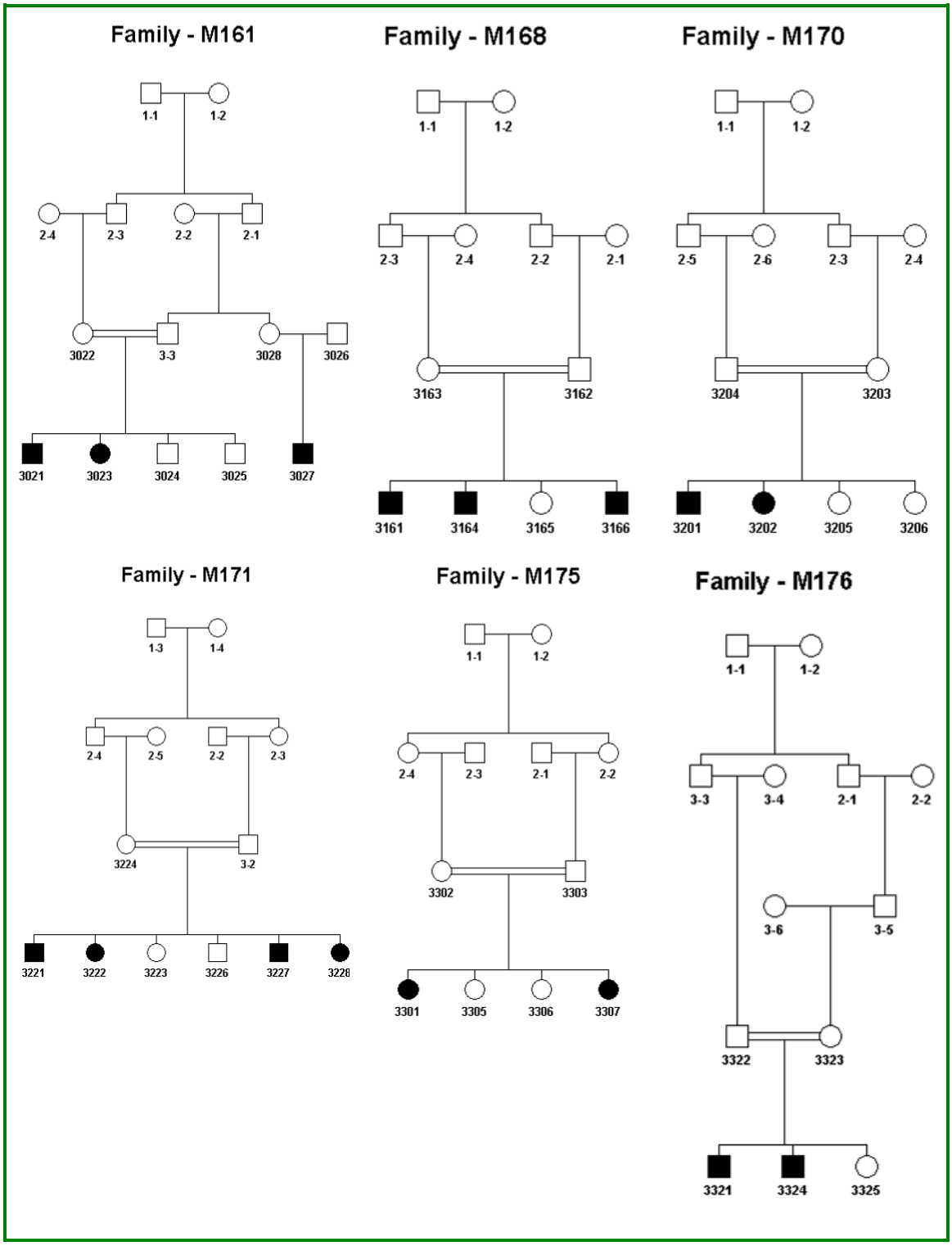
Family - M161
1-1
1-2
2-4
2-3
2-2
2-1
3022
3-3
3028
3026
3021
3023
3024
3025
3027
Family - M168
1-1
1-2
2-3
2-4
2-2
2-1
3163
3162
3161
3164
3165
3166
Family - M170
1-1
1-2
2-5
2-6
2-3
2-4
3204
3203
3201
3202
3205
3206
Family - M171
1-3
1-4
2-4
2-5
2-2
2-3
3224
3-2
3221
3222
3223
3226
3227
3228
Family - M175
1-1
1-2
2-4
2-3
2-1
2-2
3302
3303
3301
3305
3306
3307
Family - M176
1-1
1-2
3-3
3-4
2-1
2-2
3-6
3-5
3322
3323
3321
3324
3325

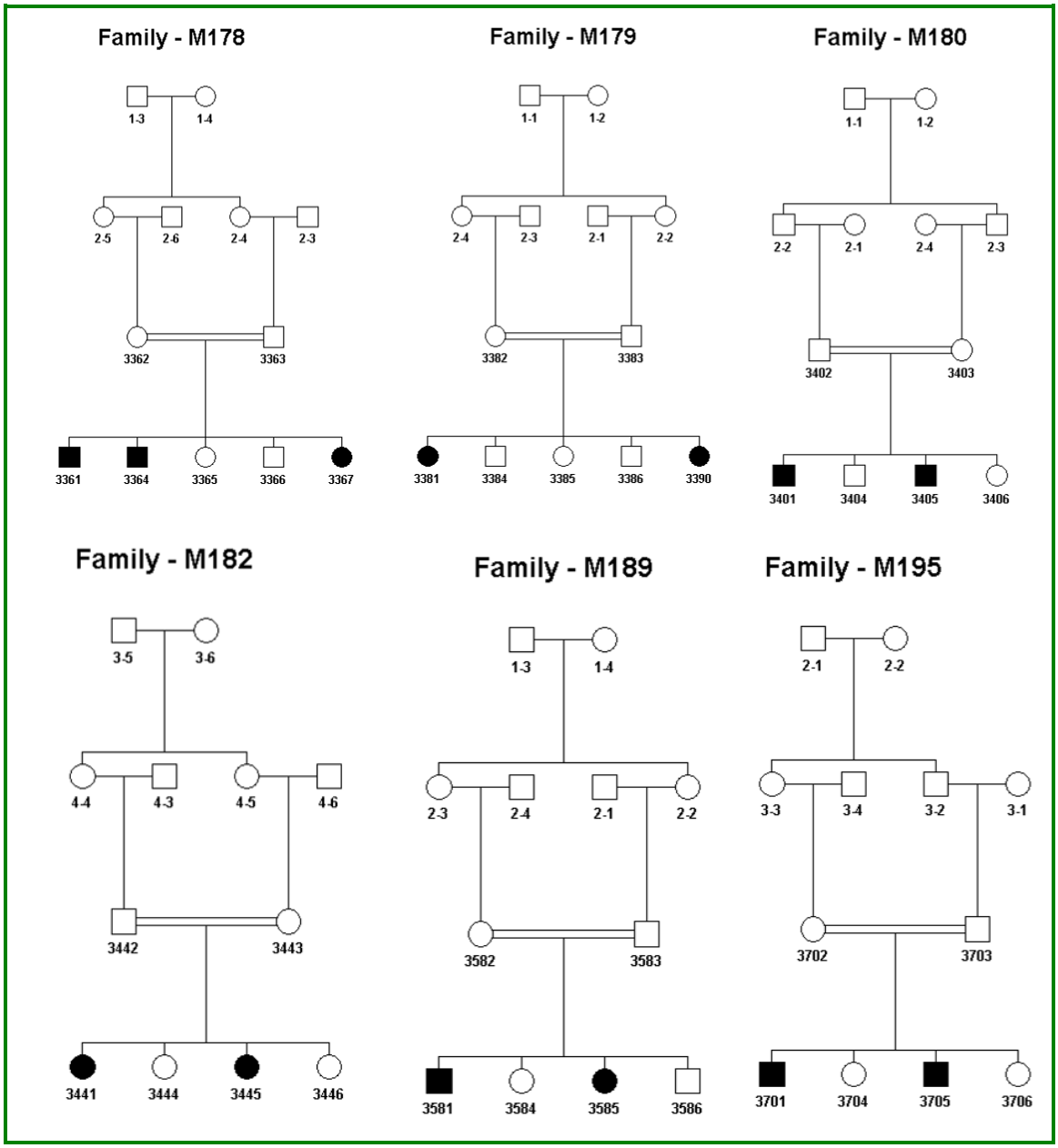
Family - M178
1-3
1-4
2-5
2-6
2-4
2-3
3362
3363
3361
3364
3365
3366
3367
Family - M179
1-1
1-2
2-4
2-3
2-1
2-2
3382
3383
3381
3384
3385
3386
3390
Family - M180
1-1
1-2
2-2
2-1
2-4
2-3
3402
3403
3401
3404
3405
3406
Family - M182
3-5
3-6
4-4
4-3
4-5
4-6
3442
3443
3441
3444
3445
3446
Family - M189
1-3
1-4
2-3
2-4
2-1
2-2
3582
3583
3581
3584
3585
3586
Family - M195
2-1
2-2
3-3
3-4
3-2
3-1
3702
3703
3701
3704
3705
3706

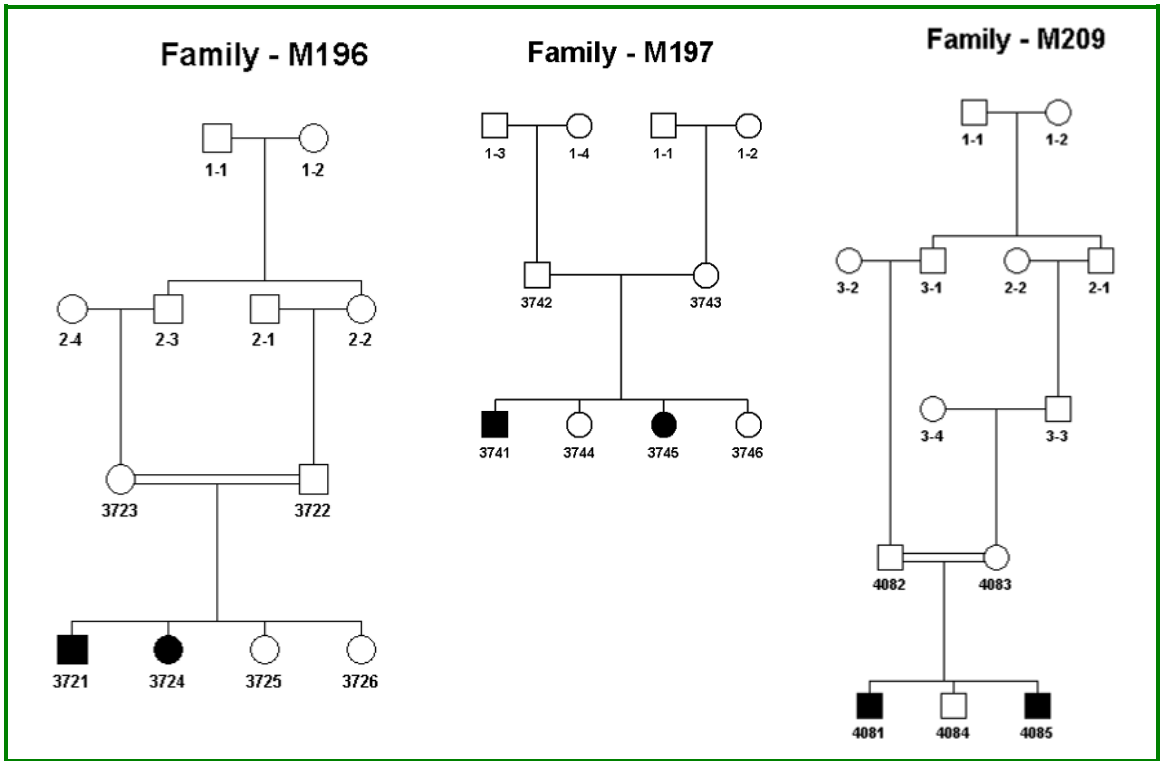
Family - M196
1-1
1-2
2-4
2-3
2-1
2-2
3723
3722
3721
3724
3725
3726
Family - M197
1-3
1-4
1-1
1-2
3742
3743
3741
3744
3745
3746
Family - M209
1-1
1-2
3-2
3-1
2-2
2-1
3-4
3-3
4082
4083
4081
4084
4085

C. Genes in MRT6 interval

Genes in MRT6 locus and their known functional information.		
A) 8 most prominent candidate MRT6 genes and available related information		
Gene	**Description**	**Information (Function, expression pattern,...)**
GRIK2	**Glutamate receptor, ionotropic, kainate 2**	Glutamate receptors mediate the majority of excitatory neurotransmission in the brain. May have a role in synaptic plasticity and may be important for learning and memory. May be involved in the transmission of light information from the retina to the hypothalamus. The protein structure and function is changed by RNA editing. Alternatively spliced transcript variants have been described. Integral membrane protein. Assembles into a kainate-gated homomeric channel that does not bind AMPA. *GRIK2* associated to *Grik5* forms functional channels. Interacts with *DLG4*. Highly expressed in brain. Expression is higher in cerebellum than in cerebral cortex.
CCNC	**Cyclin C**	A member of the cyclin family of proteins. Interacts with cyclin-dependent kinase 8 and induces the phophorylation of the carboxy-terminal domain of the large subunit of RNA polymerase II. Peak of mRNA level in the G1 phase of the cell cycle. Two transcript variants encoding different isoforms. May play a role in transcriptional regulation. Highest expression level in pancreas. High levels in heart, liver, skeletal muscle and kidney. Low levels in brain and cerebellum.
COQ3	**Coenzyme Q3 homolog, methyltransferase (yeast)**	Methyltransfrase Expressed in brain Ubiquinone biosynthesis from p-hydroxybenzoic acid
GPR145	**G protein-coupled receptor 145**	Receptor for somatostatin-28. Belongs to the g-protein coupled receptor 1 family. Activity mediated by g proteins which inhibit adenylyl cyclase. Integral membrane protein. Highly brain expressed.

GPR63	**G protein-coupled receptor 63**	G protein-coupled receptor family. Contain 7 transmembrane domains and transduce extracellular signals through heterotrimeric G proteins. One of the several different receptors for 5- hydroxytryptamine (serotonin, a biogenic hormone that functions as a neurotransmitter, a hormone, and a mitogen) Its activity is mediated by G-proteins that stimulate adenylate cyclase.
KIAA1900 (KLHL32)		Highly expressed in fetal brain and brain. Protein binding, contains 1 btb (poz) domain. BTB and kelch domain containing protein 5.
POU3F2	**POU domain, class 3, transcription factor 2**	A transcription factor that binds to the octameric DNA sequence ATGCAAAT. Share a highly homologous region, referred to as the POU domain, which occurs in several mammalian transcription factors, including the octamer-binding proteins Oct1 (POU2F1; MIM 164175) and Oct2 (POU2F2; MIM 164176), and the pituitary protein Pit1 (PIT1; MIM 173110). Class III POU genes are expressed predominantly in the CNS. May play an important role in mammalian neurogenesis by regulating their diverse patterns of gene expression. Transcription factor that binds preferentially to the recognition sequence which consists of two distinct half-sites, ('gcat') and ('taat'), separated by a nonconserved spacer region of 0, 2, or 3 nucleotides. Positively regulates the genes under the control of corticotropin-releasing hormone (crh) and crh-ii promoters. Expressed specifically in the neuroectodermal cell lineage. Highly brain expressed
SIM1	**Single-minded homolog 1 (Drosophila)**	SIM1 and SIM2 genes are Drosophila single-minded (sim) gene homologe. Transcript detected only in fetal kidney out of various adult and fetal tissues tested. Since the SIM gene plays an important role in Drosophila development and has peak levels of expression during the period of neurogenesis, it was proposed that the human SIM gene is a candidate for involvement in certain dysmorphic features (particularly the facial and skull characteristics), abnormalities of brain development, and/or mental retardation of Down syndrome. Transcriptional factor that may have pleiotropic effects during embryogenesis and in the adult. Efficient DNA binding requires dimerization with another bhlh protein. Heterodimer with arnt.
B) Genes in MRT6 locus whose sequence is not verified		

ASCC3	Activating signal cointegrator 1 complex subunit 3	Highly expressed in fetal brain.
BVES	Blood vessel epicardial substance	Encodes a member of the POP family of proteins containing three putative transmembrane domains. Expressed in cardiac and skeletal muscle and may play an important role in development of these tissues. The mouse ortholog may be involved in the regeneration of adult skeletal muscle and may act as a cell adhesion molecule in coronary vasculogenesis. Two transcript variants encoding the same protein have been found for this gene. No brain expression reported
C6orf167		Fetal brain expressed
C6orf168		involved in transport of proteins into the mitochondrion. mitochondrial outer membrane. Interacts with metaxin 1. Highly expressed in brain
C6orf66		Hormone-regulated proliferation-associated 20 Highly expressed in cerebellum and brain
FBXL4	F-box and leucine-rich repeat protein 4	A member of the F-box protein family which is characterized by an approximately 40 amino acid motif, the F-box. The F-box proteins constitute one of the four subunits of ubiquitin protein ligase complex called SCFs (SKP1-cullin-F-box), which function in phosphorylation-dependent ubiquitination. The F-box proteins are divided into 3 classes: Fbws containing WD-40 domains, Fbls containing leucine-rich repeats, and Fbxs containing either different protein-protein interaction modules or no recognizable motifs. The protein encoded by this gene belongs to the Fbls class and, in addition to an F-box, contains at least 9 tandem leucine-rich repeats. Probably constitutes the primary response element required for the generation or interpretation of the signal that induces glucose repression. Is not an essential protein. Involved in substrate recognition in ubiquitin-dependent degradation.necessary for the glucose repression pathway. Expressed constitutively at low levels.

FHL5	Four and a half LIM domains 5	Coordinately expressed with activator of cAMP-responsive element modulator (CREM). Associated with CREM and confers a powerful transcriptional activation function. (CREM acts as a transcription factor essential for the differentiation of spermatids into mature spermatozoa) Interacts with znf638. Contains multiple polyadenylation sites. Expressed in skeletal muscle and heart. highly expressed in prostate and testis , also brain expressed.
FUT9	Fucosyltransferase 9 (alpha (1,3) fucosyltransferase)	One of several alpha-3-fucosyltransferases that can catalyze the last step in the biosynthesis of Lewis antigen, the addition of a fucose to precursor polysaccharides. Synthesizes the LeX oligosaccharide, which is expressed in organ buds progressing in mesenchyma during human embryogenesis. Catalyzes alpha-1,3 glycosidic linkages. Type ii membrane protein. membrane-bound form in trans cisternae of golgi (by similarity). Highly expressed in brain
KIAA0776		Hypothetical protein LOC23376
Manea	Mannosidase, endo-alpha	Expressed in placenta and prostate (very low expression in brain), involved in carbohydrate metabolism.
POPDC3	Popeye domain containing 3	Membrane, multi-pass membrane protein. Expressed in cardiac and skeletal muscle May play an important role in heart development. Expressed predominantly in skeletal muscle and detected in heart
PRDM13	PR domain containing 13	May function as a transcription factor. (By similarity)
PREP	Prolyl endopeptidase	Cytosolic prolyl endopeptidase that cleaves peptide bonds on the C-terminal side of prolyl residues within peptides that are up to approximately 30 amino acids long. Reported to be involved in the maturation and degradation of peptide hormones and neuropeptides. Low levels of expression in the brain.

D. Clinical features and M097 family structure

MRT6 was identified as a result of linkage analysis in family M097 with 6 affected individuals. The degree of mental retardation in the affected family members ranged from mild to severe. Patient IV:1 had an IQ of 30 at the age of 50 years. His youngest sister (IV:4) had mild mental retardation. Patients V:2 and V:9 also suffered from mild mental retardation, and patient V:8 had an IQ of 55 (moderate MR). The patients had neither neurological problems, nor congenital malformations, nor facial dysmorphisms. Body height, weight and head circumference were normal in all patients. For patient V:9 we performed an MRI scan, which revealed no morphological abnormalities. Standard 450 G-band karyotyping had ruled out the possibility of visible chromosomal aberrations as a cause of MR and fragile-X testing was done for above mentioned affected individuals by PCR, ruling out the possibility of fragile-X syndrome as a cause of MR. Sample collection and clinical evaluation procedures were carried out with the informed consent of the parents.

Initially 7 family members from whom DNA was available were genotyped (Figure D-a). Linkage analysis showed a single homozygous region on chromosome 6 in all affected individuals. Later, because this relatively large haplotype in the affected from branch 1 was similar to the core family, a consanguinity was proposed in the branch 1 which was confirmed after re-evaluation of the family (Figure D-b). Having access to additional samples from the family, linkage analysis was re-performed.

The results showed a homozygous region common between affected individuals in the core family and branch 1, (Najmabadi et al. 2006) but not in the only affected individual in branch 2. As the only common linkage interval between affected individuals of core family and branch 1 was not homozygous in the

affected from branch 2 and as the phenotype in this family is pure mental retardation, the condition in the affected individual of branch 2 might have occurred due to other genetic or environmental factors and therefore this branch of the pedigree was not considered for the final linkage analysis. This yielded a 10Mb interval between markers rs2246786 and rs720225 with a parametric LOD score of 4.3.

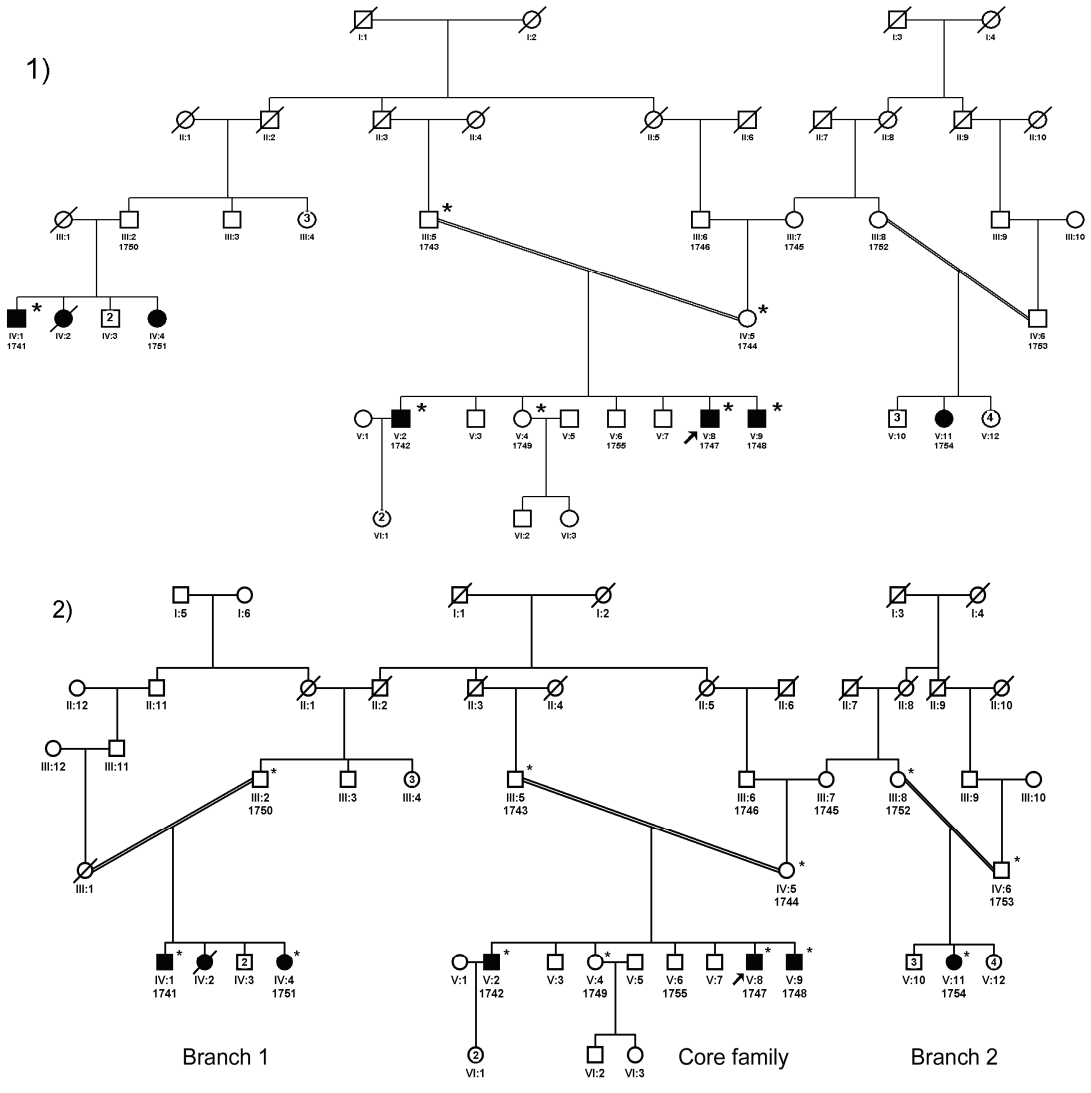

Figure D: 1) Family M097 initial pedigree. 2) Family M097 completed pedigree. Genotyped family members are marked with asterisks.

E. *GRIK2* splice variants and their importance

GRIK2 has 2 major transcripts, GLUR6a and b (See figure 1-3b;(Gregor et al. 1993). They are expressed in the same brain regions and co-assemble in native receptors (Coussen et al. 2005). Interestingly, although the two splice variants do not significantly differ in their functional properties, they can co-assemble into the same heteromeric complex in native and recombinant receptors, bringing into close proximity different sets of interacting cytosolic proteins (Figure E1).

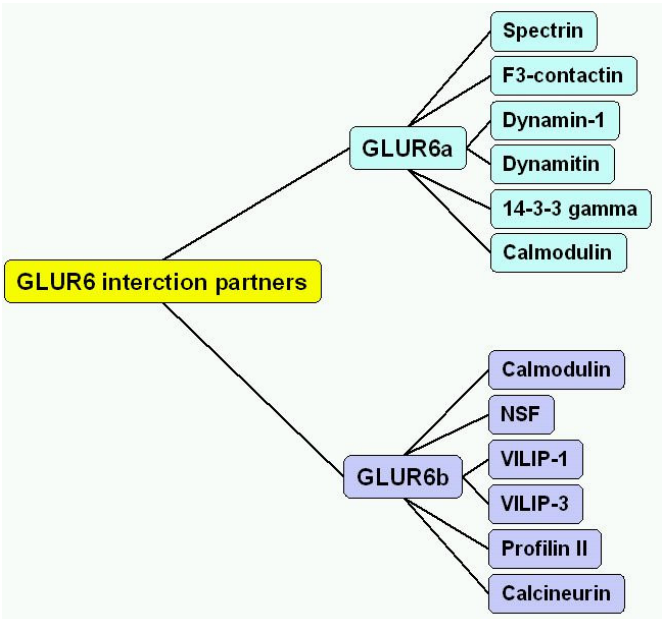

Figure E1: Wide difference in the spectrum of the GLUR6a and GLUR6b interaction partners (Coussen et al. 2005).

A third variant, GluR6c, contains an insertion of the 15 C-terminal exon and has only been described in human (Barbon et al. 2001). During the cloning of the *GRIK2* full-length cDNA, we also identified a new transcript in which 171 bp sequence from inrton 1 was spliced. We could confirm existence of this transcript with PCRs using primers located in so called ”exon1b”. Although based on the reading frame this

transcript will be truncated in the middle of “exon1b” but such transcripts might play a role in the regulation of the *GRIK2* expression in transcriptional level (Figure E2).

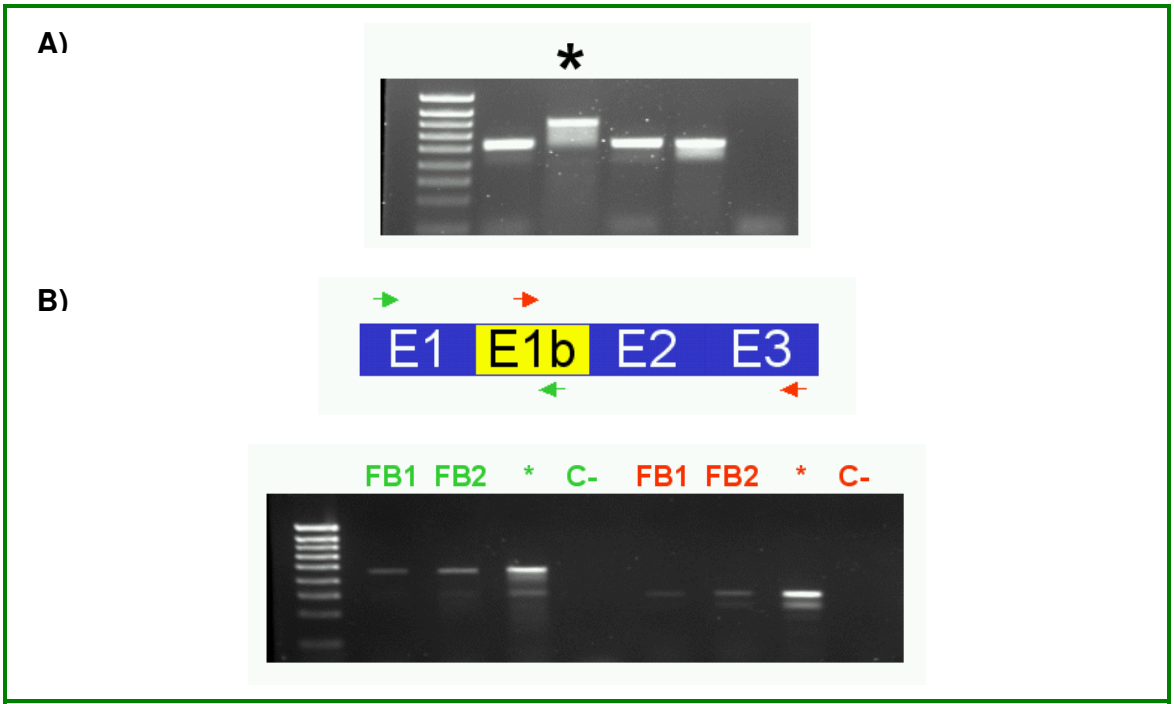

Figure E2: Existence of other *GRIK2* splice variants. A) Amplification of the cloned cDNAs revealed a clone with aberrant size marked with *. B) Sequencing of the aberrant cloned cDNA showed inclusion of an extra sequence between exons 1 and 2. Arrows show the position of the exon specific primers used for validation. C) PCR using exon specific primers confirmed existence of new transcript in the fetal brain. E: Exon, FB: Fetal brain cDNA, *: Aberrant clone which was first identified.

Other splice variants were also observed in the RT-PCR experiments. (See Figure 3-27A) As even short sequence differences can give different binding abilities to this protein, it is necessary to study expression pattern of GLUR6 in the different tissues and time frames during development in detail in order to get a better understanding of the GLUR6 functions.

F. Southern blots

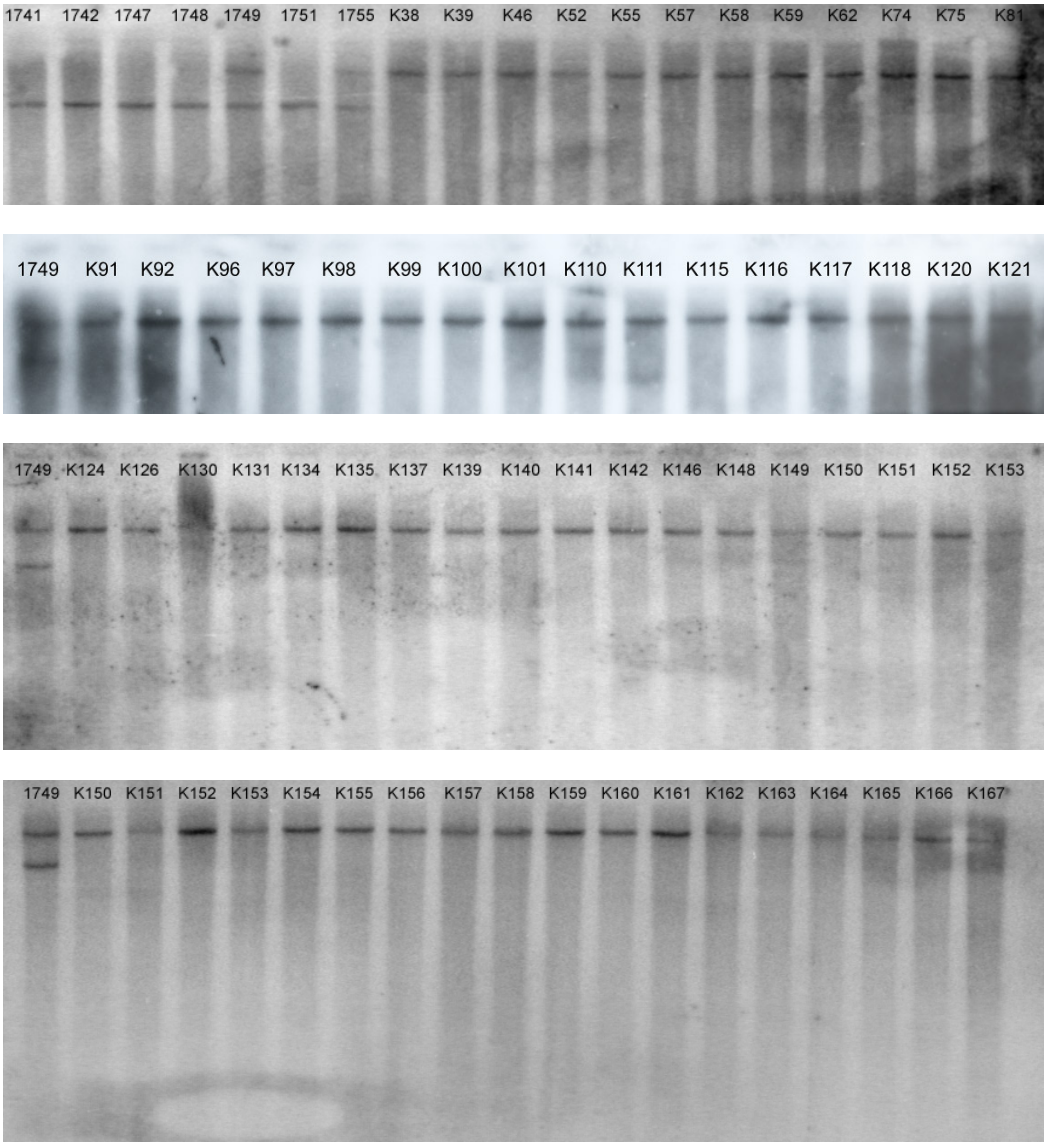

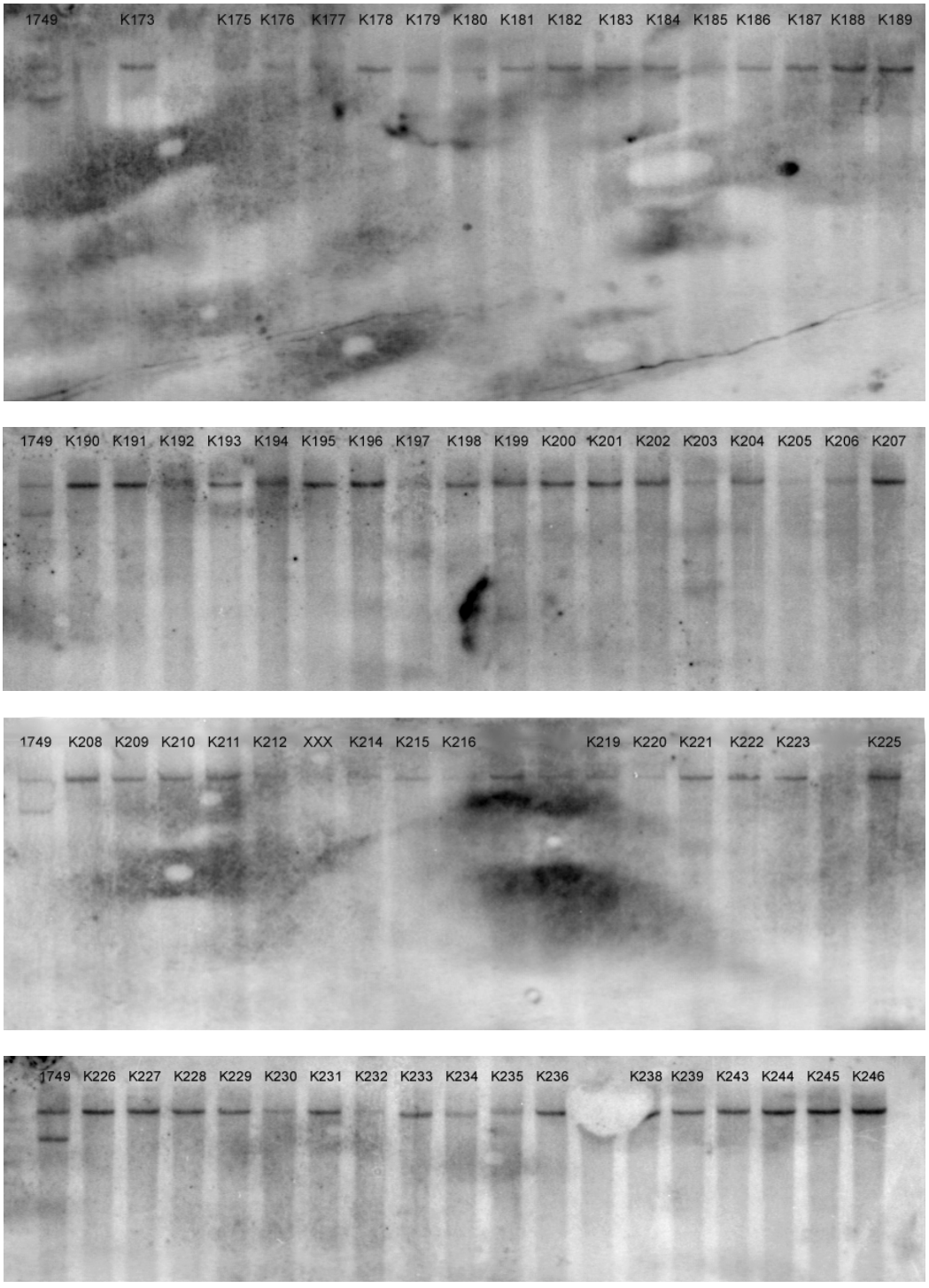
1749 K173 K175 K176 K177 K178 K179 K180 K181 K182 K183 K184 K185 K186 K187 K188 K189
1749 K190 K191 K192 K193 K194 K195 K196 K197 K198 K199 K200 K201 K202 K203 K204 K205 K206 K207
1749 K208 K209 K210 K211 K212 XXX K214 K215 K216 K219 K220 K221 K222 K223 K225
1749 K226 K227 K228 K229 K230 K231 K232 K233 K234 K235 K236 K238 K239 K243 K244 K245 K246

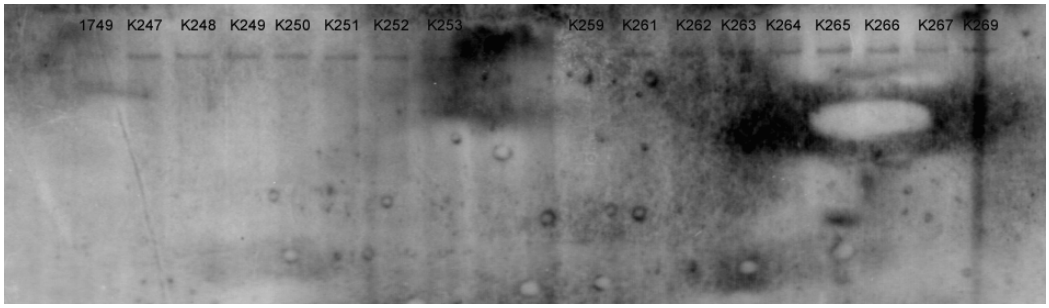

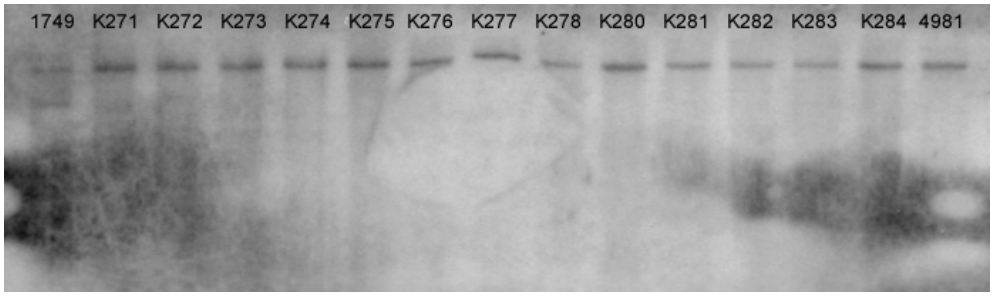

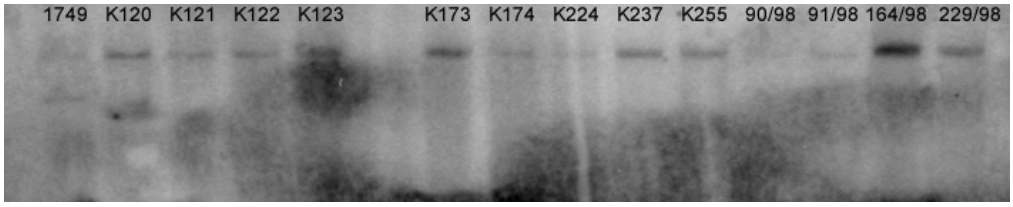

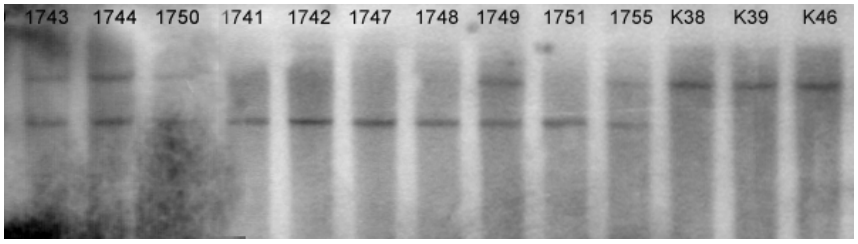

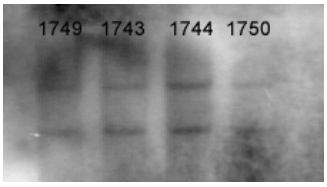

Figure F: Southern blots showing co-segregation of *GRIK2* deletion in M097 family and absence of the deletion in the controls. Numbers 1741-1755 belong to the M097 family and the rest of the numbers indicate the genomic DNA from German healthy individuals used as controls. DNA from a carrier of the deletion (1749) is loaded on the first lane as control for all blots. Upper band: 11 kb wild-type *GRIK2*, Lower band: 6.7 kb *GRIK2Δ.*

8. Summary

Non-syndromic mental retardation is still one of the most important and largely unresolved problems in genetic health care. Autosomal forms are far more common than X-linked ones, but in contrast to the latter, they are still largely unexplored.

In this study, homozygosity mapping in 48 consanguineous Iranian families with nonsyndromic autosomal recessive mental retardation (NS-ARMR) made it possible to determine the chromosomal localization of at least 5 novel mental retardation loci (MRT4-8) for this condition. The data suggest that in the Iranian population NS-ARMR is very heterogeneous, and they argue against the existence of frequent gene defects that account for more than a few percent of the cases.

Furthermore, this thesis describes a complex mutation in the ionotropic glutamate receptor 6 gene (*GRIK2, GLUR6;* [MIM 138244]) at the MRT6 locus, which cosegregates with mild to severe NS-ARMR in a large consanguineous Iranian family. The predicted gene product lacks the first ligand binding domain, the adjacent transmembrane domain and the putative pore-loop, suggesting a complete loss of function of the GLUR6 protein, which is supported by electrophysiological data. This finding provides the first proof that GLUR6 is indispensable for higher brain functions in man. It can be expected that future studies of this and other ionotropic kainate receptors will yield valuable contributions to understanding the pathophysiology of mental retardation, but also shed light on human brain function in general.

9. Zusammenfassung

Unspezifische geistige Behinderung ist eine der nach wie vor wichtigsten und weitgehend ungelösten Herausforderungen für das Gesundheitswesen einer Gesellschaft. Autosomal vererbte Formen sind dabei häufiger als X-chromosomal vererbte Formen, aber im Gegensatz zu letzeren sind erstere noch nahezu unerforscht.

In der vorliegenden Studie wurde Homozygotiekartierung in 48 konsanguinen iranischen Familien mit unspezifischer autosomal rezessiv vererbter mentaler Retardierung (NS-ARMR) durchgeführt, was die Identifizierung von fünf neuen Loci (MRT4-8) für diese Behinderung ermöglichte. Die Daten legen nahe, dass NS-ARMR in der iranischen Bevölkerung sehr heterogen ist und stellen damit die Existenz von häufigen ursächlichen Gendefekten die in mehr als einem geringen Prozentsatz der NS-ARMR Fälle auftreten in Frage.

Darüber hinaus wird über eine komplexe Mutation im *GRIK2* (*GLUR6;* [MIM 138244]) Gen berichtet. *GRIK2* kodiert für den ionotropen Glutamatrezeptor 6 und liegt im MRT6 Locus, welcher in einer großen iranischen Familie mit leichter bis mittelschwerer geistiger Behinderung kosegregiert. Dem theoretisch zu erwartenden Produkt des defekten Gens fehlen die erste Ligandenbindungsdomäne, der daran anschließende membranständige Teil, sowie die mutmaßlich an der Porenbildung beteiligte Molekülschleife. Dies legt einen vollständigen Funktionsverlust des Proteins nahe, was durch die Ergebnisse elektrophysiologischer Experimente im Rahmen der vorliegenden Arbeit unterstützt wird. Damit liefert diese Arbeit einen ersten Beweis dafür, dass dem Glutamatrezeptor 6 eine fundamentale Bedeutung für höhere Hirnfunktionen des Menschen zukommt. Es ist zu erwarten, dass weitergehende Untersuchungen dieses und anderer ionotroper Kainatrezeptoren in der Zukunft neue wertvolle Beiträge zum besseren Verständnis der Pathophysiologie geistiger Behinderung, aber auch der Funktion des menschlichen Gehirns im Allgemeinen liefern werden.